A comparison of doxorubicin and doxorubicinol in rat heart and liver tissue following anthracycline administration

by

Pamela Chenard

A thesis submitted as a partial fulfillment
of the requirements for the degree of
Master of Science (MSc) in Biology

The Faculty of Graduate Studies
Laurentian University
Sudbury, Ontario, Canada

THESIS DEFENCE COMMITTEE/COMITÉ DE SOUTENANCE DE THÈSE
Laurentian Université/Université Laurentienne
Faculty of Graduate Studies/Faculté des études supérieures

Title of Thesis
Titre de la these A COMPARISON OF DOXORUBICIN AND DOXORUBICINOL IN RAT HEART AND LIVER TISSUE FOLLOWING ANTHRACYCLINE ADMINISTRATION

Name of Candidate
Nom du candidat Chenard, Pamela

Degree
Diplôme Master of Science

Department/Program
Département/Programme Biology

Date of Defence
Date de la soutenance

April 13, 2015
avril 13, 2015

APPROVED/APPROUVÉ

Thesis Examiners/Examinateurs de thèse:

Dr. David MacLean
(Supervisor/Directeur de thèse)

Dr. T.C. Tai
(Committee member/Membre du comité)

Dr. Kabwe Nkongolo
(Committee member/Membre du comité)

Dr. Christopher Phenix
(External Examiner/Examinateur externe)

Approved for the Faculty of Graduate Studies
Approuvé pour la Faculté des études supérieures
Dr. David Lesbarrères
M. David Lesbarrères
Acting Dean, Faculty of Graduate Studies
Doyen intérimaire, Faculté des études supérieures

ACCESSIBILITY CLAUSE AND PERMISSION TO USE

Abstract

This study examined the pharmacokinetic profile of the chemotherapeutic drug doxorubicin (DOX), and of its main metabolite doxorubicinol (DOXOL) in male Sprague-Dawley rats. HPLC was used to evaluate both the effect of dose (1.5 mg/kg vs. 4.5 mg/kg) and the effect of recovery time (24, 24, 72, 96, 120, 144, 168 and 192 hours) from the bolus intraperitoneal injection on plasma, liver and heart concentrations. Fluorescence microscopy allowed for qualitative analysis of DOX in liver and heart sections. Plasma concentrations of both drug and metabolite were relatively stable over the examination period. The pattern of response was similar in the liver, although DOX concentrations were decreased after 192 hours, preceded by a spike in DOXOL at 168 hours. The 4.5 mg/kg dose produced increased concentrations of DOX at several of the initial sampling time points in this tissue. In heart tissue, concentrations of DOX steadily decreased for both doses and a dose response was evident until 144 hours. No differences were distinguishable between time-points nor between doses beyond 144 hours. The concentration of DOXOL in this tissue was elevated after 24 hours and subsequently remained stable. Interestingly, DOX and DOXOL remained detectable at 192 hours post-injection for all samples. Fluorescence microscopy results consistently revealed sections that indicated the presence of DOX and were representative of the tissues being analyzed. It was observed that following injection, DOX entered the nuclei of cells rather rapidly and seemingly in proportion to the dose administered. This localization was less apparent as time progressed. These findings strongly suggest that DOX was rapidly absorbed, distributed and metabolized, however its elimination patterns remain unclear. The fact that concentrations remained relatively stable in plasma and liver, and fixed in heart tissue after 144 hours, implies that it is stored in cardiac

tissue, and also potentially in other compartments, allowing for constant re-introduction and re-distribution. Remarkably, an increase in the dose administered did not produce greater accumulation of either drug or metabolite over time in any of the tissues analyzed, therefore the mechanism(s) responsible for the uptake and distribution within the tissues appear to be rate limiting (dose-independent). Nevertheless, the residual amounts of DOX and DOXOL in the heart and liver suggest the possibility of further accumulation upon repeated injections, supporting previous findings suggesting that cumulative doses of DOX are extremely damaging and can result in cardioxicity.

Keywords

Doxorubicin pharmacokinetics, Doxorubicin, Doxorubicinol, Chromatography, Fluorescence microscopy, Cardiotoxicity

Acknowledgements

The completion of this Master's thesis would not have been possible without the contributions of several people. First and foremost, I am extremely grateful to my advisor, Dr. David MacLean for his constant guidance, supportive feedback, constructive criticism and infinite patience during the progress of this project. His knowledge and integrity have made him an indescribably valuable mentor throughout my research and academic career. Thank you, Dave, for being a true role model and inspiring me to never give up, and for the proof that hard work and dedication are the genuine ways to success. I am also very thankful to my advisory committee members Dr. TC Tai and Dr. Kabwe Nkongolo for their excellent suggestions and support over the course of my graduate studies. I would also like to thank my external examiner, Dr. Chris Phenix.

To my colleague and PhD candidate, Sergio Fabris, I am also incredibly grateful. Thank you for the many hours of discussion, for help with the early morning experiments and the late night analysis, for the advice, the corrections and the coffees. I also extend my thanks to Lindsay Anderson, a summer intern in the MacLean lab, for her help in completion of experiments and analysis. In addition, I would like to thank the staff of the Animal Care Facility at Laurentian University for the training and knowledge that they provided.

Finally, the completion of this project and of my degree would not have been possible without the financial support of NSERC as well as the personal research funding I have received from a very generous and kind third party, who wish to remain anonymous.

Abbreviations

AC – Adriamycin cyclophosphamide
AKR – Aldo-keto reductase
ANOVA – Analysis of variance
CBR – Carbonyl reductase
CHF – Congestive heart failure
DAPI – 4’,6-diamidino-2-phenylindole
DNR – Daunorubicin
DNROL – Daunorubicinol
DOX – Doxorubicin
DOXOL – Doxorubicinol
FEC – Fluorouracil epirubicin cyclophosphamide
HER-2 – Human epidermal growth factor 2
HPLC – High performace liquid chromatography
IBC – Inflammatory breast cancer
IP – Intraperitoneal
IV – Intravenous
MRI – Magnetic resonance imaging
ROS – Reactive oxygen species
TNM – Tumor node metastasis
TOP – Topoisomerase
TOP1 – Topoisomerase I
TOP2 – Topoisomerase II
TRITC – Tetramethylrhodamine isothyocyanate
UV – Ultraviolet

Table of Contents

Thesis Defence Committee....ii

Abstract....iii

Acknowledgements....v

Abbreviations....vi

List of Tables....x

List of Figures....xi

Chapter 1: Introduction....1

1.1 Breast Cancer....1

1.1.1 General Introduction....1

1.1.2 Types of Breast Cancer and Diagnosis....2

1.1.3 Current Treatment Strategies....4

1.2 Doxorubicin....6

1.2.1 Drug Discovery and Design....6

1.2.2 Mechanisms of Chemotherapeutic Action....7

1.2.2.1 General Introduction....7

1.2.2.2 DNA Intercalation....8

1.2.2.3 Topoisomerase II Inhibition....8

1.2.3 Experimental Detection Methods....10

1.2.3.1 General Introduction....10

1.2.3.2 High Performance Liquid Chromatography Quantification....10

1.2.3.3 Fluorescence Microscopy Detection....12

1.3 Pharmacokinetics....13
1.3.1 General Introduction....13
1.3.2 Current Pharmacokinetic Understanding of Doxorubicin....14
1.3.2.1 Absorption into Systemic Circulation....14
1.3.2.2 Distribution to Peripheral Compartments....15
1.3.2.3 Metabolism....16
1.3.2.4 Excretion and Elimination....17
1.3.3 Mechanisms of Cardiotoxicity....18
1.3.3.1 General Introduction....18
1.3.3.2 Theory I: Reactive Oxygen Species....18
1.3.3.3 Theory II: Doxorubicinol....20
Chapter 2: Purpose and Objectives....24
Chapter 3: Materials and Methods....25
3.1 Animals and Experimental Design....25
3.2 Pre-experimental Protocol....26
3.3 Experimental Protocol....27
3.4 Post-experimental Protocol....27
3.4.1 Blood Samples....27
3.4.2 Tissue Samples....28
3.5 Analysis....28
3.5.1 High Performance Liquid Chromatography....28
3.5.1.1 Plasma Samples....28
3.5.1.2 Heart Tissue Samples....28

3.5.1.3 Liver Tissue Samples....29
3.5.1.4 HPLC Analysis....29
3.5.2 Histological Fluorescence Examinations....30
3.5.2.1 Slide Preparation....30
3.5.2.2 Fluorescence Microscopy....31
3.6 Statistics....32
Chapter 4: Results....33
4.1 HPLC Analysis....33
4.1.1 Plasma Samples – Doxorubicin....33
4.1.2 Plasma Samples – Doxorubicinol....34
4.1.3 Liver Tissue Samples – Doxorubicin....36
4.1.4 Liver Tissue Samples – Doxorubicinol....39
4.1.5 Heart Tissue Samples – Doxorubicin....42
4.1.6 Heart Tissue Samples – Doxorubicinol....45
4.1.7 Heart vs. Liver....48
4.2 Fluorescence Microscopy....50
4.2.1 Liver Tissue Samples....50
4.2.2 Heart Tissue Samples....53
Chapter 5: Discussion....57
5.1 Experimental Design....58
5.2 Plasma Compartment....60
5.3 Liver Compartment....62
5.4 Heart Compartment....63

5.5 Fluorescence Microscopy.....66

5.5.1 Liver.....67

5.5.2 Heart.....68

Chapter 6: Conclusions.....70

References.....72

Appendix I: Supplementary Materials and Methods.....85

Appendix II: Supplementary Results.....95

List of Tables

Table 1. Experimental animal groups.....26

Table 2. Doxorubicin concentrations in plasma samples.....35

Table 3. Doxorubicinol concentrations in plasma samples.....35

Table 4. Doxorubicin concentrations in tissue samples.....49

Table 5. Doxorubicinol concentrations in tissue samples.....49

Table 6. HPLC gradients.....90

List of Figures

Figure 1. Normal female breast anatomy and histology.....1

Figure 2. TNM Classification System and stage categorization.....3

Figure 3. Treatment options and process of decision making for cancer therapy.....5

Figure 4. The chemical structures of DOX and DNR.....7

Figure 5. Interaction of DOX and DNA.....9

Figure 6. HPLC flow scheme and typical HPLC display.....11

Figure 7. Emission spectrum of varying concentrations of DOX.....12

Figure 8. Simple pharmacokinetic pathway with first principles and examples.....14

Figure 9. Routes of DOX metabolism.....17

Figure 10. ROS formation and the effects of oxidative stress.....19

Figure 11. Mechanisms of DOXOL cardiotoxicity.....21

Figure 12. Slide layout example.....31

Figure 13. Liver doxorubicin concentrations after 1.5 mg/kg dose administration.....36

Figure 14. Liver doxorubicin concentrations after 4.5 mg/kg dose administration.....37

Figure 15. Liver doxorubicin concentrations for both doses.....38

Figure 16. Liver doxorubicinol concentrations after 1.5 mg/kg dose administration.....39

Figure 17. Liver doxorubicinol concentrations after 4.5 mg/kg dose administration.....40

Figure 18. Liver doxorubicinol concentrations for both doses.....41

Figure 19. Heart doxorubicin concentrations after 1.5 mg/kg dose administration.....42

Figure 20. Heart doxorubicin concentrations after 4.5 mg/kg dose administration.....43

Figure 21. Heart doxorubicin concentrations for both doses.....44

Figure 22. Heart doxorubicinol concentrations after 1.5 mg/kg dose administration.....45

Figure 23. Heart doxorubicinol concentrations after 4.5 mg/kg dose administration.....46

Figure 24. Heart doxorubicinol concentrations for both doses.....47

Figure 25. Histological slide images of liver from animals treated with 1.5 mg/kg DOX.....51

Figure 26. Histological slide images of liver from animals treated with 4.5 mg/kg DOX.....51

Figure 27. Histological slide images of liver from animals treated with both doses of DOX.....52

Figure 28. Histological slide images of treated versus control liver tissue.....53

Figure 29. Histological slide images of heart from animals treated with 1.5 mg/kg DOX.....54

Figure 30. Histological slide images of heart from animals treated with 4.5 mg/kg DOX.....54

Figure 31. Histological slide images of heart from animals treated with both doses of DOX.....55

Figure 32. Histological slide images of treated versus control heart tissue.....56

Figure 33. IP injection in the rat.....86

Figure 34. Histological images of heart tissue.....95

Figure 35. Histological images of liver tissue.....96

Chapter 1: Introduction

1.1 Breast Cancer

1.1.1 General Introduction

Cancer is commonly defined as the uncontrolled growth and division of abnormal cells and often leads to a malignant tumor that has the potential to spread through metastasis and affect other parts of the body. It is generally classified by the organ or body part in which it originates. For example, breast cancer originates in breast tissue and is typically a carcinoma, which is a cancer that originates in the epithelial layer of the ducts or the lobules of the breast (Figure 1) (Masood and Kameh 2002, American Cancer Society 2013).

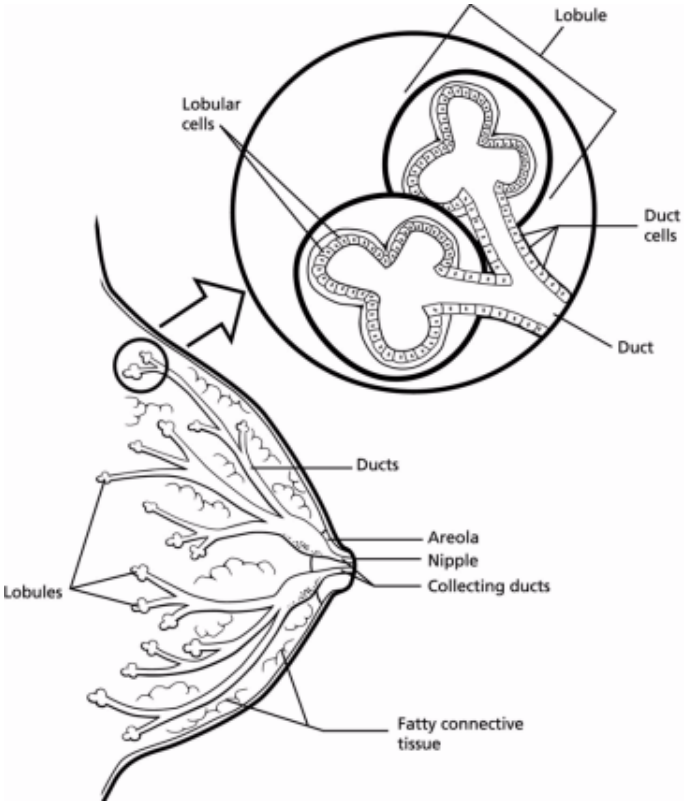

Figure 1: Normal female breast anatomy and histology (American Cancer Society 2013)

According to the Canadian Breast Cancer Foundation (2014), approximately 25% of all cancers diagnosed in women over the age of 20 are breast cancer in nature, making it one of the most prevalent. It is also the second leading cause of cancer-related deaths among women. In fact, it is predicted that 5,000 women will die from breast cancer in 2014, despite an 88% five-year survival rate for women treated for the disease. In addition, it is important to note that although patients may survive breast cancer, they have a lifetime risk of developing other complications as a result of the cancer treatment particularly with respect to the cardiovascular system, which can range anywhere from hypertension and arrhythmias to congestive heart failure (CHF) (Sparreboom et al. 2002, Menna et al. 2012).

1.1.2 Types of Breast Cancer and Diagnosis

There are several different types of breast cancers which are generally categorized based on their level of invasiveness and their location in breast tissue. Non-invasive types of breast cancers are also called *in-situ* carcinomas and originate in either the epithelium of the lobules or of the ducts (Masood and Kameh 2002, Canadian Breast Cancer Foundation 2013, American Cancer Society 2013). Non-invasive types are localized to the lumen of the lobule or duct and do not breach the lining or basement membrane between the epithelium and the surrounding connective tissue and these types of breast cancers are therefore not metastatic (Masood and Kameh 2002, Neal and Hoskin 2009). Invasive types of breast cancers are also called *infiltrating* carcinomas and can originate in the same two locations as non-invasive breast cancers, however, as the name suggests, invasive types are able to breach the basement membrane, infiltrate the blood and lymph vessels and metastasize to other parts of the body (Masood and Kameh 2002, Neal and Hoskin 2009, Canadian Breast Cancer Foundation 2012, American Cancer Society 2013). In

addition, another type of invasive breast cancer is inflammatory breast cancer (IBC), which is less common than other invasive types of breast cancers, and does not present with typical symptoms. This type is typically difficult to diagnose and often is mistaken for infection (Canadian Breast Cancer Foundation 2013, American Cancer Society 2013).

Diagnosis begins with detection through imaging methods, such as mammograms, ultrasounds or magnetic resonance imaging (MRI). A biopsy is then performed to assess whether the growth is benign or malignant, and depending on the type of biopsy, the invasiveness of the malignancy can also be determined. From this point on, staging and grading of the cancer can be done. Staging uses the TNM (Tumor Node Metastasis) Classification System to categorize cancers based on how advanced the disease is, for example Stage 0 being the least advanced and Stage IV being the most advanced (Figure 2) (Neal and Hoskin 2009, Canadian Breast Cancer Foundation 2013). Grading then classifies the aggressiveness of the cancer by microscopically observing the cancer cells to evaluate their appearance and behaviour (Canadian Breast Cancer Foundation 2013). Cells that more closely resemble normal breast tissue cells are more likely to have slower growth and less ability to spread.

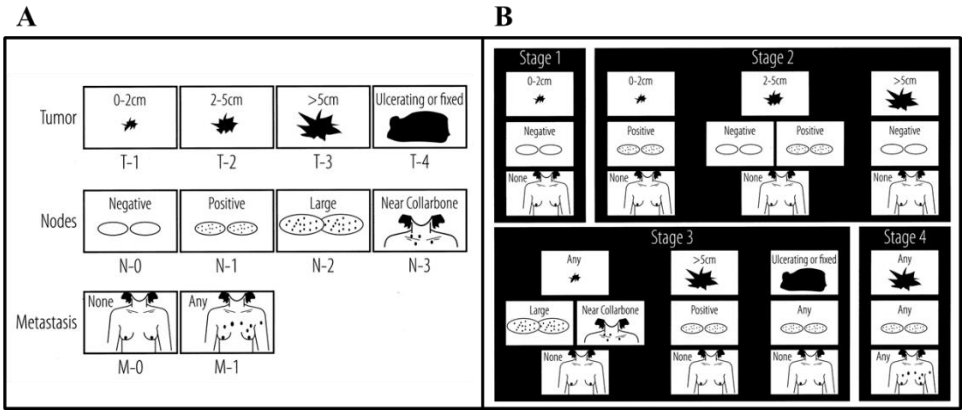

Figure 2: A. TNM (Tumor Nodes Metastasis) Classification System B. Stage categorizing system used with TNM (adapted from Canadian Breast Cancer Foundation 2013).

Newer methods of classifying breast cancers are emerging. Determining the estrogen receptor status of cancer cells is becoming increasingly practiced, since higher levels of certain estrogen receptors may lead to more successful treatment with specific hormone therapies (Heldring et al. 2007, American Cancer Society 2013). Quantifying human epidermal growth factor 2 protein (HER-2) in cancer cells is also becoming routine, since high levels of HER-2 protein generally indicate a more aggressive type of cancer. Early identification can again enhance the outcomes of treatment by using targeted therapies (Pruthi 2012, American Cancer Society 2013). The purpose of each of these diagnostic methods is to determine the patient's prognosis and develop the best possible treatment strategy for the specific type and stage of cancer.

1.1.3 Current Treatment Strategies

Depending on the final diagnosis of the patient, as well as other factors such as age and medical history, different treatment strategies can be implemented (Figure 3). Radical treatment is generally advised when the intention is long-term control or elimination of the disease, for example with Stage I, II or III cancers (Neal and Hoskin 2009). In these cases, the first line of treatment is surgery and can range from lumpectomy to radical mastectomy. Lumpectomy is a procedure for removing the tumor and a small area of surrounding breast tissue, while radical mastectomy is the excision of the entire breast, pectoralis muscles and axillary contents (Neal and Hoskin 2009, American Cancer Society 2013). Radical mastectomy is generally only applied if the growth has significantly invaded the underlying muscle. Following any surgical procedure that conserves some of the affected breast and where there is a perceived risk of local recurrence, radiotherapy and sometimes adjuvant chemotherapy or hormone therapy is recommended (Neal and Hoskin 2009).

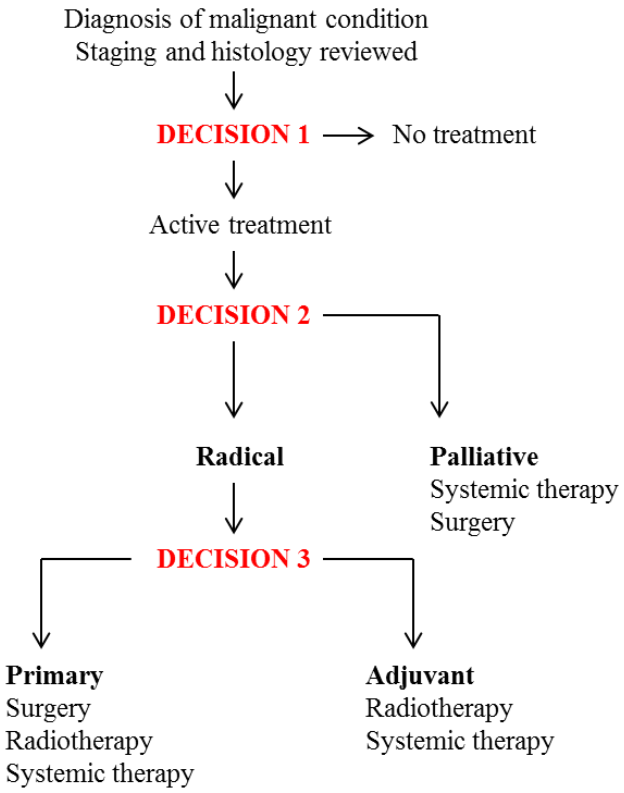

Figure 3: Treatment options and process of decision making for cancer therapy (adapted from Neal and Hoskin 2009)

In cases where the tumor is inoperable, such as with very advanced Stage III or Stage IV cancers, the primary form of treatment is chemotherapy. In such cases, a palliative approach is generally taken, although surgery can also be used in these scenarios to relieve physical impairment arising from the tumor. There are several chemotherapy regimens currently used to treat advanced cases of breast cancer, most of which are anthracycline-containing combinations of several drugs. Frontline breast cancer chemotherapy combinations include AC (adriamycin, cyclophosphamide) and FEC (fluorouracil, epirubicin, cyclophosphamide) (Neal and Hoskin 2009). Adriamycin (doxorubicin) and epirubicin represent the anthracyclines in these regimens, which intercalate into DNA to ultimately inhibit cell division. Anthracyclines have been shown to exhibit significant anti-neoplastic or anti-tumor activity (Section 2.2). Cyclophosphamide is an

alkylating agent and works by cross-linking DNA to prevent replication and inhibit cell division (Jonge et al. 2005), while fluorouracil is a pyrimidine analog which can incorporate into DNA and RNA to prevent replication and inhibit cell division (Iyer and Ratain 1999).

As previously mentioned, having received cancer treatment leaves survivors with a lifetime risk of developing other health complications. Each of the treatment options described above produce adverse effects that can range from nausea and vomiting to infertility and severe cardiac problems such as CHF (Sparreboom et al. 2002, Menna et al. 2012). The possibility of producing such negative effects may preclude patients presenting with other health conditions, or patients with very advanced stages of the disease from receiving treatment (Neal and Hoskin 2009). Thus more research or investigations into new drugs or drug combinations would be beneficial for long-term patient survival.

1.2 Doxorubicin

1.2.1 Drug Discovery and Design

Doxorubicin (DOX), also known as adriamycin, is an anti-cancer chemotherapeutic drug classified as an anthracycline antibiotic. Anthracyclines were discovered in Italy and France in the 1950s through the identification of a mutated strain of the bacteria *Streptomyces peucetius* (Arcamone 1985, Sparreboom et al. 2002). Daunorubicin (DNR) was the original pigmented antibiotic isolated from this bacterial strain, from which DOX was later derived in the 1960s as a less harmful chemotherapeutic option which has been in use since the mid-1970s (Arcamone 1985).

DOX and DNR are almost structurally identical as both molecules consist of a tetracyclic ring structure containing adjacent quinone and hydroquinone groups and a methoxy substituent at C-4 in the first ring. These characteristics constitute the planar aromatic portion of each molecule. Both structures also contain an amino-sugar portion, daunosamine, attached at C-7 of the fourth ring by a glycosidic linkage. The only difference between these chemicals is that DOX contains a primary alcohol at C-14, whereas DNR contains a methyl at this location (Figure 4) (Minotti et al. 2004, Menna et al. 2012).

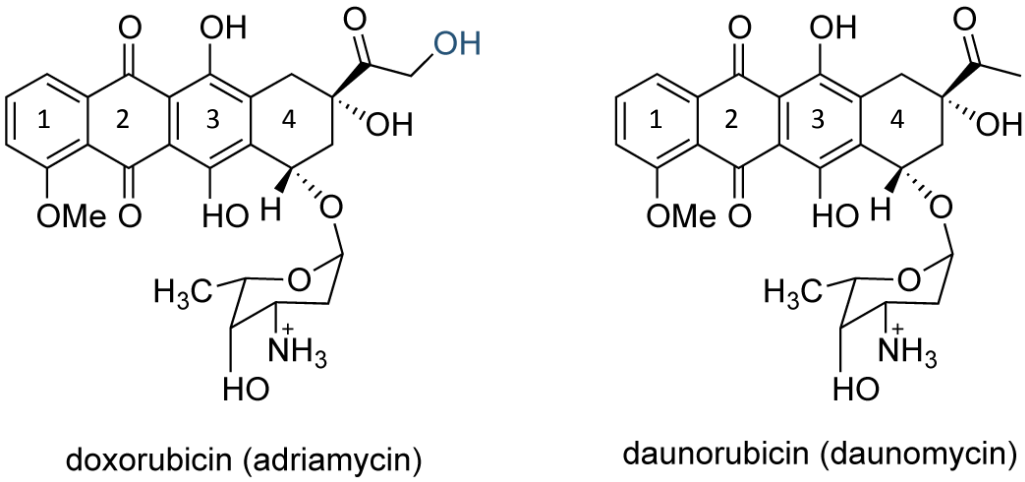

Figure 4: The chemical structures of DOX (left) and DNR (right) (adapted from ATDBio 2013)

1.2.2 Mechanisms of Chemotherapeutic Action

1.2.2.1 General Introduction

There are two main mechanisms of action for anthracyclines. Both mechanisms have been heavily researched and provide excellent insight into why DOX is a very effective anti-tumor agent. The DNA intercalation mechanism assumes DOX directly inhibits the replication of DNA, therefore stopping cellular division. The topoisomerase II (TOP2) mechanism allows for

DNA intercalation, but suspects that DOX plays more of a bridging role in the covalent binding of TOP2 to the DNA molecule (Sparreboom et al. 2002, Minotti et al. 2004).

1.2.2.2 DNA Intercalation

DOX anti-tumor activity has long been attributed to its ability to intercalate directly with DNA molecules. Intercalation is believed to occur with the planar tetracyclic ring portion of the molecule fitting into a major groove of the DNA. This interaction is then stabilized by the daunosamine moiety binding in the minor groove (Figure 5) (Frederick et al. 1990). There has been some debate as to whether the intercalation is specific to nucleic acid base pairs. Some studies have found that DOX intercalates more readily between adjacent guanine-cytosine pairings, possibly relating to the potential for increased hydrogen bonding (Manfait et al. 1982). Regardless, the intercalation has a direct physical effect on the structure of the DNA. This prevents the normal unwinding and replication events of the DNA molecule, thereby arresting cell division in the S phase of the cell cycle (Sparreboom et al. 2002, Minotti et al. 2004). Cells that cannot divide are pushed to apoptotic pathways, leading to cell death.

1.2.2.3 Topoisomerase II Inhibition

The second mechanism of DOX chemotherapeutic activity is inhibition of the DNA replication enzyme, TOP2. Normal topoisomerase function allows for modification of the topology of the DNA by inducing single-strand breaks by topoisomerase I (TOP1) or double-strand breaks by TOP2. The action of TOP enzymes leads to proper regulation of supercoiling of the DNA molecule. The activity of TOP enzymes is dependent on the cell cycle phase and the transcriptional activity of the cell (Binaschi et al. 2001, Sparreboom et al. 2002). DOX is

believed to inhibit TOP2 action by stabilizing an intermediate complex at the TOP2-DNA interface. First the DNA is intercalated by DOX and undergoes a double-strand break by TOP2 and then these DNA strands are subsequently covalently bound to tyrosine residues within the TOP2 protein. The orientation of the daunosamine sugar of DOX in the minor groove of the DNA molecule is thought to play a large role in the stability of the DOX-DNA-TOP2 complex (Binaschi et al. 2001). Ultimately, the cellular response to TOP2 inhibition is apoptosis (Gewirtz 1999).

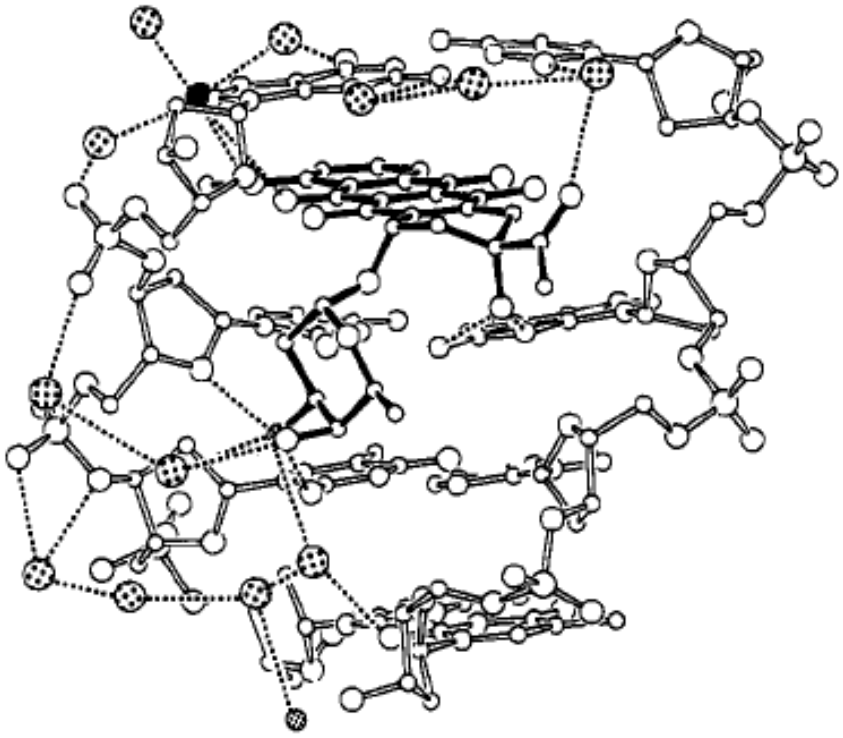

Figure 5: Interaction of DOX (solid bonds) and DNA (open bonds). Dotted lines represent hydrogen bonds (Frederick et al. 1990).

1.2.3 Experimental Detection Methods

1.2.3.1 General Introduction

Once it had been established as an anti-cancer chemotherapeutic, research on DOX revolved around its mechanism of action and clarification of its pharmacokinetic and pharmacodynamic role. This required the development of methodologies that would be capable of quantifying DOX in a given structure of interest, as well as perhaps being able to visualize it *in situ*. Two main detection methods of DOX have been greatly used in the research setting: High Performance Liquid Chromatography (quantitative) and Fluorescence Microscopy techniques (qualitative to semi-quantitative).

1.2.3.2 High Performance Liquid Chromatography Quantification

High Performance Liquid Chromatography (HPLC) is a form of pressurized column chromatography that allows identification and quantification of components in a chemical mixture (Clark 2007, Smith 2011). Normal phase HPLC uses non-polar solvents to elute non-polar components more quickly. Reversed phase HPLC is the opposite, using polar solvents to elute polar components more rapidly. As a sample is eluted from the column, it is sensed by a detector, which will relay information to a processing unit and display peaks that were detected (Figure 6) (Clark 2007, Smith 2011). The area under each peak is calculated and compared to a linear standard curve of Area vs. Concentration, in order to obtain the final concentration of the compound in the sample.

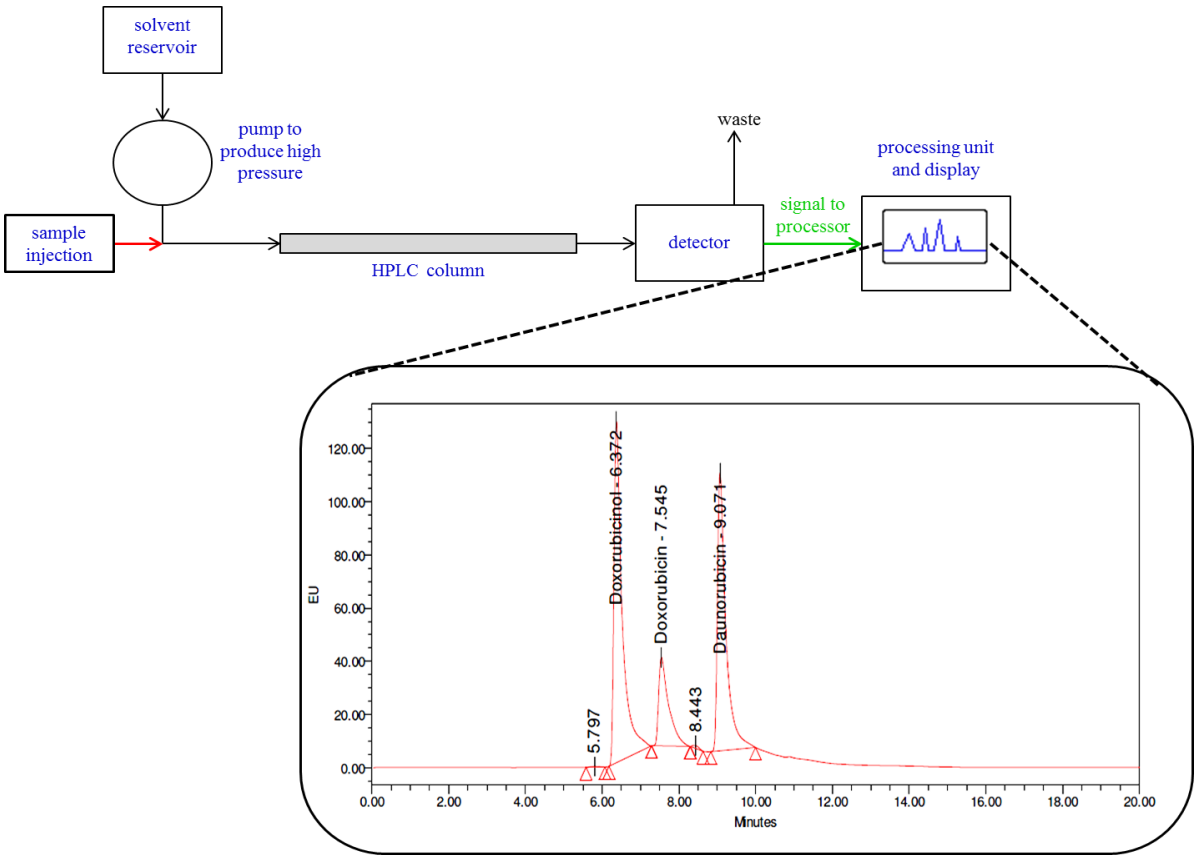

Figure 6: HPLC flow scheme (adapted from Clark 2007) and typical HPLC display (MacLean Lab 2012).

For HPLC detection and quantification of DOX, different systems, columns, detectors and processing software can be used. Reversed phase methods with fluorescence detection have been used for many years and have the advantage of being sensitive to DOX, DNR and their major metabolites. Some systems have used UV detection, while others have used HPLC detection followed by mass spectroscopy; however the sensitivity limits of mass spectroscopy have been debated as less effective (Sparreboom et al. 2002, Maudens et al. 2011).

1.2.3.3 Fluorescence microscopy detection

Since DOX is a fluorescent molecule, it can be viewed by confocal microscopy. DOX emission patterns are suitable for viewing under the TRITC emission filter, which has a centre wavelength of 590 nm and a bandwidth of 34 nm (Figure 7). Though this method is qualitative (although quantitative methods exist), it has provided insight into the localization of DOX in cancer cells as well as in tissues such as heart, liver, kidney and spleen, allowing for clarification of the drug's chemotherapeutic action within cancer cells and also its distribution throughout physiological systems (Shen et al. 2008, Susa et al. 2009, Longmuir et al. 2009, Yousefpour et al. 2011).

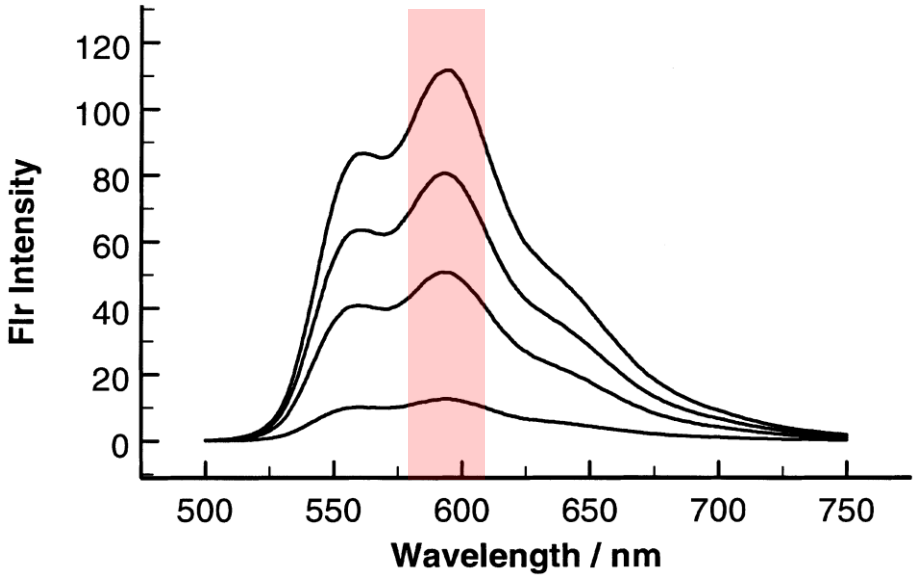

Figure 7: Emission spectrum of varying concentrations of DOX (lowest intensity is 1.0 µM, highest intensity is 20.0 µM). The grey band indicates TRITC filter emission range. (Adapted from Karukstis et al. 1998)

1.3 Pharmacokinetics

1.3.1 General introduction

Pharmacodynamics and pharmacokinetics are two avenues for understanding the mechanisms involved in the physiological response to a drug. Pharmacodynamics explains the effect of a drug on the physiological system, whether beneficial or unfavourable. Pharmacokinetics on the other hand, describes the effect of the physiological system on a drug. More specifically, pharmacokinetics studies the rate of movement of a drug from the site of administration into the systemic circulation, its subsequent distribution to peripheral regions throughout the body, and ultimately its elimination from the system (Collins and Supko 2006, Brown and Tomlin 2010).

Evidently, the time-dependent progress of a drug through a physiological system will be affected by multiple factors, which are regarded as the first principles of pharmacokinetics and include absorption, distribution, metabolism and excretion/elimination (Figure 8). Absorption can be defined by the bioavailability of a drug, which is the amount of a drug that reaches the systemic circulation following administration. This is affected by any factor influencing the transport of the drug molecule across lipid membranes. In order to exert its desired effect, a drug must be able to reach its site of action. This process is typically influenced by blood flow to the site and the ability of the drug to penetrate the tissues of the target organ. It is often numerically represented by the volume of distribution, which is the total amount of administered drug divided by the blood plasma concentration of the drug (Lehman-McKeeman 2008, Brown and Tomlin 2010). Metabolism is the breakdown of a drug into compounds that will be more easily eliminated from the system, and excretion is the route through which this elimination will occur (Parkinson 2008, Brown and Tomlin 2010).

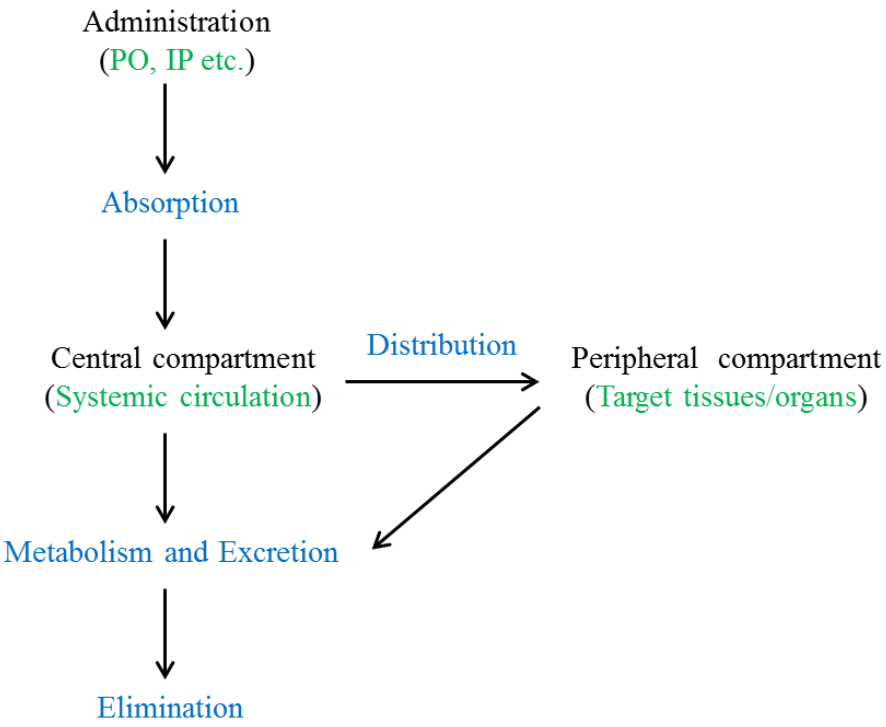

Figure 8: Simple pharmacokinetic pathway with first principles in grey and examples in brackets (adapted from Brown and Tomlin 2010).

1.3.2 Current pharmacokinetic understanding of doxorubicin

1.3.2.1 Absorption into systemic circulation

Depending on the route and duration of administration, peak plasma concentrations of DOX can vary. Generally, DOX is administered via the intra-venous (IV) route in clinical settings. However, its administration through the intra-peritoneal (IP) route has been investigated and its administration directly into the bladder is also a currently used application (Hasovits and Clarke 2012, Pfizer Canada Inc. 2012). IV administration is characterized by 100% bioavailability, meaning that 100% of the drug reaches the systemic circulation. Other routes of administration are affected by first-pass liver metabolism and other factors affecting the distribution of the drug, and result in slower absorption into the systemic circulation (Sugarbaker et al. 2011, Hasovits and Clarke 2012). It has been observed that peak plasma concentrations can be lowered with

prolonged IV administration of DOX, although this does not seem to affect the distribution of DOX to peripheral compartments (Bielack et al. 1996). Plasma binding percentages between 70-75% and volumes of distribution between 20-30 L/kg have been reported for DOX (Kontny et al. 2013). However, some studies have reported plasma binding of up to 85% (Danesi et al. 2002). Binding of a drug to plasma proteins is essential for the drug's transport throughout the physiological system, however increased plasma binding can translate to less free drug available to travel to the active site. Thus, drugs with higher levels of plasma binding can have a reduced volume of distribution and ultimately lower bioavailability (Lindup and Orme 1981). Despite its relatively high plasma binding percentages, DOX displays a high volume of distribution, which indicates that the bioavailability of DOX is unaffected.

1.3.2.2 Distribution to peripheral compartments

DOX is reported to have a very short distribution half-life of less than one hour and a relatively long elimination half-life when administered IV. Tissues are therefore rapidly exposed to DOX after administration and the duration of exposure is significant (Danesi et al. 2002, Kontny et al. 2013). It follows that DOX exhibits significant tissue binding abilities, with detectable amounts measured in liver, spleen, kidney, lung and heart (Pfizer Canada Inc. 2012, Kontny et al. 2013). Studies have revealed that drug concentrations in the heart peak within the first 24 hours following administration and that during this time the heart to plasma DOX ratio is around 40 (Grosse et al. 1999, Weiss 2011). Concentrations of the drug in the liver have been observed to be greater than in the heart, likely due to the fact that the majority of metabolism and excretion occur by means of this organ (Jacquet et al. 1998).

1.3.2.3 Metabolism

Biotransformation of DOX occurs primarily in the liver, where there is an abundance of the enzymes responsible for DOX breakdown. However, there is also evidence suggesting that a portion of DOX metabolism occurs in the heart since the presence of these enzymes in cardiac tissue has been confirmed (Olson and Mushlin 1990, O'Connor et al. 1999, Mordente et al. 2001, Danesi et al. 2002, Weiss 2011).

There are three routes through which DOX is metabolized. The first is the two-electron reduction of the C-13 carbonyl to a secondary alcohol, creating a compound named doxorubicinol (DOXOL) (functional group at ring four, Figure 4). This represents the major metabolic pathway, and it is achieved by several different aldo-keto reductases (AKRs) and carbonyl reductases (CBRs) (Figure 9) (Mordente et al. 2001, Gustafson et al. 2002). The production of DOXOL is linked to the manifestation of several adverse effects, some of them very serious (Section 3.3.3). The second metabolic route of DOX is the one-electron reduction of the quinone moiety to a semi-quinone (second ring, Figure 4). This semi-quinone can be further broken down, but often will regenerate the parent compound through oxidation (Figure 9). This redox-recycling of DOX generates several radical species, which can cause cellular damage and lead to several adverse effects (Section 3.3.2) (Menna et al. 2012). The third metabolic pathway of DOX, accounting for approximately 1-2% of metabolism, is the reductive deglycosidation which breaks the glycosidic linkage at C-7 (fourth ring, Figure 4). This produces deoxyaglycone metabolites, which have been detected but deemed inactive (Figure 9) (van Asperen et al. 1998, Gustafson et al. 2002).

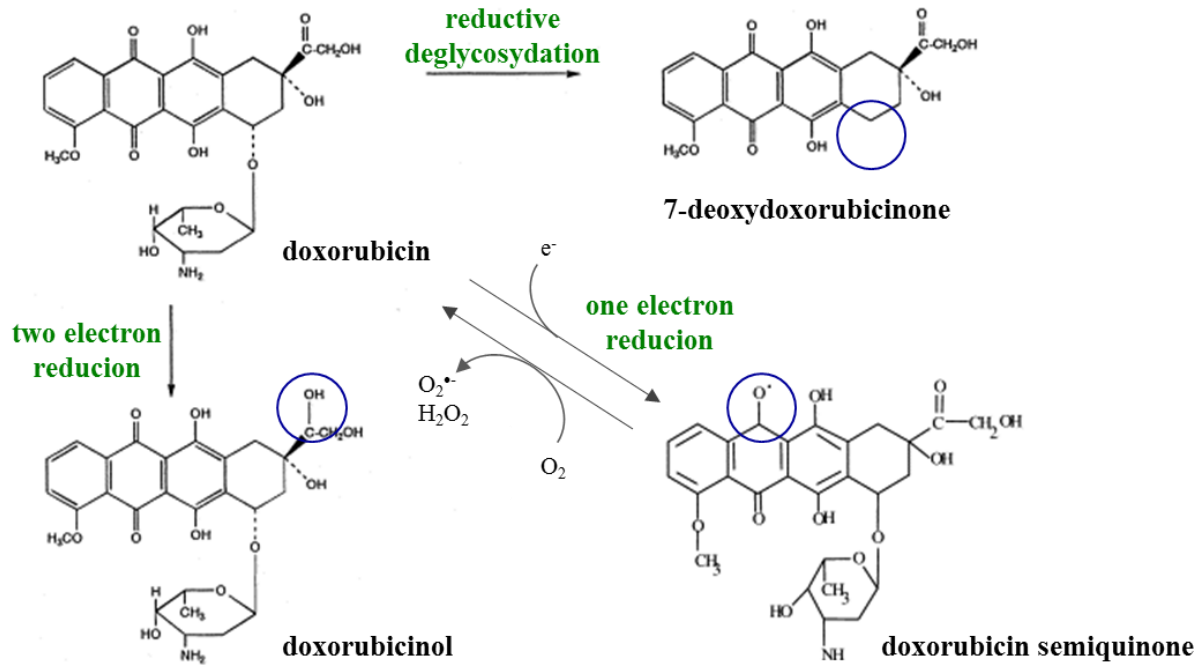

Figure 9: Routes of DOX metabolism (adapted from van Aperen et al. 1998 and Jung and Reszka 2001).

1.3.2.4 Excretion and elimination

The elimination half-life of DOX from the plasma has been described as relatively long at approximately 30 hours after IV administration, increasing the potential for exposure to tumors and tissues (Danesi et al 2002, Kontny et al. 2013). Despite this, DOX is still considered to be rapidly cleared from the plasma (Benjamin et al. 1977, Pfizer Canada Inc. 2012). Tissue binding capabilities account for the prolonged elimination of the drug from the physiological system. Roughly 5-12% is eliminated via renal excretion and 40-50% via biliary excretion over a 5-7 day period (Blum and Carter 1974, Pfizer Canada Inc. 2012, Kontny et al. 2013). Approximately 50% of biliary excretion is unchanged DOX, 20-30% is DOXOL and the balance consists of other minor metabolites (Blum and Carter 1974, Danesi et al. 2002). Due to the significance of

biliary excretion in the elimination of the drug from the physiological system, establishment of liver health is of key clinical relevance (Danesi et al. 2002).

1.3.3 Mechanisms of cardiotoxicity

1.3.3.1 General introduction

Though DOX is an effective anti-neoplastic agent that has been in use for over 40 years, there are serious limitations to its therapeutic use. The administration of the drug is accompanied by warnings of maintaining total cumulative doses of treatment under 550 mg/m^2, since exceeding this dose is associated with a greatly increased incidence of cardiac-related problems such as CHF (Pfizer Canada Inc. 2012). Even lower cumulative doses ranging from 240-400 mg/m^2 of DOX have been linked with delayed onset of CHF or asymptomatic cardiac abnormalities (Menna et al. 2012). Many have sought to investigate the mechanisms by which these toxic effects are generated and current thinking attributes the majority of the problem to the metabolism of DOX. Present theories of DOX induced toxicity include the generation of reactive oxygen species (ROS) through metabolic processes and the generation of toxic metabolites which can directly affect cardiac tissue.

1.3.3.2 Theory I: Reactive oxygen species

Reactive oxygen species such as superoxide anion ($O_2^{\bullet -}$) have the ability to induce cellular damage and apoptosis when present at elevated levels in a physiological system (Beattie 2006). Quinone-containing anti-cancer drugs have been reported to produce ROS through metabolic pathways (Olson and Mushlin 1990). Notably, DOX is suspected to redox-recycle such that its metabolism results in the formation of a semi-quinone that rapidly regenerates the parent

quinone, releasing ROS into the system (Figure 10) (Olson and Mushlin 1990, Minotti et al. 2004). In addition to this cycling, a release of iron from intracellular stores occurs, leading to the formation of more potent ROS molecules (Minotti et al. 2004).

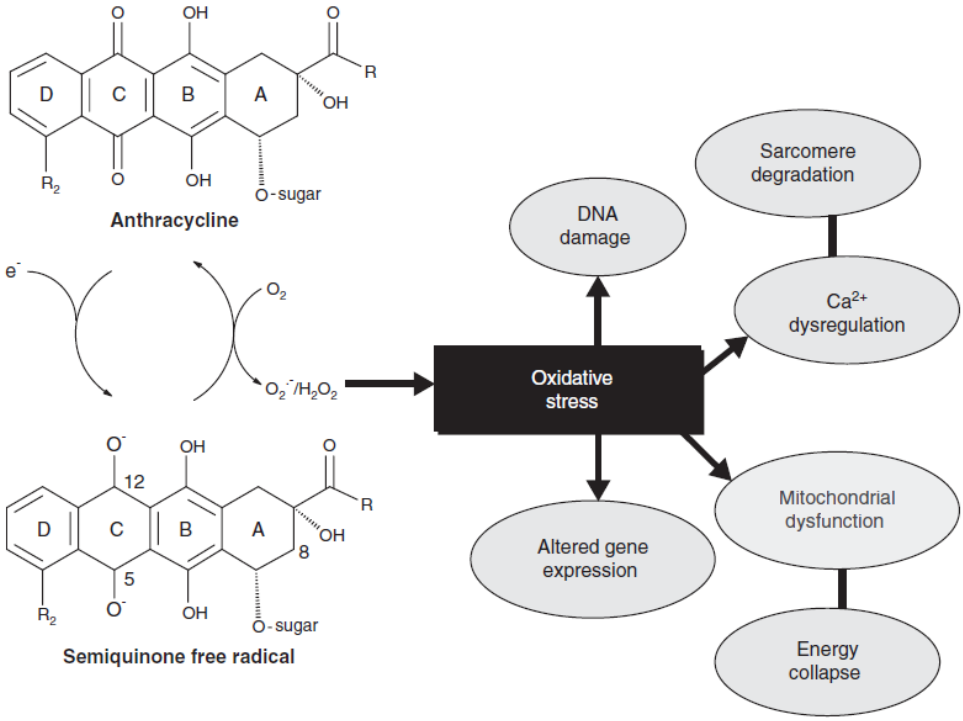

Figure 10: ROS formation and the effects of oxidative stress (Menna et al. 2012)

ROS generation has been hypothesized to contribute to the cardiotoxic effects of DOX administration in several ways (Figure 10). ROS can induce the release of calcium from stores in cardiomyocytes and impede its storage in these cells. This can result in impaired contractility and relaxation of the heart. ROS is also associated with increased mitochondrial dysfunction and cardiomyocytes, being rich in mitochondria, are therefore greatly affected (Olson and Mushlin 1990, Menna et al. 2012). Another influence is the fact that cardiomyocytes generally have poor stores of ROS-detoxifying or neutralizing enzymes, leading to increased intracellular ROS and further complications (Menna et al. 2012).

Though there is much support for the theory of ROS formation as a key player in cardiotoxicity development with anthracycline use, there are noteworthy inconsistencies. Attempts to reverse the effects of ROS by supplementing treatment regimens with antioxidants were successful in smaller animal subjects but less-so in larger ones (Olson and Mushlin 1990, Menna et al. 2012). ROS formation has been shown to occur rapidly with the administration of supraclinical concentrations of DOX, however at clinically relevant doses there is a delayed detection, perhaps indicating increases in ROS are a secondary result of cellular disruption through other mechanisms (Minotti et al. 2004). Finally, DOX-induced cardiotoxicity can be a delayed process, sometimes manifesting years after treatment. Although cardiomyocytes are deficient in ROS-neutralizing enzymes and are therefore sensitive to ROS exposure, the theory of ROS-induced cardiotoxicity does not support a delayed onset model (Menna et al. 2012).

1.3.3.3 Theory II: Doxorubicinol

As previously mentioned, the metabolic breakdown of DOX produces several metabolites. The main route, the two-electron reduction of the C-13 carbonyl group, results in the formation of the secondary alcohol DOXOL (Figure 9). The production of DOXOL has been suspected for some time to contribute to the cardiotoxic effects of anthracycline use. DOXOL was observed to accumulate more readily in cardiac tissue than DOX and where this occurred there was a general increase in the development of severe cardiac complications such as cardiomyopathy and CHF (Olson and Mushlin 1990, Cusack et al. 2002, Menna et al 2012).

The activity of DOXOL as a cardiotoxin has been attributed to two main mechanisms of action (Figure 11). First, studies revealed that DOXOL is a potent inhibitor of ATPase pumps of the

sarcoplasmic reticulum, which regulate the flux of calcium and magnesium. In addition, it also inhibits the f_0-f_1 proton pump of the mitochondria and the sodium-potassium ATPase and sodium-calcium exchanger of the sarcolemma (Boucek et al. 1987, Olson and Mushlin 1990). This leads to a disruption in energy metabolism, ion concentration gradients and calcium movement, which translates to severe cardiac function impairment and cardiotoxicity (Mordente et al. 2001). Second, DOXOL has been shown to facilitate cardiotoxicity by iron-dependent mechanisms. The accumulation of DOXOL converts aconitase/iron regulatory protein-1 (aconitase/IRP-1), a protein crucial to iron homeostasis, into a "null protein", essentially a non-active protein (Minotti et al. 1998, Brazzolotto et al. 2003). The influence of IRP-1 on cellular regulatory and metabolic pathways is extensive, and its inactivity leads to metabolic disruption, loss of iron homeostasis and impairment of the contraction-relaxation cycle of the heart by misplacement of iron ions (Minotti et al. 2004).

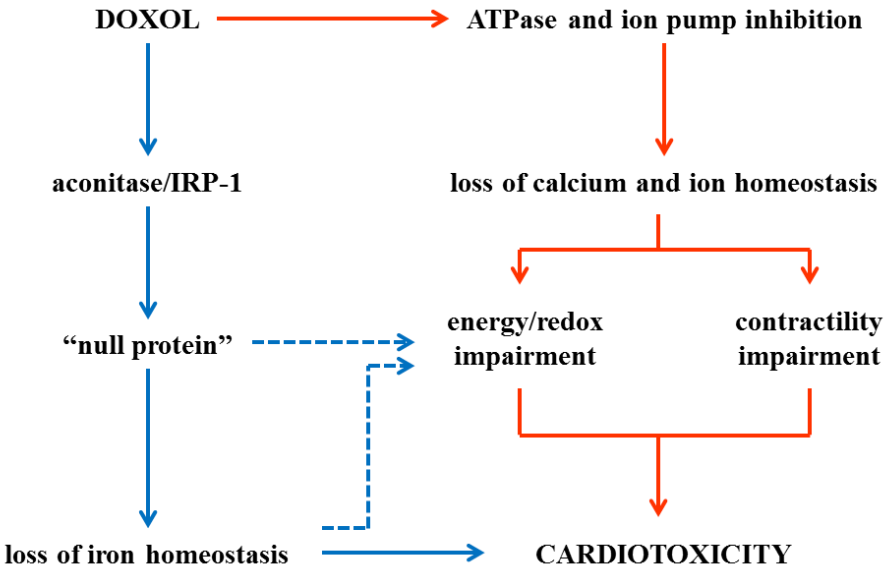

Figure 11: Mechanisms of DOXOL cardiotoxicity (adapted from Minotti et al. 2004).

As with the ROS formation theory of DOX cardiotoxicity, there are several limitations to the secondary alcohol metabolite theory. Studies involving other anthracyclines such as DNR, have found that not only do they also produce secondary alcohol metabolites, but they do so to a greater extent in cardiac tissue. However, an accumulation of daunorubicinol (DNROL) did not correlate to an increased incidence of cardiac-related problems like CHF (Minotti et al. 2004, Menna et al. 2012). Other problems with the DOXOL hypothesis originate in the enzymatic differences between animals and humans receiving treatment. In rats, metabolism of DOX occurs primarily through CBRs, whereas in humans it occurs mainly via the AKRs. The regulation of these enzymatic pathways differs enough to introduce the possibility that net levels of DOXOL produced in the heart of animal subjects could not be extrapolated to represent actual human values (Minotti et al. 2004). Despite these inconsistencies, it is generally accepted that it is important to attempt to control the amount of secondary alcohol metabolites being formed in order to avoid future risk of cardiac complications (Minotti et al. 2004, Menna et al. 2012).

While investigations into the pharmacokinetics of DOX have provided insight into its active metabolic pathways, similar studies of the alleged cardiotoxic metabolite DOXOL are lacking. As previously mentioned, it has been observed that where DOXOL accumulates in the heart, cardiac dysfunction and difficulties emerge, however the time-dependent exposure of tissues to DOXOL during DOX breakdown has yet to be fully elucidated. Furthermore, the validity of the use of supraclinical concentrations of DOX during experiments and subsequent application of the findings to dissimilar scenarios has been questioned. In addition, the duration of time used in previous observations, while supplying results for either the immediate 24 hours following administration or weekly “snap shots” following multiple weekly or bi-weekly administrations,

has been deficient in presenting a thorough pharmacokinetic representation of DOX. The present study was therefore developed in order to address these issues surrounding the pharmacokinetics of both DOX and its major metabolite DOXOL.

Chapter 2: Purpose and Objectives

The purpose of the present study was to examine and clarify the pharmacokinetics of the anthracycline chemotherapeutic DOX using a rat model. The main goal was to provide insight into the physiological behaviour of the drug, as well as of its main metabolite DOXOL. This was to be examined over an eight day period after one bolus administration of either 1.5 or 4.5 mg/kg dose of DOX. The heart was chosen as one of the organs to be studied due to its implications in the severe negative effects of DOX treatment. The liver was chosen as another organ of interest since the majority of DOX metabolism occurs in this tissue. Finally, the plasma was also analysed to confirm the presence of the drug and metabolite in the systemic circulation. The main objectives of the study are outlined below.

Objective 1: Administer either 1.5 or 4.5 mg/kg IP injections of DOX to animals and quantify the drug and its main metabolite (DOXOL) in the plasma and the tissues of interest using High Performance Liquid Chromatography (HPLC), to determine the effect of dose on the pharmacokinetics of both compounds.

Objective 2: Allow a varying period of recovery following the administration of each dose, beginning at 24 hours post-injection and continuing every 24 hours until 192 hours post-injection, and quantify DOX and DOXOL at each time point using HPLC to assess the effect of time on the pharmacokinetics of both compounds.

Objective 3: Use fluorescence microscopy of prepared histological slides of the tissues of interest to confirm presence of the drug and/or its metabolite in treated animal samples as compared to controls.

Chapter 3: Materials and Methods

All procedures involving the use of experimental animals were approved by the Laurentian University Animal Care Committee under protocol number 2009-06-01, and were performed at the Laurentian University Animal Care Facility. They also complied with all Canadian Council on Animal Care guidelines.

3.1 Animals and Experimental Design

One-hundred and two (102) male Sprague-Dawley rats weighing approximately 250 g were purchased from Charles River Laboratories, Montreal, Québec. They were purchased in groups of 25-30 animals, and were housed at the Laurentian University Animal Care Facility under a 12 hour light and dark alternation cycle at a facility temperature between 22-24°C. They were fed with rodent chow and water *ad libitum* and were allowed a one week acclimation period before the commencement of the experiments.

Animals were divided into sixteen groups of six. Half of these groups received a low dose (1.5 mg/kg) of DOX (supplied by the North-Eastern Ontario Cancer Centre, Sudbury, ON) and the other half received a high dose (4.5 mg/kg). With respect to the eight groups that received the low dose, each group was to recover for a different duration of time post-injection. These recovery times varied by intervals of 24 hours, and spanned an eight day period. The same time frame applied to the eight groups that received the high dose (Table 1). A seventeenth group of six rats represented the control animals.

Table 1: Experimental animal groups

		Time post-injection (hrs)							
Dose (mg/kg)		24	48	72	96	120	144	168	192
0	n=6 (controls)								
1.5		n=6	n=6	n=6	n=6	n=6	n=6	n=6	n=6
4.5		n=6	n=6	n=6	n=6	n=6	n=6	n=6	n=6

3.2 Pre-experimental Protocol

On the day of the injection of anthracycline, rats were weighed and the volume of injection was calculated based on whether the animal was to receive 1.5 or 4.5 mg/kg DOX. They were then anesthetized using the EZ-150 vaporizer unit (EZ-Anesthesia, Euthanex Corporation, Palmer, PA) according to the anesthesia standard operating procedure outlined in the main protocol (2009-06-01). This allowed precise control over the proportion of Isoflurane® (Walden Animal Clinic, Lively, ON) to oxygen (Praxair, Sudbury, ON), which the animals received. Initially, rats were anesthetized at a rate of 5% Isoflurane® in 100% oxygen in an induction chamber until they were unresponsive to toe pinch. They were then transferred to the surgical bed where their snouts were placed into a nose cone which delivered 1.5-2% Isoflurane® in 100% oxygen. Here the plane of anesthesia was maintained by testing with toe pinches while the animal received the injection. After the administration of the IP injection, rats were removed from the nose cone and placed back into their appropriately labelled cages, where they were monitored until they completely recovered from anesthesia. On the day of the experiment, rats were again anesthetized according to the procedure above, and were maintained at 1.5-2% Isoflurane® in 100% oxygen for the duration of all experimental procedures. Rat body temperature was

maintained between 36-37°C using a heating lamp, and regular checks of the depth of anesthesia were performed by toe pinches and by monitoring respiration rates. The carotid artery was isolated and cannulated for arterial blood sampling and patency was maintained by periodic flushing with 0.3 mL of heparinized saline.

3.3 Experimental Protocol

Animals were maintained at 1.5-2% Isoflurane® in 100% oxygen for a four hour period. The first hour constituted the equilibration period, where the animal's plane of anesthesia was monitored and any systemic changes incurred by the isolation of the carotid artery were allowed to stabilize. Every hour, for the remaining three hour period, 0.3 mL samples of blood were taken from the cannulated carotid artery. Once all blood samples were collected, the rat was euthanized by inducing an overdose of Isoflurane®. This was accomplished by increasing the percentage of Isoflurane® in 100% oxygen until the animal's breathing was arrested. This was followed by immediate decapitation in order to ensure the animal would not recover.

3.4 Post-experimental Protocol

3.4.1 Blood Samples

Once a blood sample was removed from the cannulated artery, it was transferred from the sample syringe to a vial and immediately centrifuged (15,000 rpm) to separate the formed elements from the plasma. The plasma was then removed from the sample and placed in a separate vial. Both the blood pellet and plasma vial were then placed on ice and upon completion of the experiment all samples were stored at -80°C until analyzed.

3.4.2 Tissue Samples

Once the animal was euthanized, it was returned to the surgical bed where the heart and liver were removed and weighed. Tissues were then appropriately packaged and immediately placed on ice. Upon completion of the experiment samples were stored at -80°C until analyzed.

3.5 Analysis

3.5.1 High Performance Liquid Chromatography (HPLC)

3.5.1.1 Plasma Samples

Samples were removed from the -80°C freezer, and allowed to thaw. 100 µL of plasma was added to 133 µL of a 50/50 40% zinc/100% methanol solution containing 0.625 µM DNR as an internal standard (Appendix I). This mixture was vortexed for 2 minutes using an eppendorf® Thermomixer R at a temperature of 4°C. The samples were then centrifuged at 13,000 rpm for 10 minutes. 100 µL of supernatant was placed into an HPLC vial and analyzed.

3.5.1.2 Heart Tissue Samples

For each rat, the whole frozen heart was removed from the -80°C freezer and was quartered into left and right atria and ventricles. Each chamber was sectioned into thirds, and one of these thirds of the left ventricle was sectioned into a 30-50 mg sample. This sample was then homogenized using a Qiagen TissueLyser® system for a total of four minutes. A 0.067 M potassium phosphate solution containing 0.625 µM DNR as an internal standard was the primary extraction solution. To ensure sample consistency, the volume of extraction solution used was proportional to the size of the tissue sample. Therefore a concentration of 100 mg of tissue per 1.0 mL was calculated for every sample. 150 µL of the homogenate was added to 200 µL of the

50/50 40% zinc/100% methanol solution. This mixture was vortexed and centrifuged as described above and 100 µL of supernatant was placed into an HPLC vial and analyzed.

3.5.1.3 Liver Tissue Samples

For each rat, the whole frozen liver was removed from the -80°C freezer. Without being allowed to thaw completely, a 30-50 mg sample was removed from the anterior lobe. This sample was then homogenized using the same method and primary extraction solution as above. Similar to the processing for the heart tissue samples, a concentration of 100 mg of tissue per 1.0 mL was maintained for every sample. 150 µL of the homogenate was added to 200 µL of the 50/50 40% zinc/100% methanol solution. This mixture was vortexed and centrifuged as described above. Again, 100 µL of supernatant was placed into an HPLC vial and analyzed.

3.5.1.4 HPLC Analysis

HPLC analysis was performed using a Waters HPLC System with a reversed phase ACE-CN 250x4.6 mm column and fluorescence detection at 480 nm excitation and 560 nm emission. HPLC eluents were set at a flow rate of 1mL/min using a gradient method and an injection volume of 80 µL was used for all standards and samples (Appendix I).

Empower 2 Software was used to calculate standard curves of Area vs. Concentration. The software also integrated the resulting sample chromatographs and provided the area for DOX, DOXOL and DNR, from which the concentration of each component was calculated. In order to achieve the final concentration of each component within the sample, the values obtained were corrected to account for any loss of sample during preparation by the use of an internal standard

(DNR). Dilution factors were also taken into consideration and the values were adjusted accordingly.

3.5.2 Histological Fluorescence Examination

3.5.2.1 Slide Preparation

Histological slides were prepared using a frozen tissue cutting method. Using the Leica® CM3050 S cryostat system, samples of the right ventricle of the heart and the anterior lobe of the liver, previously embedded in Tissue-Tek® O.C.T. Compound (Sakura Finetek USA), were manually sectioned at a 30 µm thickness and placed on VWR® Superfrost® Plus Micro Slides (Figure 12). VWR® Cover slips were then mounted with approximately 10-12 µL of Vectashield® Fluorescence Mounting Medium with DAPI (Vector Laboratories Inc.), and the edges were sealed with clear nail polish. Leica® suggestions for optimal cryostat and object temperatures were used for both tissue types. It is important to note that sections from the right ventricle and not the left were used for preparation of histological slides. Though it would have been preferable to use sections from the left ventricle, there was the fear of not having enough sample of left ventricle to run both HPLC analysis and histological analysis, therefore the right ventricle was used as an alternative.

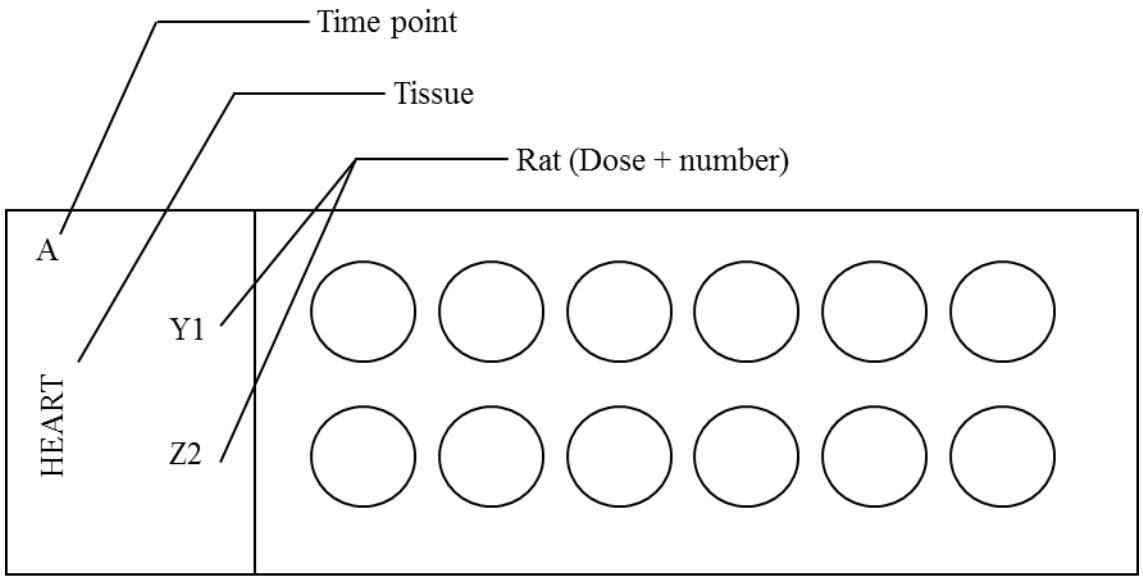

Figure 12: Slide layout example. Slide of heart tissue prepared for rats AY1 (24 hrs, 1.5 mg/kg) and AZ2 (24 hrs, 4.5 mg/kg). Each slide contained samples from; one tissue type (heart or liver), one time point, and one rat from each dose.

3.5.2.2 Fluorescence Microscopy

Histological slides were observed using a Nikon Eclipse 90i Fluorescence Microscope with QImaging Retiga EXi camera and two computer software programs. First, iControl© software was used to bring the slide into focus and allow for manual observation of the prepared slide. Second, SimplePCI 6 ©1995-2005 was used to allow computer observation of the slide as well as to perform capture and adjustment of the image. Once the section was brought into focus at 40X magnification, it was captured under two different fluorescence filters, DAPI (440 nm, 40 nm bandwidth) and TRITC (590 nm, 34 nm bandwidth). This was repeated for each section. Contrast settings were adjusted identically for all heart images (DAPI Low: 1, High: 255 and TRITC Low: 0, High: 30), in order to distinguish any changes in fluorescence from the control image, between doses or between time points. The same was done for liver images (DAPI Low: 1, High: 255 and TRITC Low: 0, High: 70). Hence, a qualitative determination of DOX concentration in both tissues of interest was made.

3.6 Statistics

Statistical analysis and figure preparation of HPLC data were performed using GraphPad InStat 3 and GraphPad Prism 4 software. Outliers were calculated and removed from each data set, and the number of animals was adjusted to reflect this change. Any sample with an undetectable reading from HPLC analysis was re-analyzed and if the value was detectable, this value was incorporated into the data set. If however the reading remained undetectable it was designated a value of zero and was still included in mean calculations and therefore in statistical analyses. Using the adjusted raw data, the mean concentration for each group was calculated (in μmol/kg for tissue samples and in nmol/L for plasma samples) and it was this value that was used in all statistical analyses. Comparisons between experimental groups were performed. For each tissue individually, comparisons of concentrations between each time point for a specific dose were done using ANOVAs and comparisons of concentrations between doses at each specific time point were done using un-paired t-tests. Comparisons of concentration between heart and liver tissue at each time point were done using un-paired t-tests also. Finally, comparisons of experimental groups to control groups were accomplished by using one-sample t-tests. For all analyses, significance was defined as $p<0.05$ and all values were expressed as mean ± standard error of the mean.

Supplementary methods are shown in Appendix I.

Chapter 4: Results

HPLC quantification was performed on samples extracted from control animals to ensure that no other endogenous substance had the same retention time as DOX, DOXOL or DNR. All values for control samples were undetectable by HPLC, and were therefore designated a value of zero as described in the Chapter 3, Section 3.6.

4.1 HPLC Analysis

4.1.1 Plasma Samples – Doxorubicin

All concentrations of DOX measured at both doses were elevated ($p<0.05$) as compared to controls except at the 1.5 mg/kg dose at 48 hours post-injection, which was only approaching significance. At the 1.5 mg/kg dose, the concentration of DOX in the plasma was relatively stable over the 192 hour period with a spike in concentration at 96 hours (41.45 ± 17.95 nmol/L) that was greater ($p<0.05$) than values measured at 24, 72, 120, 144 and 168 hours (4.06 ± 0.22 nmol/L, 1.92 ± 0.14 nmol/L, 1.50 ± 0.10 nmol/L, 0.95 ± 0.18 nmol/L, 1.91 ± 0.33 nmol/L, respectively). At the 4.5 mg/kg dose, there were no statistically significant differences between the post-injection time points. However, there was a slight increase in concentration at the 96 hour period, thus a similar pattern was observable for both doses, though for the higher dose these differences were not as extreme.

When comparisons between doses were made, the DOX concentrations at the 4.5 mg/kg dose were greater ($p<0.05$) than at the 1.5 mg/kg dose at 24 hours (12.06 ± 2.21 nmol/L vs. 4.06 ± 0.22 nmol/L, respectively), 72 hours (11.69 ± 1.99 nmol/L vs. 1.92 ± 0.14 nmol/L, respectively),

120 hours (4.33 ± 0.29 nmol/L vs. 1.50 ± 0.10 nmol/L, respectively) and 144 hours (7.49 ± 0.84 nmol/L vs. 0.95 ± 0.18 nmol/L, respectively) (Table 2).

4.1.2 Plasma Samples – Doxorubicinol

All concentrations of DOXOL measured at both doses were significantly greater than controls. Though there were significant decreases between 24 hours (1.02 ± 0.14 nmol/L) and 72, 120 and 192 hours (0.63 ± 0.07 nmol/L, 0.61 ± 0.06 nmol/L and 0.60 ± 0.19 nmol/L, respectively) at the 1.5 mg/kg dose, the concentrations remained relatively constant over time. At the 4.5 mg/kg dose this consistency was even more evident as there were no differences in concentration between time points. The 4.5 mg/kg dose produced greater concentrations ($p<0.05$) of DOXOL at 48 (0.64 ± 0.06 nmol/L at 1.5 mg/kg and 4.77 ± 3.41 nmol/L at 4.5 mg/kg) and 72 hours (0.63 ± 0.07 nmol/L at 1.5 mg/kg and 0.99 ± 0.13 nmol/L at 4.5 mg/kg) (Table 3).

Table 2: Doxorubicin concentrations (in nmol/L) in plasma samples

Dose (mg/kg)	Time post-injection (hours)							
	24	48	72	96	120	144	168	192
1.5	ᵅ4.06 ± 0.22	5.99 ± 3.51	ᵅ1.92 ± 0.14	41.45 ± 17.95	ᵅ1.50 ± 0.10	ᵅ0.95 ± 0.18	ᵅ1.91 ± 0.33	20.34 ± 7.55
4.5	*12.16 ± 2.21	7.00 ± 0.53	*11.69 ± 1.99	29.09 ± 15.80	*4.33 ± 0.29	*7.49 ± 0.84	2.37 ± 0.44	3.68 ± 0.44

Data are presented as mean ± SEM. * Denotes significant difference ($p<0.05$) between doses at each time point. ᵅ Denotes significant difference from 96 hours. Although not indicated, all values were significantly different from controls.

Table 3: Doxorubicinol concentrations (in nmol/L) in plasma samples

Dose (mg/kg)	Time post-injection (hours)							
	24	48	72	96	120	144	168	192
1.5	1.02 ± 0.14	0.64 ± 0.06	ᵅ0.63 ± 0.07	0.88 ± 0.11	ᵅ0.61 ± 0.06	0.73 ± 0.13	0.75 ± 0.06	ᵅ0.60 ± 0.19
4.5	1.26 ± 0.17	*4.77 ± 3.41	*0.99 ± 0.13	1.01 ± 0.13	0.93 ± 0.39	0.71 ± 0.20	0.59 ± 0.12	0.49 ± 0.13

Data are presented as mean ± SEM. * Denotes significant difference ($p<0.05$) between doses at each time point. ᵅ Denotes significant difference from 24 hours. Although not indicated, all values were significantly different from controls.

4.1.3 Liver Tissue Samples – Doxorubicin

At the 1.5 mg/kg dose, liver DOX concentrations initially decreased from 2.79 ± 0.46 µmol/kg at 24 hours to 0.57 ± 0.12 µmol/kg at 96 hours ($p<0.05$). The concentration of DOX then increased from 96 hours to 2.89 ± 0.60 µmol/kg at 120 hours ($p<0.05$). Although the subsequent decrease to 1.04 ± 0.13 µmol/kg at 144 hours was not significant, the increase measured from 144 hours to 4.15 ± 1.52 µmol/kg at 168 hours was. After 168 hours, the concentration dramatically decreased to 0.78 ± 0.07 µmol/kg at 192 hours ($p<0.05$). At all time points this dose was elevated as compared to controls ($p<0.05$) and the overall decrease of 2.01 ± 0.26 µmol/kg DOX concentration between 24 and 192 hours, although not statistically significant, was observed to be marked (Figure 13).

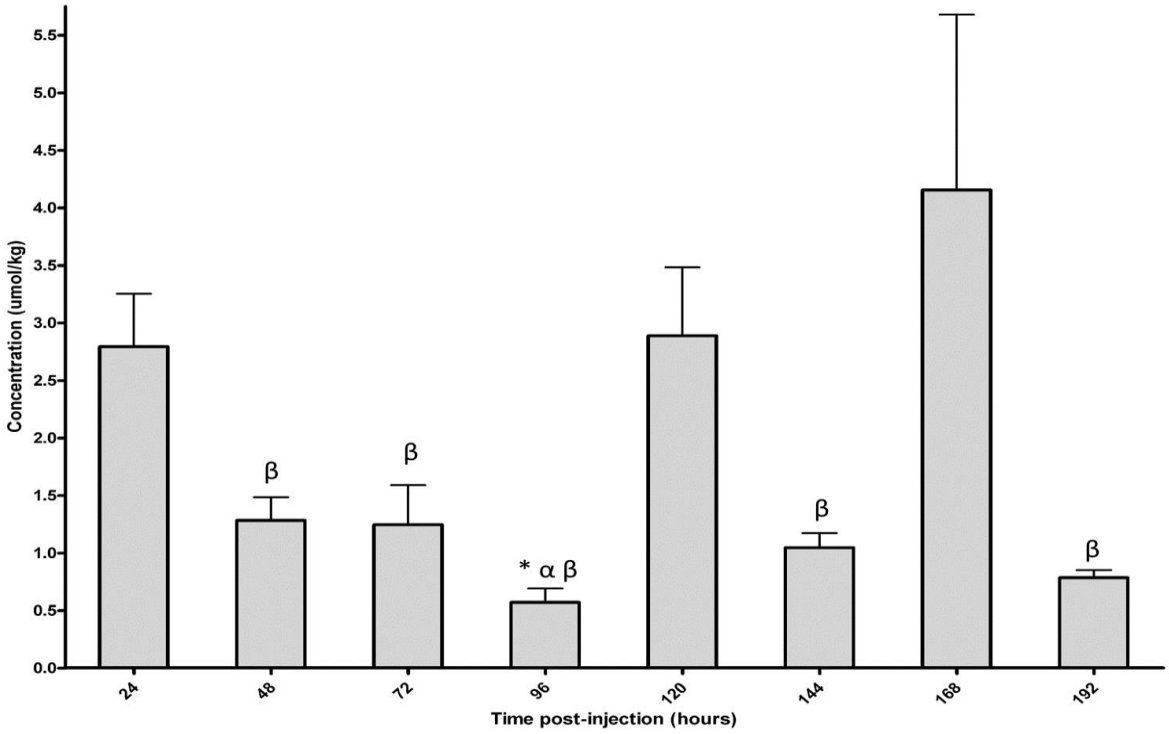

Figure 13: Liver doxorubicin concentrations after 1.5 mg/kg dose administration. Data are presented as mean ± SEM. * Denotes significant difference ($p<0.05$) from 24 hours post-injection. $^{\alpha}$ Denotes significant difference ($p<0.05$) from 120 hours post-injection. $^{\beta}$ Denotes significant difference ($p<0.05$) from 168 hours post-injection. Although not indicated, all values were significantly different from controls.

At the 4.5 mg/kg dose, liver concentrations of DOX were unchanged until 192 hours post-injection (0.74 ± 0.23 µmol/kg). Although the concentration did decrease between 24 and 48 hours (6.62 ± 0.93µmol/kg and 3.58 ± 0.68 µmol/kg respectively), and seemingly increased between 120 hours and 144 hours (2.90 ± 0.82 and 5.54 ± 1.25 µmol/kg respectively), only the decreases between 24 hours and 192 hours and between 144 hours and 192 hours were significant. At all time points this dose was elevated compared to controls ($p<0.05$) and the overall DOX concentration decreased by 5.89 ± 0.58 µmol/kg between 24 and 192 hours ($p<0.05$) (Figure 14).

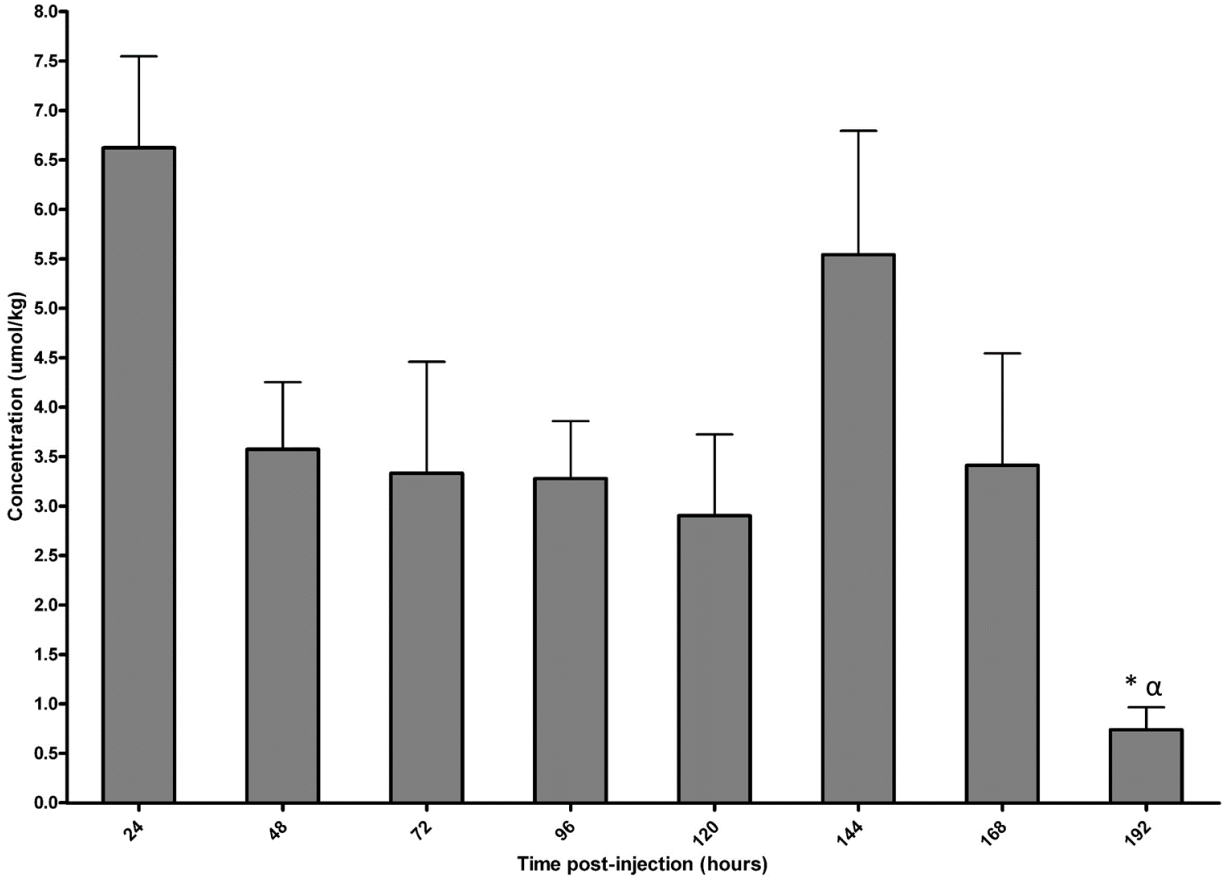

Figure 14: Liver doxorubicin concentrations after 4.5 mg/kg dose administration. Data are presented as mean ± SEM. * Denotes significant difference ($p<0.05$) from 24 hours post-injection. α Denotes significant difference ($p<0.05$) from 144 hours post-injection. Although not indicated, all values were significantly different from controls.

Upon comparison of both doses, it was found that the concentration of DOX in the liver was greater at the 4.5 mg/kg dose than the 1.5 mg/kg dose at 24 hours (6.62 ± 0.93 vs. 2.79 ± 0.46 µmol/kg, respectively), 48 hours (3.58 ± 0.68 vs. 1.28 ± 0.20 µmol/kg, respectively), 96 hours (3.28 ± 0.58 vs. 0.57 ± 0.12 µmol/kg, respectively) and 144 hours (5.54 ± 1.25 vs. 1.04 ± 0.13 µmol/kg, respectively) ($p<0.05$) (Figure 15).

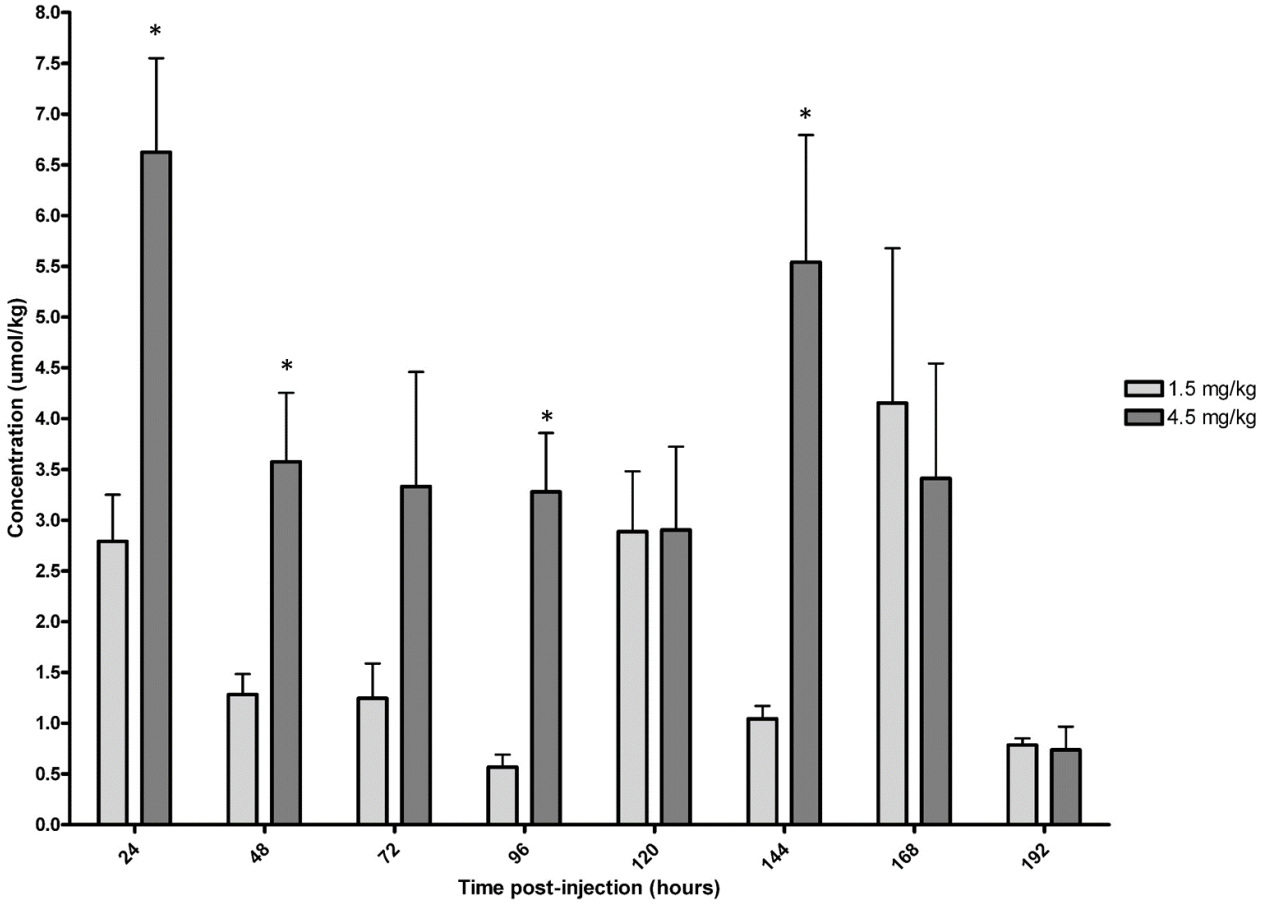

Figure 15: Liver doxorubicin concentrations for both doses. Data are presented as mean ± SEM. * Denotes significant difference ($p<0.05$) between doses. Although not indicated, all values were significantly different from controls.

4.1.4 Liver Tissue Samples – Doxorubicinol

Following injection at the 1.5 mg/kg dose, there was an increase from 0.10 ± 0.02 µmol/kg at 24 hours to 0.71 ± 0.25 µmol/kg at 168 hours ($p<0.05$). The concentration subsequently decreased from 168 hours to 0.19 ± 0.04 µmol/kg at 192 hours ($p<0.05$). At all time points this dose was also elevated as compared to controls ($p<0.05$) and there were no differences between the concentrations measured at 24 and 192 hours post-injection (Figure 16).

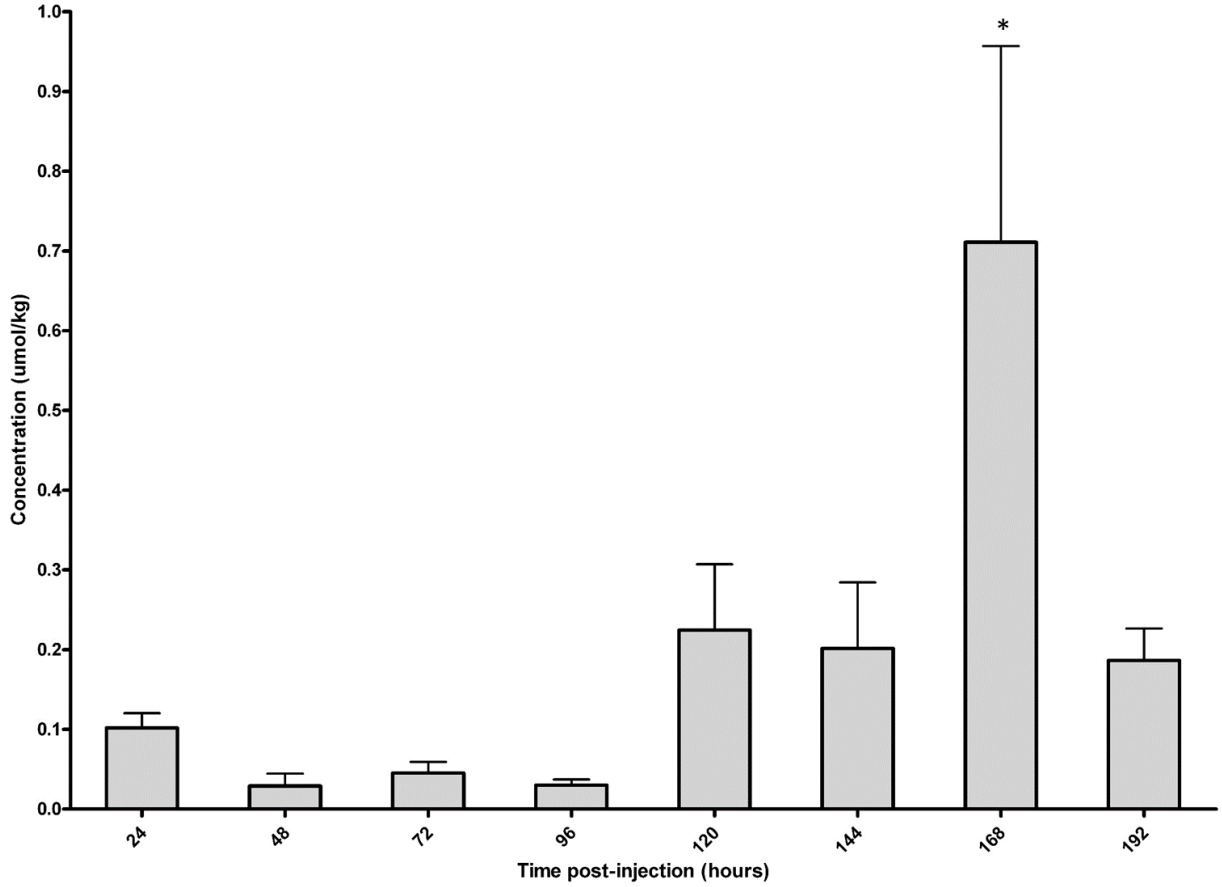

Figure 16: Liver doxorubicinol concentrations after 1.5 mg/kg dose administration. Data are presented as mean ± SEM. * Denotes significant difference ($p<0.05$) from all other time points. Although not indicated, all values were significantly different from controls.

Similarly, at the 4.5 mg/kg dose, the concentration of DOXOL remained stable between 24 hours (0.12 ± 0.02 µmol/kg) and 144 hours (0.13 ± 0.05 µmol/kg) after which it increased to 0.58 ± 0.17 µmol/kg at 168 hours ($p<0.05$) and remained elevated at 192 hours (0.34 ± 0.10 µmol/kg). At all time points this dose was elevated as compared to controls ($p<0.05$) and there were no differences between the concentrations measured at 24 hours and 192 hours post-injection (Figure 17).

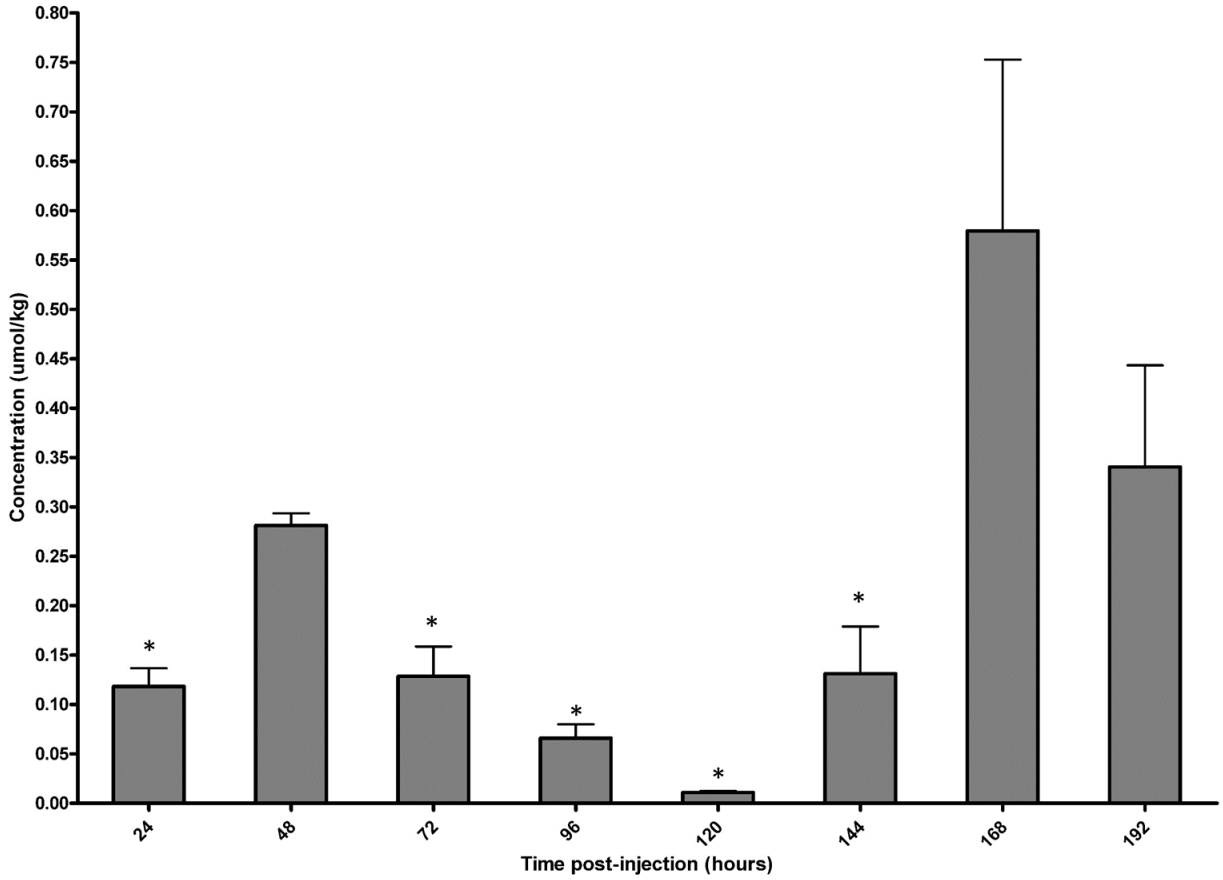

Figure 17: Liver doxorubicinol concentrations after 4.5 mg/kg dose administration. Data are presented as mean ± SEM. * Denotes significant difference ($p<0.05$) from 168 hours post-injection. Although not indicated, all values were significantly different from controls.

Upon comparison of both doses, it was found that the concentration of DOXOL in the liver was greater at the 4.5 mg/kg dose than the 1.5 mg/kg dose at 48 hours (0.28 ± 0.01 vs. 0.03 ± 0.02 µmol/kg, respectively), 72 hours (0.13 ± 0.03 vs. 0.05 ± 0.01 µmol/kg, respectively) and 96 hours (0.07 ± 0.01 and 0.03 ± 0.01 µmol/kg respectively) ($p<0.05$). Conversely, the concentration of DOXOL was greater at the 1.5 mg/kg dose than the 4.5 mg/kg dose at 120 hours (0.22 ± 0.08 vs. 0.01 ± 0.00 µmol/kg, respectively) ($p<0.05$) (Figure 18).

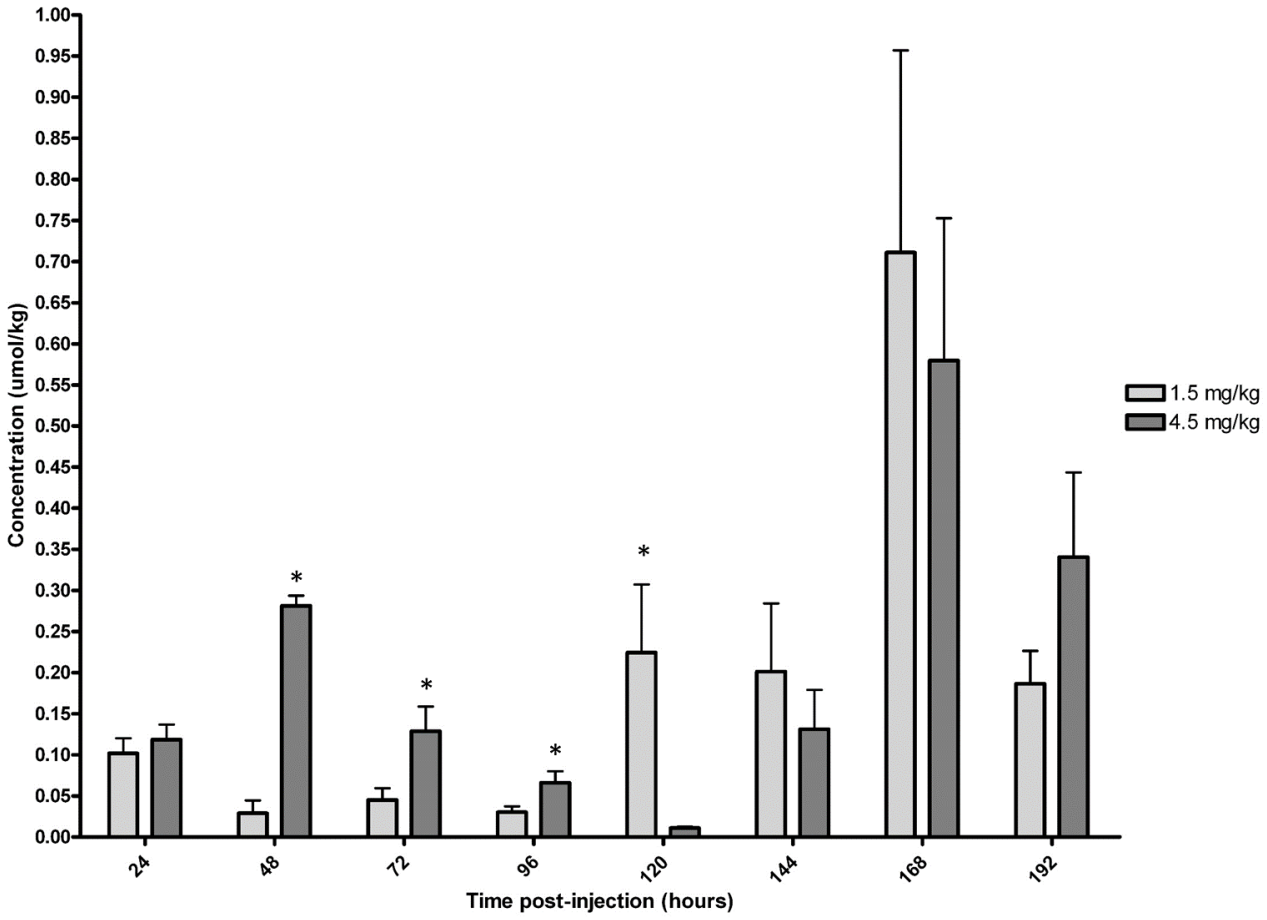

Figure 18: Liver doxorubicinol concentrations for both doses. Data are presented as mean ± SEM. * Denotes significant difference ($p<0.05$) between doses. Although not indicated, all values were significantly different from controls.

4.1.5 Heart Tissue Samples – Doxorubicin

At the 1.5 mg/kg dose, DOX concentrations decreased from 0.84 ± 0.09 µmol/kg at 24 hours to 0.32 ± 0.05 µmol/kg at 48 hours ($p<0.05$) after which, no further significant changes in DOX concentrations were observed. At all time points this dose resulted in elevated DOX concentrations in heart tissue as compared to controls ($p<0.05$) and an overall decrease of 0.57 ± 0.10 µmol/kg from 24 hours to 192 hours was observed ($p<0.05$) (Figure 19).

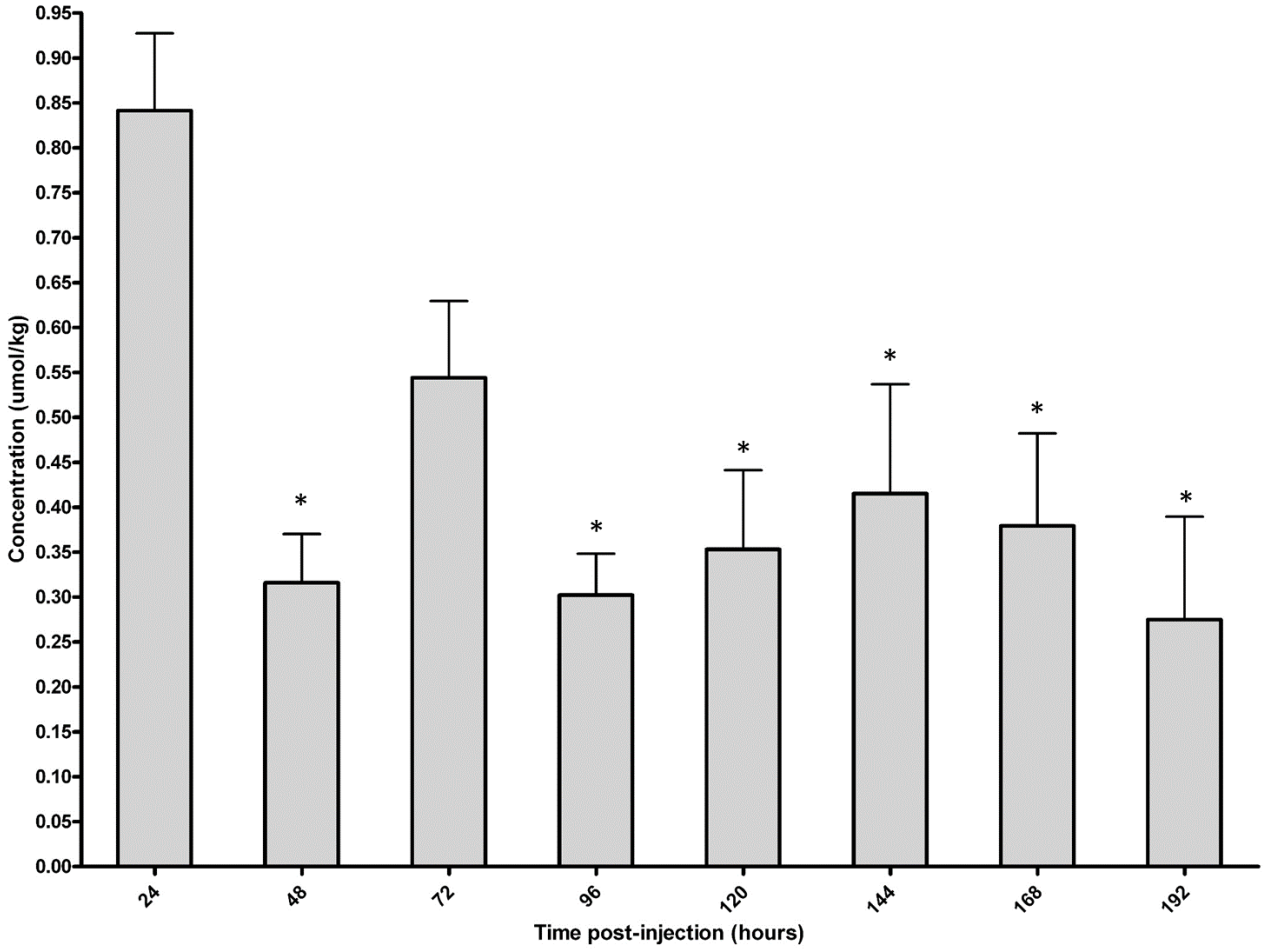

Figure 19: Heart doxorubicin concentrations after 1.5 mg/kg dose administration. Data are presented as mean ± SEM. * Denotes significant difference ($p<0.05$) from 24 hours post-injection. Although not indicated, all values were significantly different from controls.

At the 4.5 mg/kg dose, an initial decrease from 1.94 ± 0.27 µmol/kg at 24 hours to 1.02 ± 0.07 µmol/kg at 72 hours ($p<0.05$) was observed in DOX concentrations, followed by a steady decrease in DOX throughout the remainder of the experiment. Decreases ($p<0.05$) were also noted between 48 hours (1.23 ± 0.13 µmol/kg) and 168 hours (0.34 ± 0.08 µmol/kg) and between 48 hours and 192 hours (0.30 ± 0.03 µmol/kg). At all time points this dose was elevated as compared to controls ($p<0.05$) and the concentration decreased by 1.64 ± 0.15 µmol/kg over the 192 hour duration of the experiment ($p<0.05$) (Figure 20).

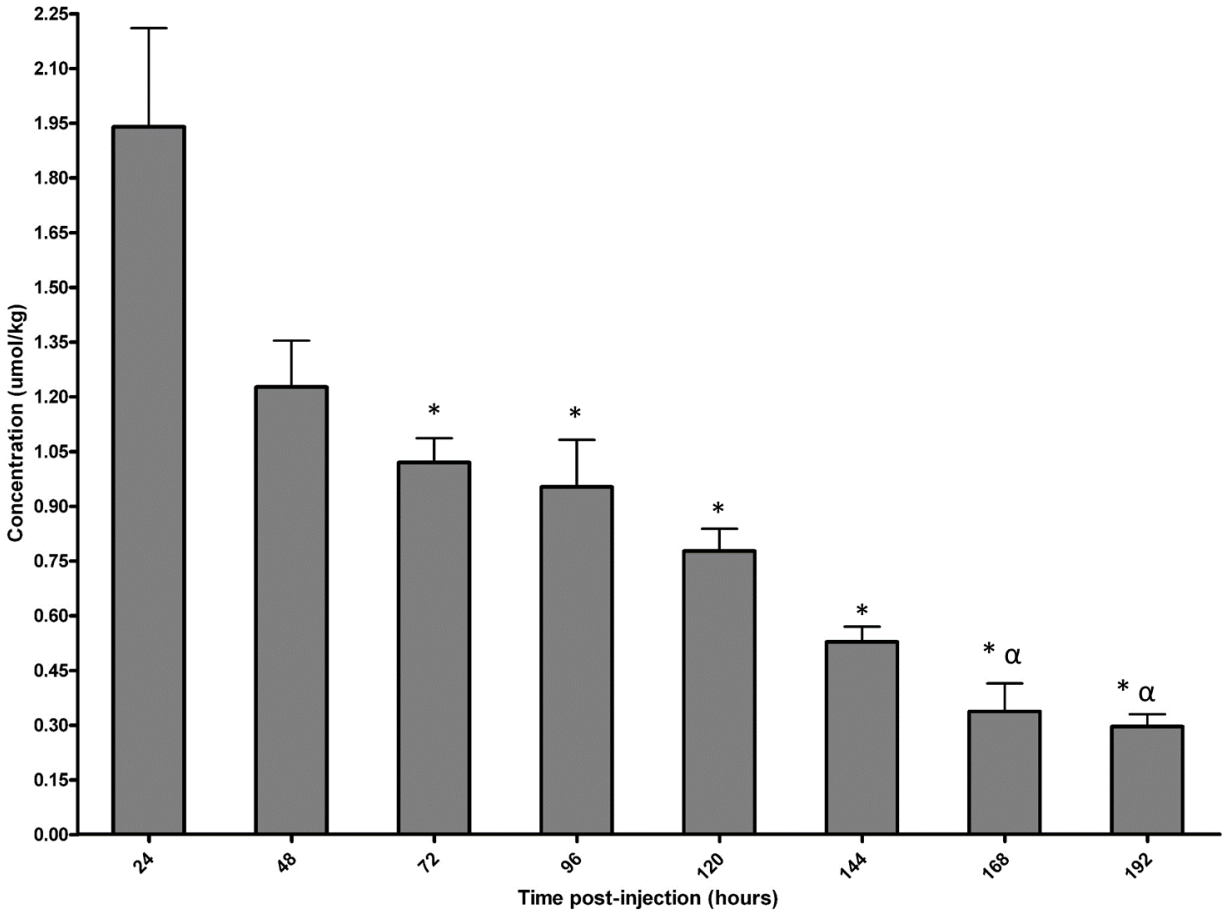

Figure 20: Heart doxorubicin concentrations after 4.5 mg/kg dose administration. Data are presented as mean ± SEM. * Denotes significant difference ($p<0.05$) from 24 hours post-injection. $^{\alpha}$ Denotes significant difference ($p<0.05$) from 48 hours post-injection. Although not indicated, all values were significantly different from controls.

Upon comparison of both doses, it was found that the concentration of DOX in the heart was greater at the 4.5 mg/kg dose than the 1.5 mg/kg dose at 24 hours (1.94 ± 0.27 vs. 0.84 ± 0.09 µmol/kg, respectively), 48 hours (1.23 ± 0.13 vs. 0.32 ± 0.05 µmol/kg, respectively), 72 hours (1.02 ± 0.07 vs. 0.54 ± 0.09 µmol/kg, respectively), 96 hours (0.95 ± 0.13 vs. 0.30 ± 0.05 µmol/kg, respectively) and 120 hours (0.78 ± 0.06 vs. 0.35 ± 0.09 µmol/kg, respectively) ($p<0.05$), although for the last three time points, there were no differences between the concentrations measured at each dose (Figure 21).

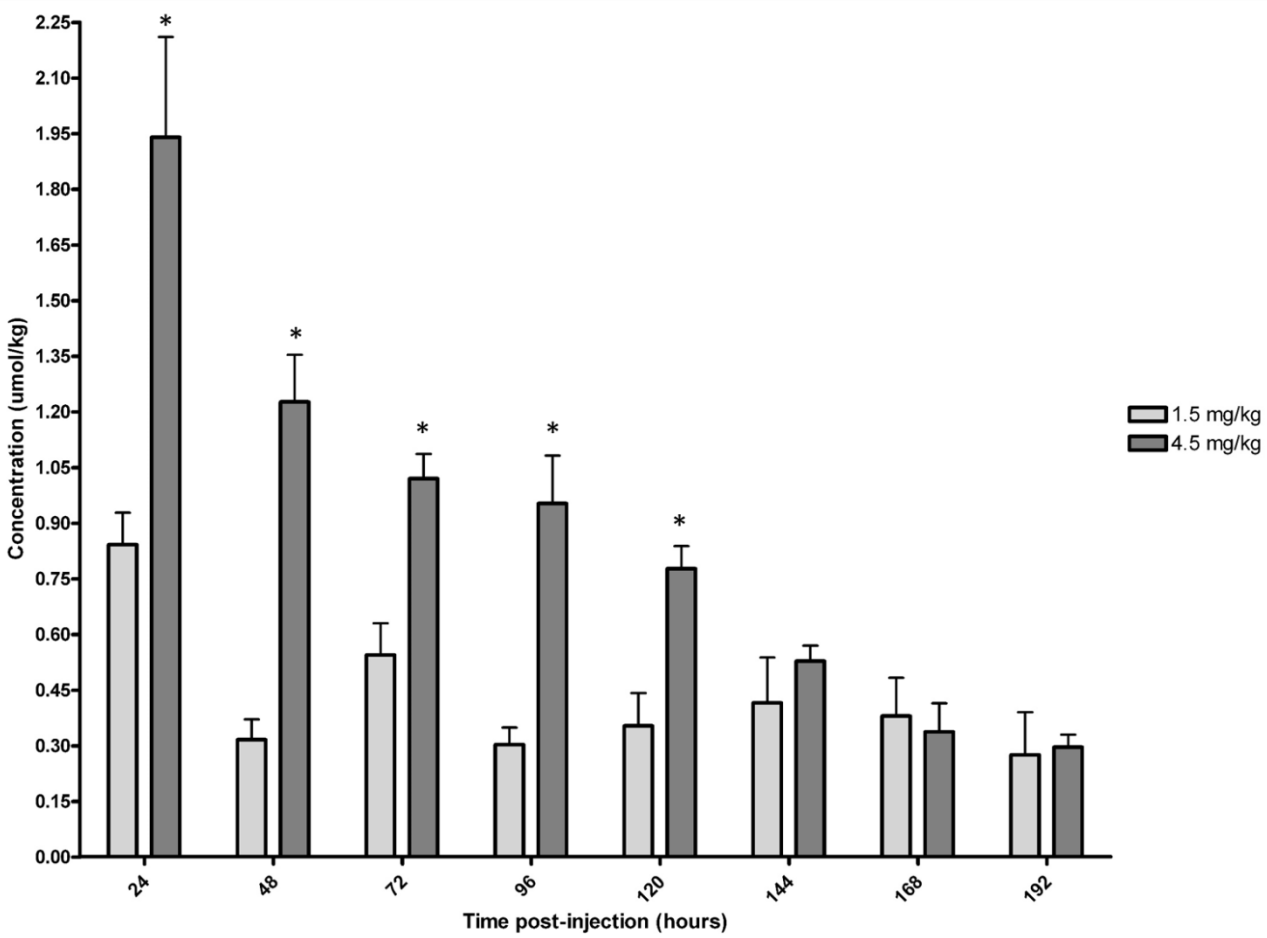

Figure 21: Heart doxorubicin concentrations for both doses. Data are presented as mean ± SEM. * Denotes significant difference ($p<0.05$) between doses. Although not indicated, all values were significantly different from controls.

4.1.6 Heart Tissue Samples – Doxorubicinol

At the 1.5 mg/kg dose, there was a non-significant increase in DOXOL concentration between 0.02 ± 0.003 µmol/kg at 24 hours and 0.10 ± 0.05 µmol/kg at 72 hours. Although this increase was not significant, the subsequent decrease from 72 hours to 96 hours (0.01 ± 0.002 µmol/kg) was ($p<0.05$). Following this point, the DOXOL concentration no longer varied, remaining elevated until 192 hours (0.03 ± 0.007 µmol/kg) ($p<0.05$). At all time points this dose was elevated as compared to controls ($p<0.05$) and the concentration change between 24 and 192 hours was not significant (Figure 22).

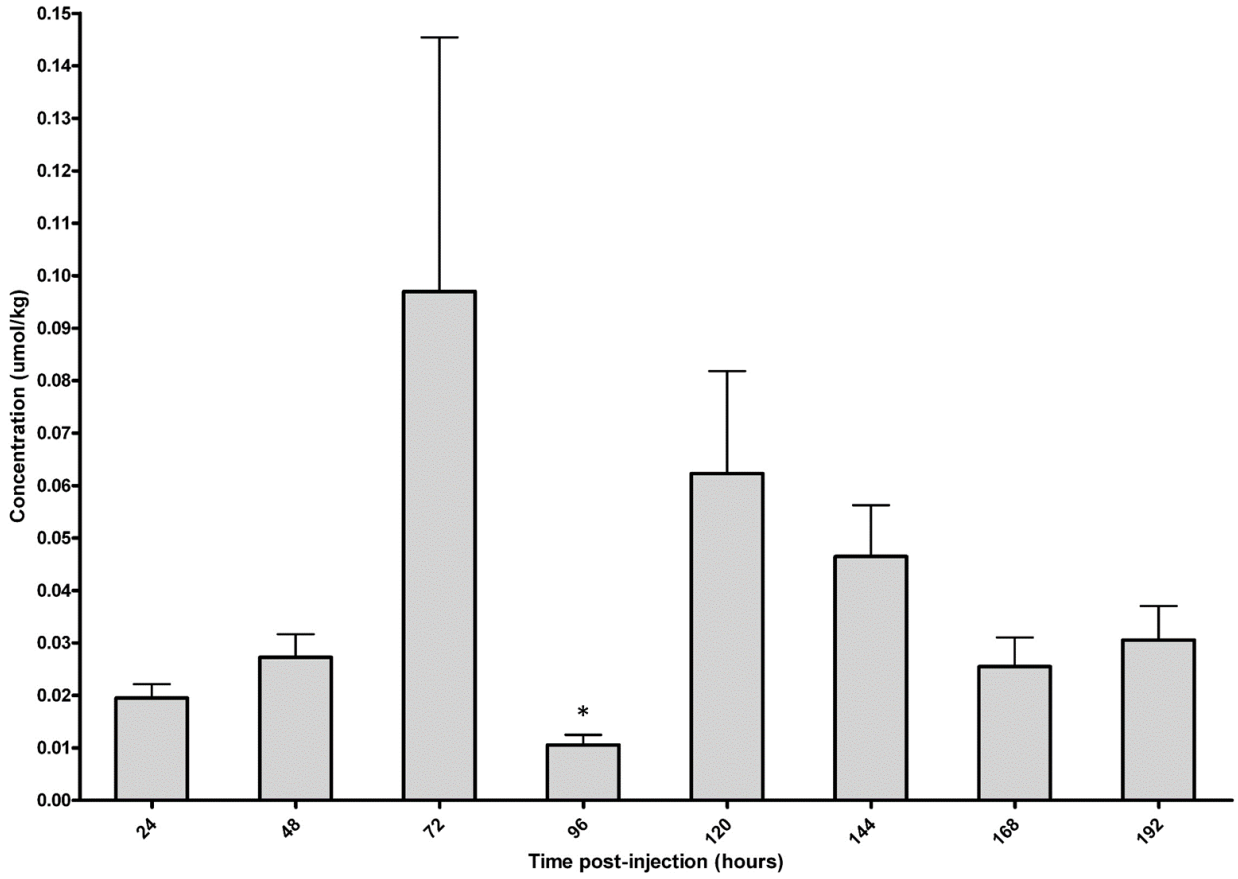

Figure 22: Heart doxorubicinol concentrations after 1.5 mg/kg dose administration. Data are presented as mean ± SEM. * Denotes significant difference ($p<0.05$) from 72 hours post-injection. Although, not indicated, all values were significantly different from controls.

At the 4.5 mg/kg dose, the increase in DOXOL concentration between 0.06 ± 0.01 µmol/kg at 24 hours and 0.13 ± 0.02 µmol/kg at 72 hours as well as the subsequent decrease to 0.04 ± 0.008 µmol/kg at 96 hours were significant ($p<0.05$). A secondary increase then occurred between 96 hours and 144 hours (0.10 ± 0.03 µmol/kg) ($p<0.05$). The following decrease to 0.03 ± 0.01 µmol/kg at 192 hours was not significant from the 144 hour concentration, though it was significantly lower ($p<0.05$) than the DOXOL concentration at 72 hours post-injection. At all time points this dose was elevated as compared to controls ($p<0.05$) and the concentration change between 24 and 192 hours was not significant (Figure 23).

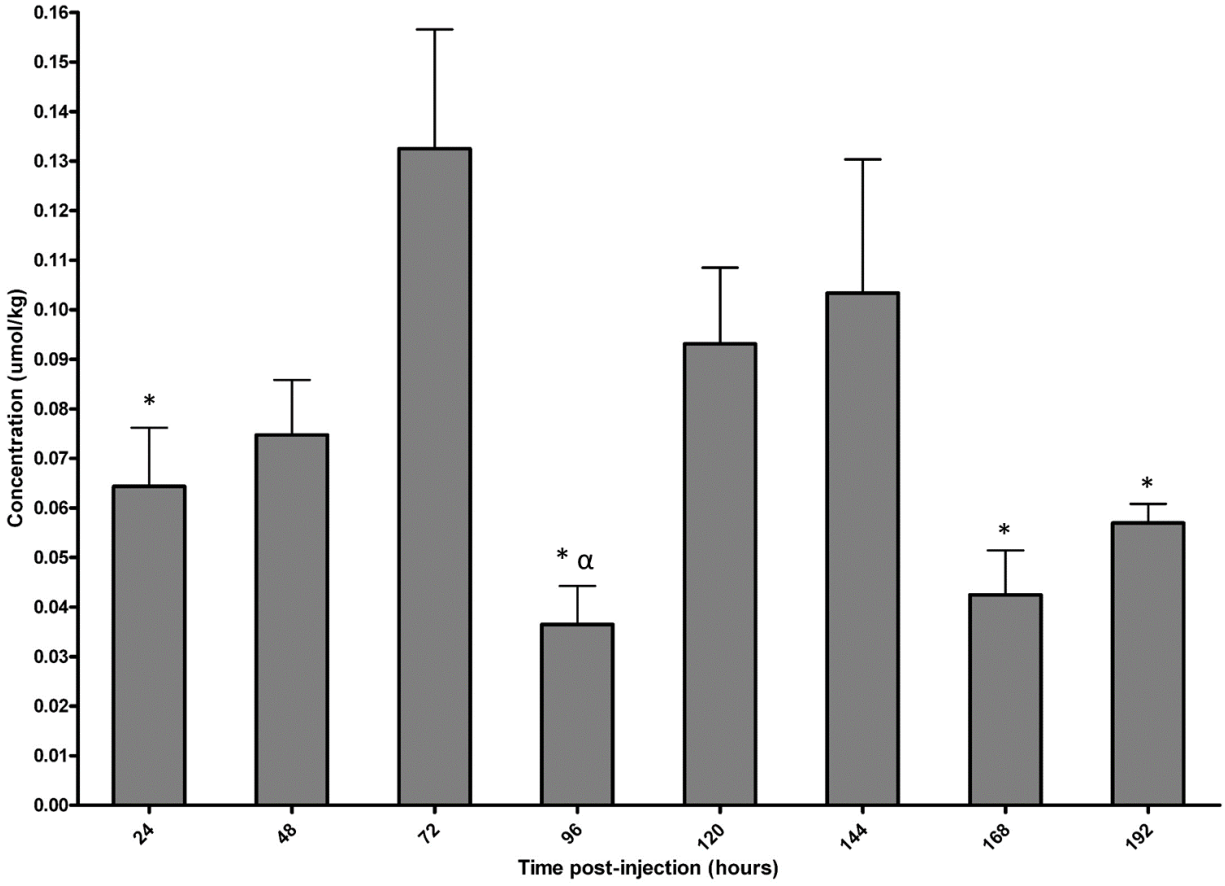

Figure 23: Heart doxorubicinol concentrations after 4.5 mg/kg dose administration. Data are presented as mean ± SEM. * Denotes significant difference ($p<0.05$) from 72 hours post-injection. α Denotes significant difference ($p<0.05$) from 144 hours post-injection. Although not indicated, all values were significantly different from controls.

Upon comparison of both doses, it was found that the concentration of DOXOL in the heart was greater at the 4.5 mg/kg dose than the 1.5 mg/kg dose at 24 hours (0.06 ± 0.01 vs. 0.02 ± 0.003 µmol/kg, respectively), 48 hours (0.08 ± 0.01 vs. 0.03 ± 0.004 µmol/kg, respectively), 96 hours (0.04 ± 0.01 vs. 0.01 ± 0.002 µmol/kg, respectively) and 192 hours (0.06 ± 0.004 vs. 0.03 ± 0.007 µmol/kg, respectively) ($p<0.05$) (Figure 24).

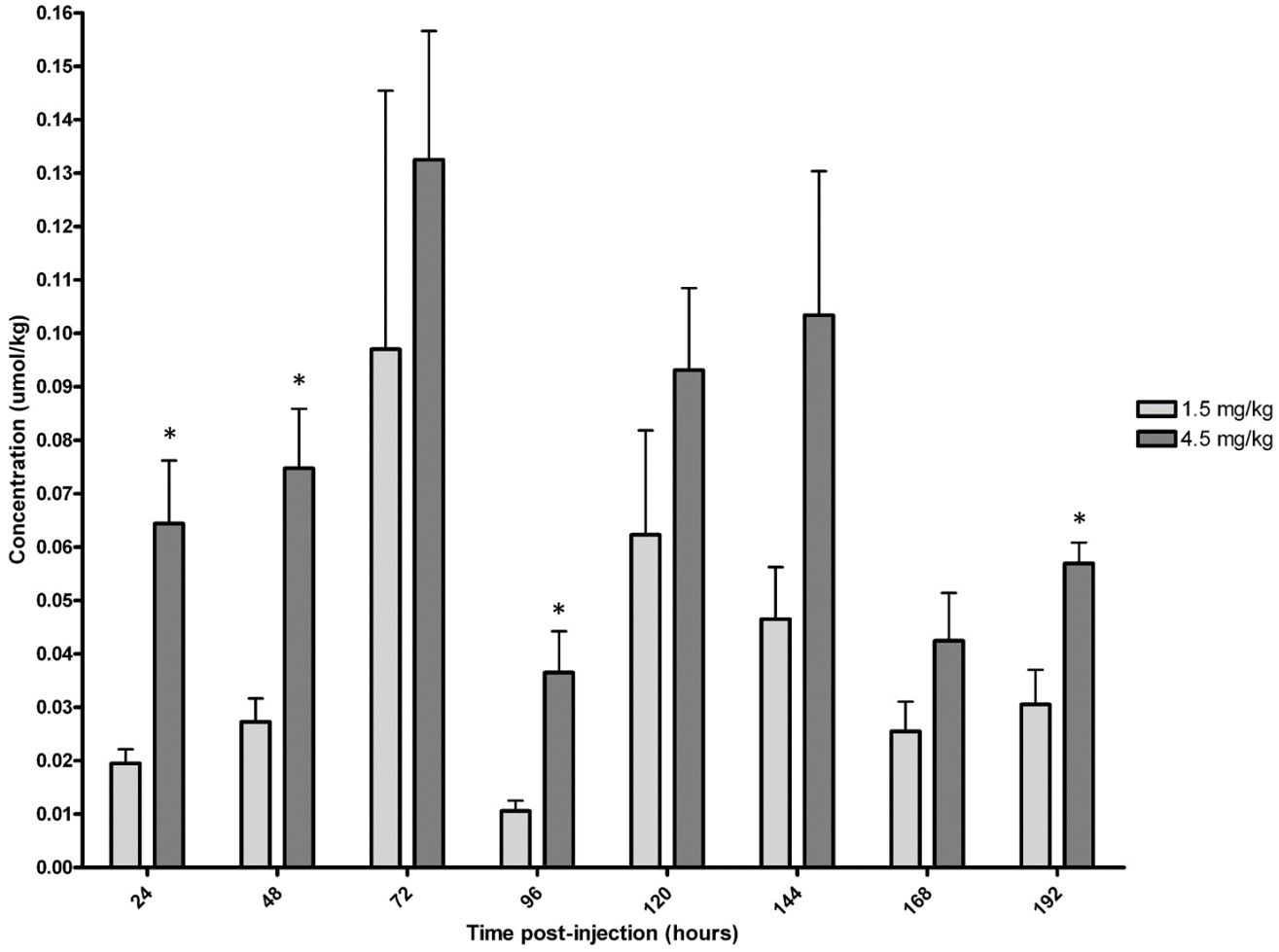

Figure 24: Heart doxorubicinol concentrations for both doses. Data are presented as mean ± SEM. * Denotes significant difference ($p<0.05$) between doses. Although not indicated, all values were significantly different from controls.

4.1.7 Heart vs. Liver

Upon comparison of heart and liver tissue concentrations, DOX was more concentrated ($p<0.05$) in the liver than in the heart at both the 1.5 mg/kg and the 4.5 mg/kg doses. However, at the higher dose, at both 72 and 192 hours post-injection, the concentrations of DOX in the liver, though higher than those in the heart, were not significantly elevated (Table 4).

Furthermore, DOXOL was more concentrated ($p<0.05$) in the liver than in the heart at the 1.5 mg/kg dose, with the exception of 48 hours post-injection, at which point the difference was negligible. Similarly, the DOXOL concentration was greater ($p<0.05$) in the liver than in the heart at the 4.5 mg/kg dose, however in this case there were three exceptions. At 72 and 144 hours, the difference between heart and liver concentrations was negligible. Whereas at 120 hours, the DOXOL concentration in the heart was actually greater ($p<0.05$) than that in the liver (Table 5).

Table 4: Doxorubicin concentrations (in µmol/kg) in tissue samples

		Time post-injection (hours)							
Dose (mg/kg)	Tissue	24	48	72	96	120	144	168	192
1.5	Heart	0.84 ± 0.09	0.32 ± 0.05	0.54 ± 0.09	0.30 ± 0.05	0.35 ± 0.09	0.42 ± 0.12	0.38 ± 0.10	0.28 ± 0.12
	Liver	*2.79 ± 0.46	*1.28 ± 0.20	*1.24 ± 0.34	*0.57 ± 0.12	*2.89 ± 0.60	*1.04 ± 0.13	*4.15 ± 1.52	*0.78 ± 0.07
4.5	Heart	1.94 ± 0.27	1.23 ± 0.13	1.02 ± 0.07	0.95 ± 0.13	0.78 ± 0.06	0.53 ± 0.04	0.34 ± 0.08	0.30 ± 0.03
	Liver	*6.62 ± 0.93	*3.58 ± 0.68	3.33 ± 1.13	*3.28 ± 0.58	*2.90 ± 0.82	*5.54 ± 1.25	*3.41 ± 1.13	0.74 ± 0.23

Data are presented as mean ± SEM. * Denotes higher ($p<0.05$) DOX concentration between the two tissues at each dose. Although not indicated, all values were significantly different from controls.

Table 5: Doxorubicinol concentrations (in µmol/kg) in tissue samples

		Time post-injection (hours)							
Dose (mg/kg)	Tissue	24	48	72	96	120	144	168	192
1.5	Heart	0.02 ± 0.003	0.03 ± 0.004	0.10 ± 0.05	0.01 ± 0.002	0.06 ± 0.02	0.05 ± 0.01	0.03 ± 0.01	0.03 ± 0.01
	Liver	*0.10 ± 0.02	0.03 ± 0.02	*0.05 ± 0.01	*0.03 ± 0.01	*0.22 ± 0.08	*0.20 ± 0.08	*0.71 ± 0.25	*0.19 ± 0.04
4.5	Heart	0.06 ± 0.01	0.08 ± 0.01	0.13 ± 0.03	0.04 ± 0.01	*0.09 ± 0.02	0.10 ± 0.03	0.04 ± 0.01	0.06 ± 0.004
	Liver	*0.12 ± 0.02	*0.28 ± 0.01	0.13 ± 0.03	*0.07 ± 0.01	0.01 ± 0.002	0.13 ± 0.05	*0.58 ± 0.17	*0.34 ± 0.10

Data are presented as mean ± SEM. * Denotes higher ($p<0.05$) DOXOL concentration between the two tissues at each dose. Although not indicated, all values were significantly different from controls.

4.2 Fluorescence Microscopy

It is important to note that analysis of histological slides was purely qualitative and that no definite measure of fluorescence was applied to the images; therefore no statistical analysis was possible. It is also important to note that each of the heart and liver sample images, including control sample images, were normalized as described in Chapter 3, Section 5.2.2. Furthermore, the purpose of assessing fluorescence of the drug was not to determine localization, however images are presented alongside the DAPI filtered image (which fluoresces blue and binds to nucleic acids) in attempts to provide additional insights where possible.

4.2.1 Liver Tissue Samples

For images taken of samples treated with 1.5 mg/kg DOX, fluorescence decreased between 24 and 96 hours followed by a slight increase at 120 hours (Figure 25A), after which fluorescence seemed to remain constant between 144 and 192 hours (Figure 25B). The fluorescence level from 24 hours tended to show a continual decrease over the 192 hour examination period (Figure 25C).

For images taken of samples treated with 4.5 mg/kg DOX, fluorescence greatly increased between 24 and 72 hours, though the distribution of DOX within the tissue appeared to be less localized at the later time point (Figure 26A). Afterwards, fluorescence diminished substantially at 120 hours, followed by a slight increase at 144 hours, and then appeared to decrease yet again at 192 hours (Figure 26B). The decrease in fluorescence intensity over the 192 hour examination period was small but the disappearance of nuclear localization of DOX was substantial (Figure 26C).

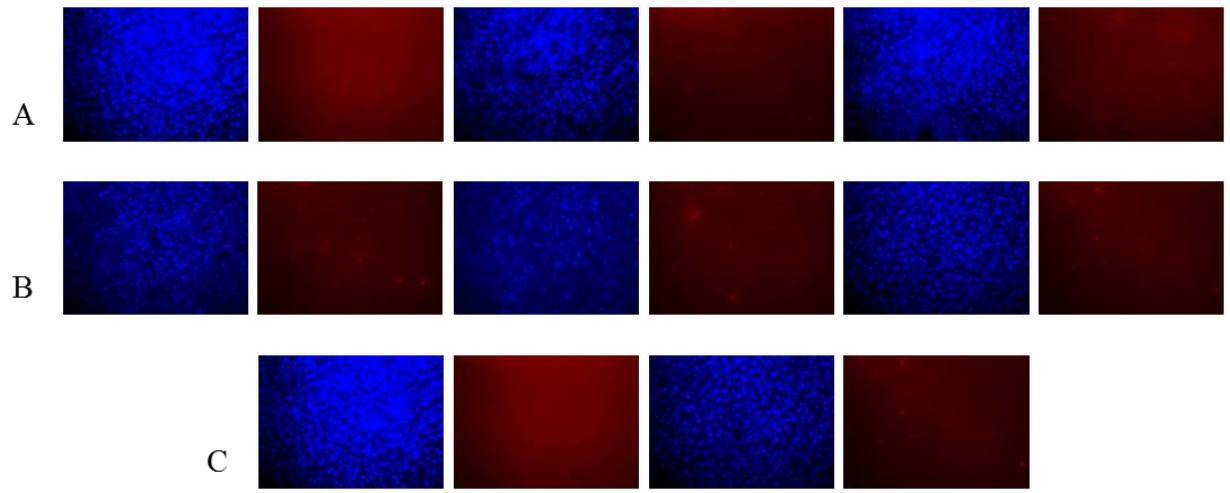

Figure 25: Histological slide images of liver from animals treated with 1.5 mg/kg DOX. DAPI filtered images reveal blue-stained nuclei, TRITC filtered images reveal drug. A) From left to right; samples from animals 24 hours, 96 hours and 120 hours post-injection. B) From left to right; samples from animals 144 hours, 168 hours and 192 hours post-injection. C) From left to right; samples from animals 24 hours and 192 hours post-injection. (All images are at 40X magnification).

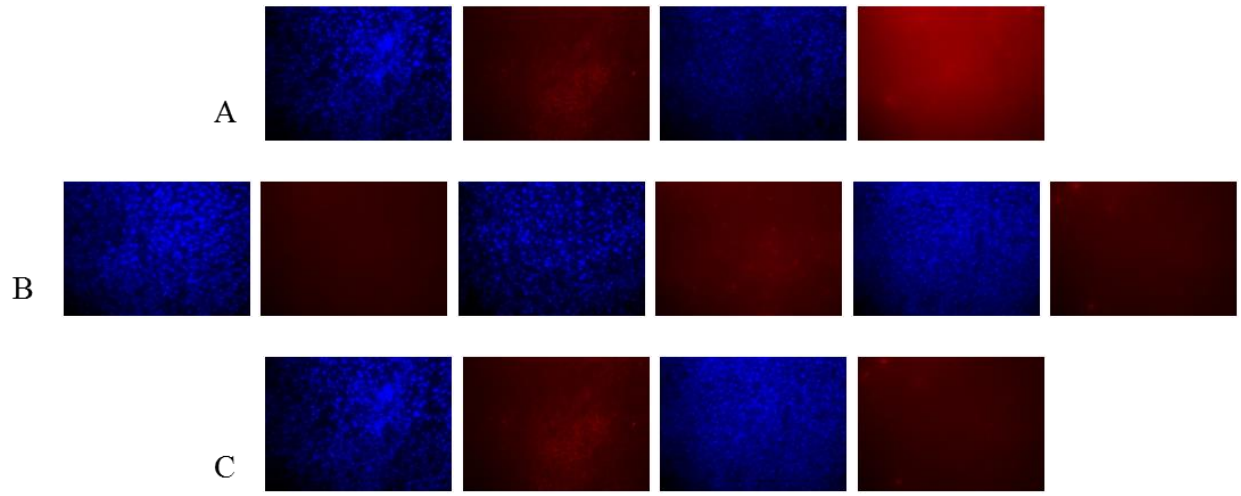

Figure 26: Histological slide images of liver from animals treated with 4.5 mg/kg DOX. DAPI filtered images reveal blue-stained nuclei, TRITC filtered images reveal drug. A) From left to right; samples from animals 24 hours and 72 hours post-injection. B) From left to right; samples from animals 120 hours, 144 hours and 192 hours post-injection. C) From left to right; samples from animals 24 hours and 192 hours post-injection. (All images are at 40X magnification).

Upon comparison of images taken of samples at both doses, it was observed that at 24 and 48 hours, more localization of DOX was apparent in images of samples from animals treated with 4.5 mg/kg despite the image of 1.5 mg/kg treated samples being brighter (Figure 27A and B). At 72 and 96 hours, the opposite was true; the fluorescence intensity was greater for those images of samples from animals that received the 4.5 mg/kg dose; however there is very little, if any localization evident (Figure 27C and D). At all other time points, any difference between doses was difficult to distinguish, especially at 192 hours (Figure 27E).

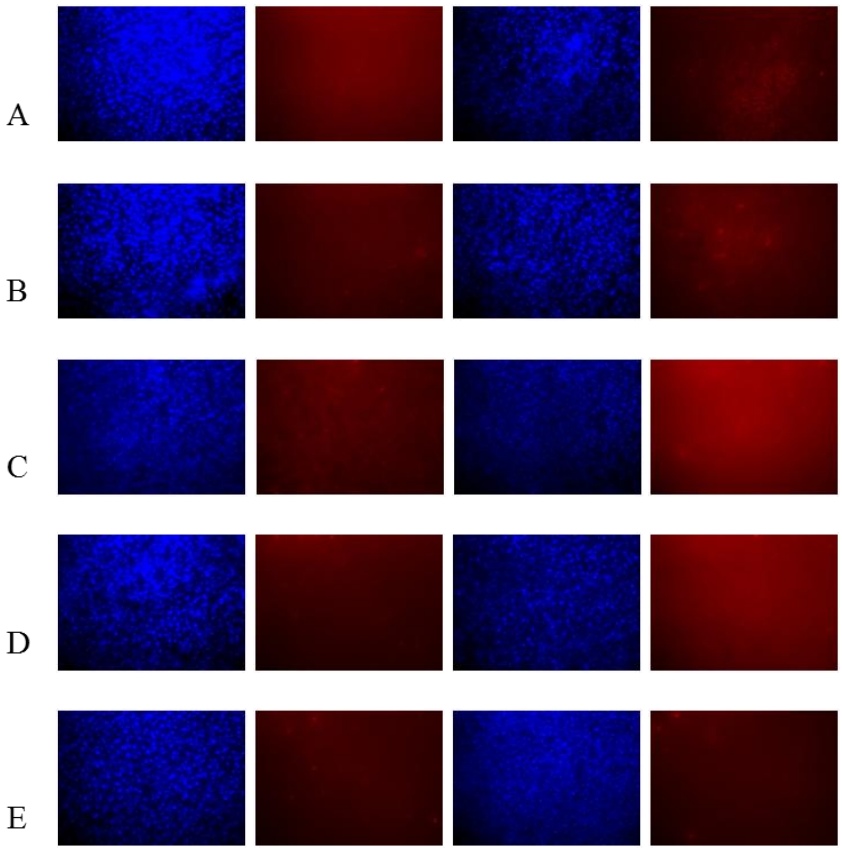

Figure 27: Histological slide images of liver from animals treated with both doses of DOX. In all panels, the two left images represent the 1.5 mg/kg dose and the two right images represent the 4.5 mg/kg dose. DAPI filtered images reveal blue-stained nuclei, TRITC filtered images reveal drug. A) 24 hours post-injection. B) 48 hours post-injection. C) 72 hours post-injection. D) 96 hours post-injection. E) 192 hours post-injection (All images are at 40X magnification).

Upon comparison of images of samples treated with either dose of DOX and controls, it was apparent that fluorescence and localization were greater for all of the images of samples from animals treated with 4.5 mg/kg DOX. Differences between controls and samples from animals treated with 1.5 mg/kg DOX, although not as pronounced as for the higher dose, were still evident (Figure 28).

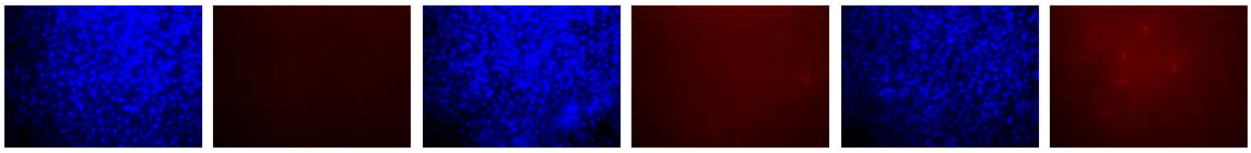

Figure 28: Histological slide images of treated versus control liver tissue. DAPI filtered images reveal blue-stained nuclei, TRITC filtered images reveal drug. From left to right: Control, 48 hours at 1.5 mg/kg, and 48 hours at 4.5 mg/kg. (All images are at 40X magnification).

4.2.2 Heart Tissue Samples

For images taken of samples treated with 1.5 mg/kg DOX, fluorescence decreased between 24 and 48 hours and then increased between 48 and 72 hours (Figure 29A). Fluorescence also seemed to decrease between 72 and 96 hours, after which point intensity appears to remain constant until 192 hours (Figure 29B). The fluorescence level from 24 hours decreased greatly over the 192 hour examination period (Figure 29C).

For images taken of samples treated with 4.5 mg/kg DOX, fluorescence greatly decreased between 24 hours and 48 hours, though DOX appeared to remain localized at 48 hours (Figure 30A). Afterwards, the intensity increased gradually to 120 hours (Figure 30B), from which time the fluorescence level decreased at 144 hours and remained constant to 192 hours (Figure 30C). Again, there was a remarkable decrease in fluorescence over the 192 hour examination period, and the decrease in localization was much more evident in samples from animals treated with the higher dose.

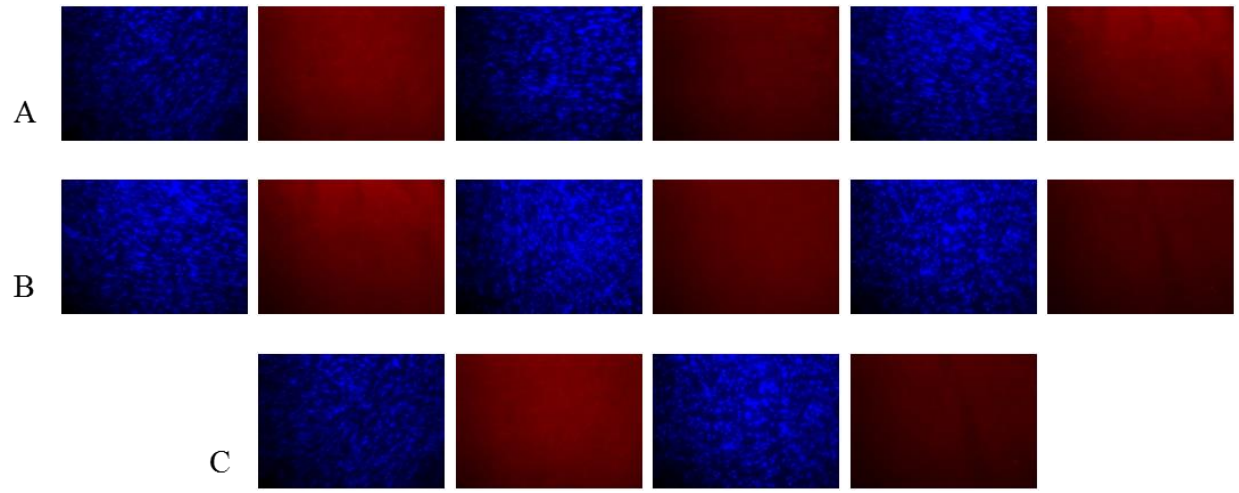

Figure 29: Histological slide images of heart from animals treated with 1.5 mg/kg DOX. DAPI filtered images reveal blue-stained nuclei, TRITC filtered images reveal drug. A) From left to right; samples from animals 24 hours, 48 hours and 72 hours post-injection. B) From left to right; samples from animals 72 hours, 96 hours and 192 hours post-injection. C) From left to right; samples from animals 24 hours and 192 hours post-injection. (All images are at 40X magnification).

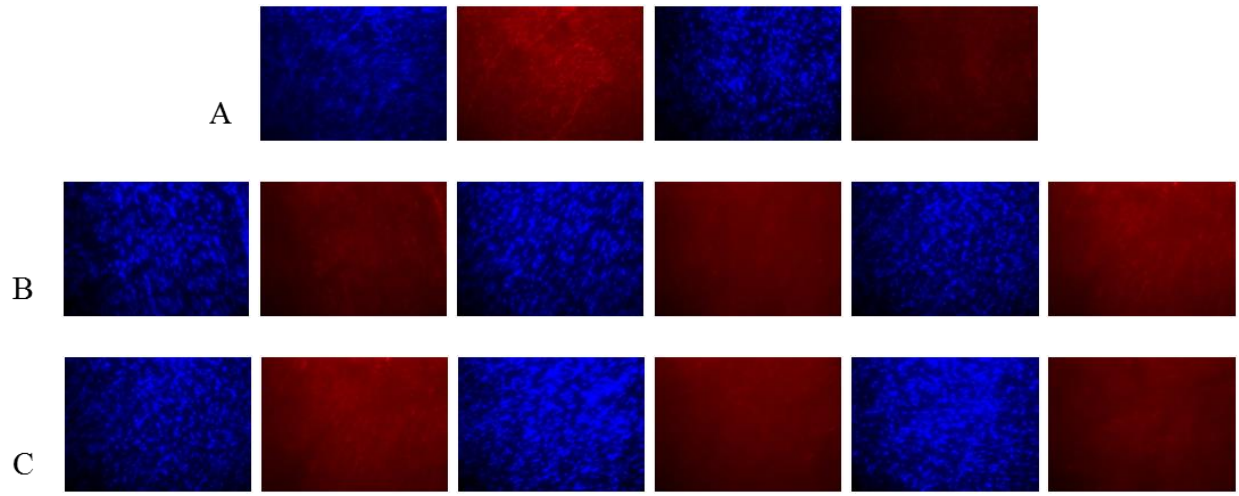

Figure 30: Histological slide images of heart from animals treated with 4.5 mg/kg DOX. DAPI filtered images reveal blue-stained nuclei, TRITC filtered images reveal drug. A) From left to right; samples from animals 24 hours and 48 hours post-injection. B) From left to right; samples from animals 72 hours, 96 hours and 120 hours post-injection. C) From left to right; samples from animals 120 hours, 144 hours and 192 hours post-injection. (All images are at 40X magnification).

Upon comparison of images taken of samples at both doses, it was observed that at 24 hours, 120 hours and 192 hours, fluorescence and localization were greater for the images of samples from animals treated with 4.5 mg/kg DOX, although as time progressed these differences became more difficult to distinguish (Figure 31). Conversely, at the 72 hour time point, it appeared that fluorescence at 1.5 mg/kg was greater than that at 4.5 mg/kg (Figure 31). At all other time points, any difference between doses was difficult to identify.

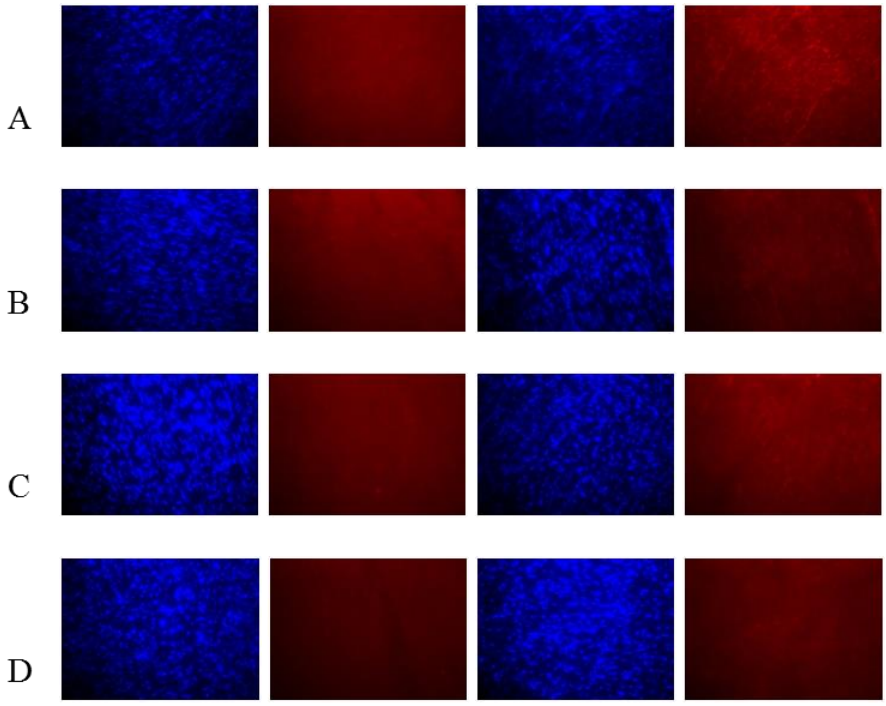

Figure 31: Histological slide images of heart from animals treated with both doses of DOX. In all panels, the two left images represent the 1.5 mg/kg dose and the two right images represent the 4.5 mg/kg dose. DAPI filtered images reveal blue-stained nuclei, TRITC filtered images reveal drug. A) 24 hours post-injection. B) 72 hours post-injection. C) 120 hours post-injection. D) 192 hours post-injection. (All images are at 40X magnification).

Upon comparison of images of samples treated with either dose of DOX and controls, it was apparent that fluorescence and localization were greater for the majority of the images of samples from animals treated with 4.5 mg/kg DOX. Differences between controls and samples from animals treated with 1.5 mg/kg DOX were not as obvious, although still observable (Figure 32).

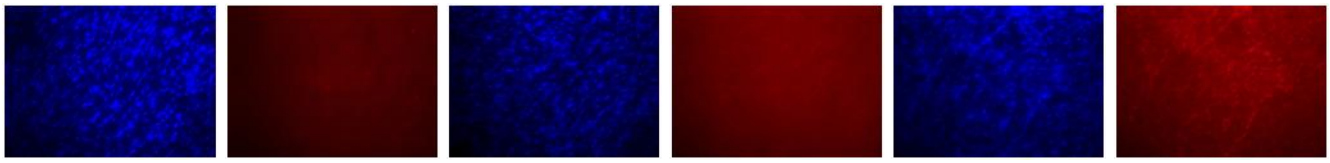

Figure 32: Histological slide images of treated versus control heart tissue. From left to right: Control, 24 hours at 1.5 mg/kg, 24 hours at 4.5 mg/kg. (All images are at 40X magnification).

Supplementary results are shown in Appendix II.

Chapter 5: Discussion

The purpose of this study was to examine and clarify the pharmacokinetics of the anthracycline chemotherapeutic DOX using a rat model. The main goal was to provide insight into the physiological behaviour of the drug, as well as of its main metabolite DOXOL, over a 192 hour period by analyzing plasma and tissue concentrations after the administration of one bolus injection of DOX.

In summary, analysis of DOX and DOXOL in plasma revealed stable concentrations for both molecules over the 192 hour examination period with an observed spike in DOX concentration at 96 hours post-injection. While a dose response was observed in the plasma at several time points for DOX, DOXOL concentrations were similar for all time points regardless of dose administered. Liver tissue exhibited a similar pattern as that of plasma, although DOX concentrations did ultimately decrease at 192 hours, preceded by a spike in DOXOL concentration indicating the potential upregulation of DOX-metabolizing enzymes at approximately 168 hours post-injection. For heart tissue, while the concentration of the metabolite remained consistent over the examination period, the concentration of DOX steadily decreased until reaching a stable concentration at 144 hours for both doses, suggesting the possibility of storage of this threshold amount in the tissue regardless of the dose administered. Moreover, these patterns of tissue responses were supported by fluorescence microscopy findings, which also provided additional insight into the localization of DOX within the tissues.

Taken together, the results of this study further elucidate the pharmacokinetic response of tissues and plasma to bolus injections of DOX over a period of time that has formerly remained uninvestigated as well as indicate that these molecules, especially DOXOL, remain in tissues for extended periods of time and may contribute to cardiotoxicity.

5.1 Experimental design

There are several aspects of the experimental design which deserve further clarification. First, the selection of time points at which samples were taken and why the two different concentrations of DOX were chosen will be addressed. Currently in the literature, DOX has been investigated in-depth for the purpose of clarifying the mechanisms by which it induces cardiotoxicity and thus cardiac conditions such as CHF. To do this, researchers have studied several critical time points. These include; 1) the immediate period, within and up to 24 hours following the administration of the dose, which has been used to assess the initial pharmacokinetics of DOX and 2) the weekly period, measuring concentrations once a week after weekly administration cycles, which has been used to assess the long-term effects of DOX (Herman et al. 1999, Gustafson et al. 2001). Very few studies have examined the behaviour of DOX over several days following a single bolus injection, and indeed none have done so for more than five days (Hayward et al. 2013). This represents a significant period of time during which the concentrations of DOX and DOXOL have not been measured. Thus, the rationale for sequentially sampling tissues and plasma every 24 hours for up to 192 hours (8 days), was for the purpose of examining this yet uninvestigated time frame. It is interesting to note that very few studies have examined this time frame, despite the fact that the elimination half-life of DOX is reported to be approximately 6-7 days (Danesi et al. 2002).

Secondly, the present study selected two different doses of DOX to be administered (1.5 mg/kg and 4.5 mg/kg). It must first be noted that a dose of 1.5 mg/kg in the rat is equivalent to approximately 9 mg/m^2, which is approximately half of a typical chemotherapeutic dose given at weekly intervals to humans (Freireich et al. 1966, Pfizer Canada Inc. 2012). However, several studies have shown that upon repeated administration of even a 1.0 mg/kg dose, rats have developed cardiomyopathy and other cardiac-related problems (Herman et al. 1998, Herman et al. 1999, Hayward and Hydock 2007). While many studies have used much higher doses to induce cardiotoxicity more rapidly, the application of the findings from these supraclinical dose studies to the typical clinical setting is not necessarily correct (Minotti et al. 2004). Therefore, as a low dose limit, the 1.5 mg/kg dose was selected, however in order to determine the effect that dose would have on tissue concentrations, it was important to have a second and higher dose to compare it with, thus a higher dose of 4.5 mg/kg was also selected. In addition, it is important to note that the intention of this study was not to induce cardiomyopathy, but to examine the pharmacokinetics of the drug and its main metabolite, thus the use of lower doses remains applicable.

Finally, the route of administration merits some clarification. In general, the administration of DOX in animal studies has been achieved by either IV or IP injection. While many animal studies have used IV administration of DOX in an attempt to mimic its administration in clinical settings, IP is also a widely accepted mode of administration, particularly in rodents. IP injection is typically much easier to achieve than IV injection, however it is associated with a slower uptake of the drug into the systemic circulation as well as first-pass metabolism effects (Hasovits and Clarke 2012). Despite the latter, studies examining the pharmacokinetics and cardiotoxic

effects of DOX using IP injection have still observed similar results to those studies using IV administration (Herman et al. 1999, Hayward and Hydock, 2007). Administration via IP injection was therefore selected for this study.

5.2 Plasma compartment

Being an important compartment responsible for the dynamics between drug delivery and elimination from tissues, the concentrations of DOX and DOXOL were measured in the plasma. As expected, no DOX was detected in control animals, however in the treated animals, although the DOX concentrations in the plasma spiked at 96 hours post-injection, they were remarkably stable over the duration of the experiment, exhibiting no significant change between the first sample time of 24 hours and the final sample time of 192 hours. This suggests that the drug entered the plasma within the first 24 hours following I.P. administration and remained in the circulation at a relatively consistent level. Past studies have revealed that DOX is rapidly cleared from the plasma (i.e. within the first 24 hours) and although in this study, no sampling was done prior to 24 hours post-injection, these data suggest that DOX is potentially stable in the circulation after an initially rapid increase (Benjamin et al. 1977, Danesi et al. 2002, Pfizer Canada Inc. 2012).

While the higher dose of the drug (4.5 mg/kg) did not consistently yield greater concentrations in the plasma, a dose response was observed at several time points. In addition, a similar pattern of response was observed for both doses, whereby concentrations increased and then remained stable, except at 96 hours. This stability could potentially be explained by the fact that DOX is known to be bound to plasma proteins to a great extent following its administration, therefore

remaining in the circulation and continually being exposed and distributed to tissues (Danesi et al. 2002, Kontny et al. 2013). It is reasonable to assume there is a finite amount of protein available in the plasma for DOX binding, therefore this could create a threshold for the concentration of DOX in the plasma over time, regardless of the dose administered. Whether or not this is in fact occurred could not be determined in this study, but may contribute to the dose response and stability of the DOX concentrations in the plasma.

In a similar fashion, the concentration of the metabolite DOXOL was also very consistent in the plasma and as anticipated, no DOXOL was detected in control samples. Concentrations were elevated after the first 24 hours and exhibited very little change during the remainder of the experiment. This indicates an associated breakdown of DOX into DOXOL consistent with previous findings from other studies (Olson and Mushlin 1990). What these data also suggest is a balance in both breakdown of the drug and elimination of the metabolite from the plasma. In order for the concentration of a molecule in a compartment to remain stable, the rate of entry and the rate of exit must be in equilibrium and this would appear to be what is occurring as reflected by the measured concentrations in the plasma.

The administration of the higher dose did not result in greater DOXOL concentrations during the first 24 hours, as compared to the lower dose. However, at the lower dose the DOXOL concentrations remained constant in the plasma after 48 hours, whereas at the higher dose they steadily decreased over time but remained relatively constant after 72 hours. Overall, the concentrations of this compound in the plasma were fairly stable, and showed only a slight decrease over time indicating that the rate of production and the rate of removal of DOXOL were

steady over time and therefore reinforce that the mechanisms responsible for DOX breakdown and elimination of metabolites function at a constant rate, regardless of the dose administered.

5.3 Liver compartment

To assist in the clarification of the processing of the drug and its conversion to DOXOL, the concentrations of DOX and DOXOL were measured in the liver. DOX concentrations over the course of the experiment were relatively constant in the liver, despite some fluctuations in concentration occurring at the lower dose (1.5 mg/kg). However, the concentration did tend to decrease by the 192 hour point. Despite the fact that the higher dose of DOX did not reveal greater concentrations at the later time points, there was a fairly clear dose-response initially.

Of further interest is the fact that even though the concentration of DOX at 192 hours was decreased with respect to that at 24 hours, DOX was still detectable, and in fact almost equal for both doses at this point. Under circumstances of repeated dosing regimens, the observation that there is residual DOX after 192 hours following a bolus injection could result in a greater accumulation of the drug in the tissue. This seems to support the fact that a cumulative dose effect of DOX has increasingly negative effects on physiological systems (Menna et al. 2012, Pfizer Canada Inc. 2012).

Upon measurement of DOXOL concentrations in the liver, it was evident that the concentration was stable, in a similar manner to its behaviour in the plasma. However, for both doses the concentration of DOXOL increased dramatically at the 168 hour time point. This sudden increase in the metabolite taken with the observation that DOX concentrations were lower at the

final 192 hour time point, suggests that upregulation of the enzymes responsible for DOX breakdown requires approximately this length of time to occur. While it is well understood that several aldo-keto reductases (AKRs) and carbonyl reductases (CBRs) are responsible for the breakdown of DOX to DOXOL, and that these enzymes are present in tissues to varying degrees and with varying affinities for the drug, there has been very little investigation into the upregulation of these enzymes over time as a result of the exposure to the drug (Kassner et al. 2008). It has been observed that some of these enzymes are upregulated in tumor tissue after exposure to DOX, contributing to the growing concern of the development of drug-resistance among certain cancer cells (Heibein et al. 2012). Furthermore, it has been found that exposure to DOX does exert changes in gene expression in cardiac tissue, and that these changes have been suggested to be linked with the cardiotoxic nature of the drug (Olson et al. 2003, Richard et al. 2011). It is therefore possible that a similar phenomenon is occurring in the liver after 168 hours post-injection, however further research and more specific quantification of enzymatic activity would be necessary to support this notion.

Despite the fact that DOX is being broken down and that DOXOL is being eliminated, they seem to remain in the body for a long period of time. This may help explain why there is still significant accumulation in the body, leading to cardiotoxic effects. It also indicates that the liver, as a detoxifying tissue, does not rapidly remove the harmful compounds.

5.4 Heart compartment

To elucidate the kinetics of DOX and DOXOL in one of the tissues that is most detrimentally affected by DOX administration, the concentration of each was quantified in the heart. Again as

anticipated, no DOX was detected in control animals but in animals receiving the treatment proved to be rapidly taken up in this tissue within the first 24 hours. Over the 192 hour experimental period, the concentration of DOX consistently decreased in heart tissue, though the rate of elimination appeared to be more rapid in response to administration of the higher dose (4.5 mg/kg). In this tissue, a dose-response was clearly identifiable, with the 4.5 mg/kg dose yielding much larger tissue concentrations of DOX than the 1.5 mg/kg dose. The exception to this arose at the 144 hour period, from which point there were no differences in DOX concentration between doses, nor between the remaining time points. This indicates that regardless of the dose administered, there was a threshold amount of DOX stored in the heart.

Indeed many studies have documented the accumulation of DOX in certain organelles, particularly in mitochondria, within cells (Anderson et al. 2004, Carvalho et al. 2014, Ichikawa et al. 2014). This accumulation is suspected to be due to the selective binding of DOX to an inner-mitochondrial membrane protein called cardiolipin. Although Anderson et al. (2004) described the manner in which cardiolipin molecules in various tissues display slightly different organizational structures and thus different affinities for DOX, it is well-supported that the mitochondria in heart tissue do express a cardiolipin protein that has DOX-binding capabilities (Rahman et al. 1985, Goormaghtigh et al. 1990, Parker et al. 2001, Claypool and Koehler 2012). Therefore, this dose-independent, stable concentration of DOX in heart tissue after 144 hours could possibly be a result of DOX binding to cardiolipin and thus its storage in cardiac mitochondria. Furthermore, when it is taken into consideration that heart tissue has a rather large quantity of mitochondria compared to other tissues, it is reasonable that liver tissue in this study did not exhibit a similar storage pattern (Carvalho et al. 2014).

The storage of DOX in the heart tissue further exemplifies concerns about dosing regimens that incorporate multiple repeated doses. It has been demonstrated a multitude of times that cumulative doses of DOX lead to increased risk for serious cardiovascular complications, cardiomyopathy and CHF (Menna et al. 2012, Pfizer Canada Inc. 2012). The results of this study reveal for the first time, the potential time-related kinetics of this very detrimental and usage-limiting effect of DOX.

However, the cardiotoxic nature of DOX has not necessarily been attributed to DOX accumulation, but to the accumulation of its main metabolite DOXOL, which has been suggested to be up to 10 times more cardiotoxic than its parent compound (Olson et al. 1988). The results of the present study show that while the concentration of DOX steadily decreases over time, the concentration of DOXOL is remarkably stable. Despite minor fluctuations in concentration presenting over the 192 hours, seemingly mimicking fluctuations observed in the plasma, the concentration of the metabolite is not different from the 24 hour time point to the final 192 hour time point. This indicates that heart tissue is consistently exposed to DOXOL, which is likely exerting very negative effects on the tissue.

Furthermore, as has been consistently observed throughout the study the effect of dose, although eliciting a dose-response in plasma and tissues regarding DOX, did not do so in a consistent fashion with respect to DOXOL. However, the findings still lead to a better understanding of the relationship between DOX and DOXOL from compartment to compartment.

5.5 Fluorescence Microscopy

While many studies have used fluorescence microscopy for the purpose of quantifying concentrations of DOX or of determining specific localization of DOX within tissues, its use in this particular study was for the confirmation of the presence of DOX within the tissues analyzed (Paschoud et al. 1985, Shen et al. 2008, Chen et al. 2012) as well as to shed light onto the general localization of the drug. The primary quantification of DOX and its metabolite DOXOL was accomplished via HPLC analysis, and in order to potentially assist in the representation of the pharmacokinetics of the drug, microscopy was utilized.

Tissue slices were mounted onto slides using a fluorescence-preserving mounting medium which contained DAPI fluorescent stain. This stain enables the visualization of nuclei by binding to nucleic acids and fluorescing blue under DAPI filter. By using this mounting medium, it was possible to obtain an idea of the cellular composition of the sample in order to determine whether or not the sections would provide representative images of the tissue being analyzed. This also allowed further visualization of the localization of DOX, and while no solid conclusions can be drawn from this qualitative analysis, it certainly provides further insights into the behaviour of the drug.

Using the TRITC filter allowed visualization of DOX, which is known to be a fluorescent molecule (Introduction: Section 2.3). There is an assumption that its metabolite DOXOL would also fluoresce under the same filter due to the fact that structurally the molecules are remarkably similar. However, from the HPLC analysis it was evident that the concentrations of DOX were orders of magnitude greater than the concentrations of DOXOL in both tissues and it was

therefore reasonable to conclude that any observable differences in fluorescence intensity were likely due to fluctuations in DOX concentration, and not DOXOL.

5.5.1 Liver

Images of liver tissue from either control animals or animals receiving treatment proved to be very representative of the tissue, as identified by visualization under the DAPI filter. All images also proved to reveal greater fluorescence under TRITC filter for treated samples as compared to control samples, indicating that DOX was in fact detectable by this method.

At both the 1.5 mg/kg and 4.5 mg/kg dose, the microscopy images revealed a similar pattern of response as was indicated by the HPLC results, with observable fluctuations in fluorescence intensity to match statistically significant changes in DOX concentrations. However, for either dose there were certain instances where the level of fluorescence of the tissue did not coincide with HPLC concentrations, which highlights one of the drawbacks of this study. While every attempt at consistency in sampling was made, it was impossible to visualize by microscopy the exact sample that was used for HPLC analysis, thereby introducing a potential source of variation in the results. Furthermore, it is important to note that due to the experimental design, samples of tissues at each time point were not from the same animal. Although dosing was performed in as accurate a manner as possible and handling of all animals and samples was consistent, it is likely that there were variations in the results simply due to the variability in the physiology of the animals at the individual level. That being said, despite the few fluctuations in fluorescence that do not appear to exactly match the HPLC results, the histological analysis does

seem to confirm the relative stability of the drug in the liver, and the eventual decrease in concentration after 192 hours post-injection.

As previously mentioned, the use of DAPI staining enabled the visualization of the cellularity of the tissue and when these images were compared to those exposed under the TRITC filter, it allowed for the observation that DOX appeared to be localized in the nuclei. While this observation was not consistent for each dose, nor for each time point, it is in agreement with the notion that DOX functions by entering the nucleus of the cell to intercalate with DNA (Frederick et al. 1990, Minotti et al. 2004). From the histology results it would appear that this nuclear localization occurred rather rapidly, and to a greater extent at the higher dose. Crivellato et al. described the detection of fluorescent nuclei in cultured hepatocytes after only 6 hours of receiving 0.1 mM of DOX, and observed that the number of fluorescent nuclei increased over 48 hours, although no examinations past this time point were performed (2000). It is important to note that only speculations may be made from the histological results of this study since no actual quantitative analyses of the histological images were performed. However, the images remain strongly supportive that DOX accumulates in the nuclei.

5.5.2 Heart

Images of heart tissue from both control and treated animals proved to be very representative of the tissue, as identified by visualization under the DAPI filter. All images also proved to reveal greater fluorescence under TRITC filter for treated samples as compared to control samples, indicating that DOX was again detectable by this method.

Similar to the liver, at both the 1.5 mg/kg and 4.5 mg/kg dose, the microscopy images revealed a similar pattern of response as was indicated by the HPLC results. Fluctuations in fluorescence intensity observed by microscopy matched statistically significant changes in DOX concentrations. In the case of heart tissue, only the 4.5 mg/kg dose revealed inconsistencies between the level of fluorescence and HPLC concentrations, and these can be accounted for by the same sources of error that were discussed for liver tissue. Again, despite a certain amount of variability, the histological images are highly representative of the overall decrease in DOX over the 192 hour examination period.

Images obtained from animals treated with 4.5 mg/kg DOX revealed rather consistently that this higher dose produced greater fluorescence intensity as well as increased nuclear localization. This was exceedingly evident at 24 hours, and gradually became less apparent over the 192 hour examination period, in a similar fashion to that observed for liver tissue. Again this indicates the possibility that DOX accumulates in the nucleus to a greater extent at higher doses, and that it targets this location rather rapidly. Overall, the fluorescence microscopy allowed for qualitative support of the quantitative analysis and provided additional insight into the possible localization of the drug.

Chapter 6: Conclusions

This study, for the first time, analyzed the pharmacokinetics of DOX and its main metabolite, DOXOL, over a 192 hour period using a single intraperitoneal injection of either 1.5 or 4.5 mg/kg of the anthracycline. HPLC analysis was completed on samples of plasma, liver and heart at 24, 48, 72, 96, 120, 144, 168 and 192 hours following the injection. Fluorescence microscopy was used to ascertain the quality of sections of liver and heart, as well as presences and localization of DOX.

1. Although concentrations of DOX and DOXOL in the plasma did not necessarily exhibit a strong dose response, they did reveal the same pattern of response in this compartment, remaining relatively stable after an initial increase within the first 24 hours. This indicates that an equilibrium in the rate of entry into and rate of exit from the plasma compartment was established for both drug and metabolite, and suggests that the underlying mechanisms of DOX breakdown and elimination function at similar and relatively constant rates.
2. In the liver concentrations of DOX were increased at 24 hours, and a clear dose response was observed for the initial time points. Similar patterns of response were exhibited after both doses, with overall decreases at 192 hours post-injection, preceded by a spike in DOXOL at 168 hours. These findings suggest that upregulation of the enzymes responsible for DOX breakdown requires approximately this length of time to occur and that the liver, as the major detoxifying organ of the body, processes DOX relatively slowly. Under fluorescence microscopy liver samples proved to be representative of the tissue and corroborated HPLC findings. It was also observed that DOX accumulated in

the nuclei of cells, and appeared to do so within the first 24 hours and in a dose-dependent fashion, which supports the known DNA-binding function of DOX.

3. In heart tissue the dose response was even more pronounced and the rate of steady decrease after initial increase at 24 hours was obvious, and more prominent after animals received the higher dose. However, concentrations of DOX reached a threshold point at 144 hours, regardless of dose, and ceased to decrease following this point, suggesting storage of the drug in cardiac tissue. Furthermore, while concentrations of DOX in the heart steadily decreased to 144 hours and then remained stable, concentrations of DOXOL remained stable over the entire duration of the examination period after initially increasing at 24 hours, indicating that the heart was constantly exposed to the harmful metabolite during this length of time. Microscopy images were once again representative of the tissue and supported the HPLC findings, and in a similar manner to liver images, revealed that DOX rapidly entered the nuclei of the cells and did so to a much greater extent at the higher dose.
4. These findings contribute to the field as they are the first to show that substantial DOX and DOXOL are still present in the plasma, liver and heart following 192 hours.

Overall, the results consistently revealed residual amounts of both DOX and DOXOL in all tissues. While no increases in the concentration of either molecule were observed in these tissues after 192 hours, their continued detection was remarkable and their storage in other tissues is entirely possible and would allow for their re-distribution within the physiological system, potentially helping to explain the obtained results. Furthermore, in repeated dosing regimens, these residual amounts could lead to further accumulation of either drug or metabolite, and eventually lead to undesirable outcomes.

References

Alvarez-Cedron, L., Sayalero, L., Lanao, J. High-performance liquid chromatographic validated assay of doxorubicin in rat plasma and tissues. (1999) *Journal of Chromatography B.* 721(2): 271-278.

American Cancer Society. *What is breast cancer?* Last revised 2013. Accessed June 2013. http://www.cancer.org/cancer/breastcancer/overviewguide/breast-cancer-overview-what-is-breast-cancer

Anderson, A., Xiong, G. and Arriaga, E. (2004) Doxorubicin Accumulation in Individually Electrophorosed Organelles. *Journal of the American Chemical Society*. 126(30): 9168-9169.

Arcamone, F. (1985) Properties of Antitumor Anthracyclines and New Developments in Their Application: Cain Memorial Award Lecture. *Cancer Research*. 45(12): 5995-5999.

ATDBio. *Nucleic Acid-Drug Interactions*. 2005-2013. Accessed June 2013. http://www.atdbio.com/content/16/Nucleic-acid-drug-interactions

Beattie, D. (2006) Bioenergetcs and Oxidative Metabolism. In Devlin, T.'s *Textbook of Biochemistry with Clinical Correlations*. 6th Ed. John Wiley & Sons. (pp.529-580).

Benjamin, R., Riggs, C., and Bachur, N. (1977) Plasma Pharmacokinetics of Adriamycin and Its Metabolites in Humans with Normal Hepatic and Renal Function. *Cancer Research*. 37(5): 1416-1420.

Bielack, S., Erttmann, R., Kempf-Bielack, B. and Winkler, K. (1996) Impact of Scheduling on Toxicity and Clinical Efficacy of Doxorubicin: What Do We Know in the Mid-Nineties? *European Journal of Cancer*. 32A(10): 1652-1660.

Binaschi, M., Bigioni, M., Cipollone, A., Rossi, C., Goso, C., Maggi, C., Capranico, G. and Animati, F. Anthracyclines: selected new developments. (2001). *Current Medicinal Chemistry. Anti-Cancer Agents*. 1(2): 113-130.

Blum, R., and Carter, S. (1974) Adriamycin. A new anticancer drug with significant clinical activity. *Annual Internal Medicine*. 80(2): 249-259.

Boucek, R., Olson, R., Brenner, D., Ogunbumni, E., Inui, M. and Fleischer, S. (1987). The major metabolite of doxorubicin is a potent inhibitor of membrane-associated ion pumps: a correlative study of cardiac muscle with isolated membrane fractions. *Journal of Biological Chemistry*. 262 (33): 15851-15856.

Brazzolotto, X., Andriollo, M., Guiraud, P., Favier, A. and Moulis, J. (2003). Interactions between doxorubicin and the human iron regulatory system. *Biochimica et Biophysica Acta*. 1593 (2-3): 209-218.

Brown, D. and Tomlin, M. (2010) Pharmacokinetic Principles. In Tomlin, M.'s *Pharmacology and Pharmacokinetics: A Basic Reader*. Springer-Verlag London Limited. (pp.13-52).

Canadian Breast Cancer Foundation. *Breast Cancer in Canada, 2013*. Last revised 2013. Accessed June 2013. http://www.cbcf.org/ontario/AboutBreastCancerMain/AboutBreastCancer/Pages/BreastCancerinCanada.aspx

Canadian Breast Cancer Foundation. *Breast Cancer Statistics*. Last revised 2014. Accessed June 2014. http://www.cancer.ca/en/cancer-information/cancer-type/breast/statistics/?region=on

Carvalho, F., Burgeiro, A., Garcia, R., Moreno, A., Carvalho, R. and Oliveira, P. (2014). Doxorubicin-induced Cardiotoxicity: From Bioenergetic Failure and Cell Death to Cardiomyopathy. *Medicinal Research Reviews*. 34(1): 106-135.

Chen, N., Wu, C., Chung, C., Hwu, Y., Cheng, S., Mou, C. and Lo, L. (2012). Probing the Dynamics of Doxorubicin-DNA Intercalation during the Initial Activation of Apoptosis by Fluorescence Lifetime Imaging Microscopy (FLIM). *PLoS ONE*. 7(9):e44947. doi: 10.1371/journal.pone.0044947

Clark, J. *High Performance Liquid Chromatography – HPLC*. 2007. Accessed June 2013. http://www.chemguide.co.uk/analysis/chromatography/hplc.html

Claypool, S. and Koehler, C. (2012). The complexity of cardiolipin in health and disease. *Trends in Biochemical Sciences*. 37(1): 32-41.

Collins, J. and Supko, J. (2006) Pharmacokinetics. In Chabner, B. and Longo, D.'s *Cancer Chemotherapy & Biotherapy: Principles & Practices*. Lippincott Williams & Wilkins, USA. (pp. 32-44).

Crivellato, E. Donini, A., Baccarani, U., Lavaroni, S., Candussio, L., Degrassi, A. and Bresadola, F. (2000). Efficiency of doxorubicin handling by isolated hepatocytes is a valuable indicator for restored cell function. *The Histochemical Journal*. 32: 535-543.

Cusack, B., Young, S., Gambliel, H. and Olson, R. (2002) Effect of aging on cardiac contractility in a rat model of chronic daunorubicin cardiotoxicity. *Cardiovascular Toxicology*. 2(2): 99-109.

Danesi, R., Foglin, S., Gennari, A., Conte, P. and Del Tacca, M. (2002). Pharmacokinetic-Pharmacodynamic Relationships of the Anthracycline Anticancer Drugs. *Clinical Pharmacokinetics*. 41(6): 431-444.

Eksborg, S., Strandler, H., Edsmyr, F., Naslund, I. and Tahvanainen, P. (1985). Pharmacokinetic study of i.v. infusions of adriamycin. *European Journal of Clinical Pharmacology*. 28(2): 205-212.

Frederick, C., Williams, L., Ughetto, G., van der Marel, G., Boom, J., Rich, A. and Wang, A. (1990) Structural Comparison of Anticancer Drug-DNA Complexes: Adriamycin and Daunomycin. *Biochemistry*. 29(10): 2538-2549.

Freireich, E J., Gehan, E A., Rall, D P. et al. (1966) Quantitative comparison of toxicity of anticancer agents in mouse, rat, dog, monkey and man. *Cancer Chemotherapy Reports*. 50(4): 219-244.

Gabizon, A., Shmeeda, H. and Barenholz, Y. (2003) Pharmacokinetics of pegylated liposomal doxorubicin – Review of animal and human studies. *Clinical Pharmacokinetics*. 42 (5): 419-436.

Gewirtz, D. (1999) A critical evaluation of the mechanisms of action proposed for the antitumor effects of the anthracycline antibiotics Adriamycin and daunorubicin. *Biochemical Pharmacology*. 57(7): 727-741

Grosse, P., Bressolle, F., Rouanet, P., Joulia, J. and Pinguet, F. (1999). Methyl-β-cyclodextrin and doxorubicin pharmacokinetics and tissue concentrations following bolus injection of these drugs alone or together in the rabbit. *International Journal of Pharmaceutics*. 180(2): 215-223.

Goormaghtigh, E., Huart, P., Praet, M., Brasseur, R. and Ruysschaert, J. (1990). Structure of the Adriamycin-cardiolipin complex. Role in mitochondrial toxicity. *Biophysical Chemistry*. 35(2-3): 247-257

Gustafson, D., Rastattier, J., Colombo, T. and Long, M. (2002) Doxorubicin Pharmacokinetics: Macromolecule Binding, Metabolism, and Excretion in the Context of a Physiologic Model. *Journal of Pharmaceutical Sciences*. 91(6): 1488-1501.

Hasovits, C. and Clarke, S. (2012) Pharmacokinetics and Pharmacodynamics of Intraperitoneal Cancer Chemotherapeutics. *Clinical Pharmacokinetics*. 51(4): 203-224.

Hayward, R. and Hydock, D. (2007) Doxorubicin Cardiotoxicity in the Rat: An In Vivo Characterization. *Journal of the American Association for Laboratory Animal Science*. 46(4): 20-32.

Hayward, R., Hydock, D., Gibson, N., Greufe, S., Bredahl, E. and Parry, T. (2013). Tissue retention of doxorubicin and its effect on cardiac, smooth and skeletal muscle function. *Journal of Physiology and Biochemistry*. 69: 177-187

Heibein, A., Guo, B., Sprowl, J., MacLean, D. and Parissenti, A. (2012). Role of aldo-keto reductases and other doxorubicin pharmacokinetic genes in doxorubicin resistance, DNA binding, and subcellular localization. *BioMed Central Cancer*. 12: 381-394. Accessed June 2014. http://www.biomedcentral.com/content/pdf/1471-2407-12-381.pdf

Heldring, N., Pike, A., Andersson, S., Matthews, J., Cheng, G., Hartman, J., Tujague, M., Strom, A., Treuter, E., Warner, M. and Gustafsson, J. (2007) Estrogen Receptors: How Do They Signal and What Are Their Targets. *Physiological Reviews*. 87(3): 905-931.

Herman, E., Zhang, J., Hasinoff, B., Tran, K., Chadwick, D., Clark, J.Jr., and Ferrans, V. (1998) Comparison of the chronic toxicity of piroxantrone, losoxantrone and doxorubicin in spontaneously hypertensive rats. *Toxicology*. 128(1): 35-52.

Herman, E., Zhang, J., Lipshultz, S., Rifai, N., Chadwick, D., Takeda, K., Yu, Z. and Ferrans, V. (1999) Correlation Between Serum Levels of Cardiac Troponin-T and the Severity of the Chronic Cardiomyopathy Induced by Doxorubicin. *Journal of Clinical Oncology*. 17(7): 2237-2243.

Ichikawa, Y., Ghanefar, M., Bayeva, M., Wu, R., Khechaduri, A., Naga Prasad, S., Kannan Mutharasan, R., Jairaj Naik, T. and Ardehali, H. (2014). Cardiotoxicity of doxorubicin is mediated through mitochondrial iron accumulation. *The Journal of Clinical Investigation*. 124(2): 617-630.

Iyer, L. and Ratain, M. (1999) 5-Fluorouracil Pharmacokinetics: Causes for Variability and Strategies for Modulation in Cancer Chemotherapy. *Cancer Investigation*. 17(7): 494-506.

Jacquet, P., Averbach, A., Stuart, O., Chang, D. and Sugarbaker, P. (1998). Hyperthermic intraperitoneal doxorubicin: pharmacokinetics, metabolism, and tissue distribution in a rat model. *Cancer Chemotherapy Pharmacology*. 41(2): 147-154

Jonge, M., Huitema, A., Rodenhuis, S. and Beijnen, J. (2005) Clinical Pharmacokinetics of Cyclophosphamide. *Clinical Pharmacokinetics*. 44(11): 1135-1164.

Jung, K. and Reszka, R. (2001). Mitochondria as subcellular targets for clinically useful anthracyclines. *Advanced Drug Delivery Reviews*. 49(1-2): 87-105.

Karukstis, K., Thompson, E., Whiles, J., and Rosenfeld, R. (1998) Deciphering the fluorescence signature of daunomycin and doxorubicin. *Biophysical Chemistry*. 73(3): 249-263.

Kassner, N., Huse, K., Martin, H., Gödtel-Armburst, U., Metzger, A., Meineke, I., Brockmöller, J., Klein, K., Zanger, U., Maser, E. and Wojnowski, L. (2008) Carbonyl Reductase 1 is a Predominant Doxorubicin Reductase in the Human Liver. *Drug Metabolism and Disposition.* 36(10): 2113-2120. Accessed March 2014. dmd.aspetjournals.org

Kontny, N., Wurthwein, G., Joachim, B, Boddy, A., Krischke, M., Fuhr, U., Thompson, P., Jorger, M., Schellens, J., Hempel, G. (2013) Population pharmacokinetics of doxorubicin: establishment of a NONMEM model for adults and children older than 3 years. *Cancer Chemotherapy Pharmacology*. 71(3): 749-763.

Lehman-McKeeman, L. (2008). Absorption, Distribution, and Excretion of Toxicants. In Klassen, C.'s *Casarette and Doull's Toxicology: The Basic Science of Poisons*. 7th Ed. McGraw-Hill Publishers. (pp. 131-160)

Lindup, W. and Orme, M. (1981) Clinical pharmacology: plasma protein binding of drugs. *British Medical Journal; Clinical Research Edition*. 282(6259): 212-214.

Longmuir, K., Haynes, S., Baratta, J., Kasabwalla, N., and Roberston, R. (2009) Liposomal delivery of doxorubicin to hepatocytes in vivo by targeting heparan sulfate. *International Journal of Pharmaceutics*. 382(1-2): 222-233.

Manfait, M., Alix, A., Jeannesson, P., Jardillier, J. and Theophanides, T. (1982) Interaction of adriamycin with DNA as studied by resonance Raman spectroscopy. *Nucleic Acids Research*. 10(12): 3803-3816.

Masood, S., and Kameh, D. (2002) Breast. In M.R. Alison's *The Cancer Handbook Volume 1* (pp. 611-616).

Maudens, K., Stove, C., and Lambert, W. (2011) Quantitative liquid chromatographic analysis of anthracyclines in biological fluids. *Journal of Chromatography B*. 897(25): 2471-2486

Menna, P., Gonzalez Paz, O., Chello, M., Covino, E., Salvatorelli, E. and Minotti, G. (2012) Anthracycline cardiotoxicity. *Expert Opinion Drug Safety*. 11(S1): S21-S36.

Minotti, G., Menna, P., Salvatorelli, E., Cairo, G. and Gianni, L. (2004) Anthracyclines: Molecular Advances and Pharmacologic Developments in Antitumor Activity and Cardiotoxicity. *Pharmacological Reviews*. 56(2): 185-229.

Minotti, G., Recalcati, S., Mordente, A., Liberi, G., Calafiore, A., Mancuso, C., Preziosi, P. and Cairo, G. (1998). The secondary alcohol metabolite of doxorubicin irreversibly inactivates aconitase/iron regulatory protein-1 in cytosolic fractions from human myocardium. *The Journal of the Federation of American Societies for Experimental Biology*. 12(7): 541-552.

Neal, AJ and Hoskin, PJ. (2009) *Clinical Oncology: Basic Principles and Practice*. Fourth ed. Hodder Arnold Publishers. Ch: 2, 6 and 8.

Olson, L., Bedja, D., Alvey, S., Cardounel, A., Gabrielson, K. and Reeves, R. (2003) Protection from Doxorubicin-Induced Cardiac Toxicity in Mice with a Null Allele of Carbonyl Reductase 1. *Cancer Research*. 63(19): 6602-6606. Accessed June 2014. http://cancerres.aacrjournals.org/content/63/20/6602.full.pdf+html

Olson, R., Mushlin, P., Brenner, D., Fleischer, S., Chang, B., Cusack, B., and Boucek, R. (1988). Doxorubicin cardiotoxicity may be due to its metabolite, doxorubicinol. *Proceedings of the National Academy of Sciences of the United States of America*. 85: 3585-3589

Olson, R. and Mushlin, P. (1990). Doxorubicin cardiotoxicity: analysis of prevailing hypotheses. *The Journal of the Federation of American Societies for Experimental Biology*. 4(13): 3076-3086.

Parker, M., King, V. and Howard, K. (2001). Nuclear magnetic resonance study of doxorubicin binding to cardiolipin containing magnetically oriented phospholipid bilayers. *Biochimica et biophysica acta*. 1514(2): 206-216.

Parkinson, A. (2008). Biotransformation of Xenobiotics. In Klassen, C.'s *Casarette and Doull's Toxicology: The Basic Science of Poisons*. 7th Ed. McGraw-Hill Publishers. (pp. 161-305)

Paschoud, N., Bignell, C. and Reinhold, H. (1985). A double fluorescence method for determining doxorubicin distribution and vascular supply in the mouse kidney. *Journal of Histochemistry and Cytochemistry*. 33(1): 73-76. Retrieved June 2014. http://jhc.sagepub .com/content/33/1/73

Pfizer Canada Inc. *Product monograph: Adriamycin®PFS doxorubicin hydrochloride injection*. Revised 2012. Accessed June 2013. http://www.pfizer.ca/en/our_products/products /monograph/150

Pruthi, S. (2012) *HER2-positive breast cancer: What is it?* Online article from Mayo Foundation for Medical Education and Research. Accessed July 2013. http://www.mayoclinic.com/ health/breast-cancer/AN00495

Rahman, A., White, G., More, N. and Schein, P. (1985). Pharmacological, toxological, and therapeutic evaluation in mice of doxorubicin entrapped in cardiolipin liposomes. *Cancer Research*. 45: 796-803

Richard, C., Ghibu, S., Delemasure-Chalumeau, S., Guilland, J., Des Rosiers, C., Zeller, M., Cottin, Y., Rochette, L. and Vergely, C. (2011). Oxidative Stress and Myocardial Gene Alterations Associated with Doxorubicin-Induced Cardiotoxicity in Rats Persists for 2 Months after Treatment Cessation. *The Journal of Pharmacology and Experimental Therapeutics*. 339(3): 807-814. Accessed June 2014. http://jpet.aspetjournals.org/content/339/3/807.full

Saskatchewan Association of Veterinary Technologists. *Rodent Anesthesia*. 2010. Accessed June 2013. http://www.savt.ca/html/conference/proceedings/Rodent_Anesthesia/index.cfm

Shen, F., Chu, S., Bence, A., Bailey, B., Xue, X., Erickson, P., Montrose, M., Beck, W. and Erickson, L. (2008) Quantitation of Doxorubicin Uptake, Efflux, and Modulation of Multidrug Resistance (MDR) in MDR Human Cancer Cells. *The Journal of Pharmacology and Experimental Therapeutics*. 324(1): 95-102.

Smith, A. (2011) The influence of systemic hypoxia on vascular and interstitial mediators of blood flow in rat skeletal muscle. Master's Thesis. *Laurentian University*.

Sparreboom, A., Nooter, K., and Verweij, J. (2002). Mechanisms of Action of Cancer Chemotherapeutic Agents: Anitumor Antibiotics. In M.R. Alison's *The Cancer Handbook Volume 2* (pp. 1333-1346).

Sugarbaker, P., Van der Speeten, K., Stuart, O. and Chang, D. (2011) Impact of surgical and clinical factors on the pharmacology of intraperitoneal doxorubicin in 145 patients with peritoneal carcinomatosis. *European Journal of Surgical Oncology*. 37(8): 719-726.

Susa, M., Iyer, A., Ryu, K., Hornicek, F., Mankin, H., Amiji, M., and Duan, Z. (2009) Doxorubicin loaded Polymeric Nanoparticulate Delivery System to overcome drug resistance in osteosarcoma. *BioMed Central Cancer*. 9: 399.

van Asperen, J., van Tellingen, O. and Beijnen, J. (1998) Determination of doxorubicin and metabolites in murine specimens by high-performance liquid chromatography. *Journal of Chromatography B: Biomedical Sciences and Applications*. 712(1-2): 129-143.

Weiss, M. (2011). Functional characterization of drug uptake and metabolism in the heart. *Expert Opinion on Drug Metabolism and Toxicology*. 7(10): 1295-1306.

Yousefpour, P., Atyabi, F., Vasheghani-Farahani, E., Movahedi, A., and Dinarvand, R. (2011) Targeted delivery of doxorubicin-utilizing chitosan nanoparticles surface-functionalized with anti-Her2 trastuzumab. *International Journal of Nanomedicine*. 6: 1977-1990.

Appendix I: Supplementary Materials and Methods

Pre-experimental protocol

Injection volume calculation

1. The rat to be injected was weighed and tail marked.
2. The rat weight was converted from grams to kilograms.
3. Using the following formula, the injection volume was calculated.

$$\text{injection volume (mL)} = \frac{[(\text{rat weight in kg}) \times (\text{dose in mg/kg})]}{(\text{concentration of DOX stock, 2 mg/mL})}$$

Rat anesthesia

1. The surgical suite was set up; tools gathered, working area prepared, heating lamp set-up.
2. The rat was anaesthetized in the EZ-Anesthesia host chamber by turning on the 100% oxygen tank and the Isoflurane® at 5% for 5 minutes as described by the Euthanex Corporation (2002).
3. The plane of anesthesia was examined by verifying that the rat did not respond to knocking on the chamber walls or to toe-pinch.
4. If the rat did not respond, it was transferred to operating table and put on the nose cone for continuous delivery of oxygen and Isoflurane® at 1.5-2%

Intraperitoneal (IP) injection administration

1. Once the rat was maintained on oxygen and Isoflurane® at 1.5-2%, and the plane of anesthesia was consistent, the injection was given in the lower left (LL) quadrant of the abdominal region (Supplementary Figure 1).

2. If the rat was receiving a high dose and two separate syringes had to be used, one injection was administered to the LL quadrant, and the other to the lower right (LR) quadrant of the abdominal region.

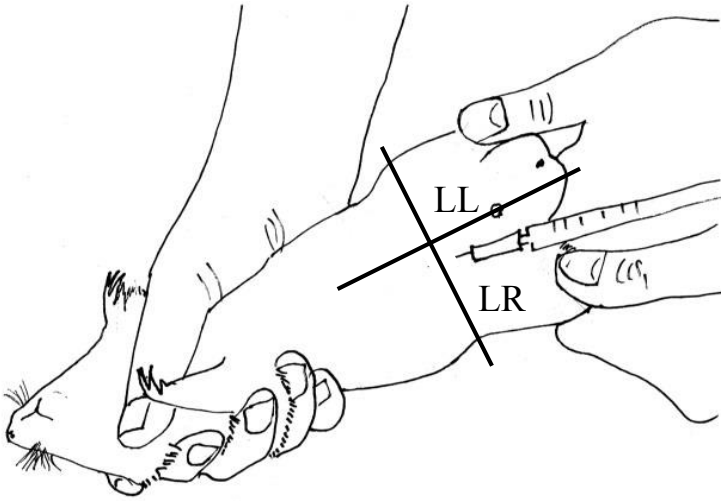

Figure 33: IP injection in the rat in the lower right (LR) abdominal quadrant (adapted from the Saskatchewan Association of Veterinary Technologists).

Recovery of the anesthetized animal

1. Once the injection had been administered, oxygen and Isoflurane® were turned off.
2. The animal was promptly replaced to their original cage and allowed to recover slowly with the lid removed.
3. The cage was labelled that the animal had received an injection of DOX.
4. Once the animal was awake, the lid to the cage was replaced and the cage was returned to its appropriate location.

Carotid artery isolation and cannulation

1. With a scalpel, a 3 cm ventral incision was made slightly to the right of the midline from the clavicle to approximately the rib cage.
2. With blunt dissection, fat tissue was removed.

3. The ventral muscle was removed by tightly tying off both ends of the muscle with suture string and subsequently cutting out the muscle. Any bleeding area was cauterized.
4. The carotid artery was isolated with forceps and three suture strings were placed underneath the artery.
5. The artery was tied off with a suture string approximately 0.5 cm upstream.
6. A micro-bulldog was used to temporarily stop blood flow posterior to the area of cannulation.
7. With a cannula and needle, the artery was pierced.
8. Needle was carefully removed, the cannula progressed gently toward the heart, and a closed three way stop cock was placed at the other end.
9. The micro-bulldog was removed, and cannula tied into place with the remaining two suture strings below the artery.
10. The three way stop cock was opened and 0.1 mL of heparnized saline was injected (1.0 mL of 1,000 IU/mL Hepalean (Organon Canada Ltd.) into 9.0 mL saline) to prevent clotting of any blood in the stop cock or cannula.

Experimental protocol

Blood collection

1. Three 0.5 mL blood collection micro-centrifuge vials were labelled.
2. Syringes were heparinised using 5 µL Hepalean (Organon Canada Ltd.)
3. Following equilibration, a 0.3 mL blood sample was drawn from the carotid artery.
4. 0.3 mL of heparinized saline was injected.
5. The sample was centrifuged at 15,000 rpm for 15 seconds.

6. Using a pipette, the plasma was removed from the blood cells and transferred to a second micro centrifuge tube, which was labelled.
7. Plasma and blood cell vials were put on ice until the conclusion of the experiment, after which point they were stored at -80°C.
8. This procedure was repeated every hour for another two hours.

Rat euthanasia

1. When the last sample was complete, the Isoflurane was turned up to 5% until the rat stopped breathing.
2. The rat was then quickly transferred to the guillotine, where it was decapitated.

Post-experimental protocol

Organ removal

1. Following decapitation, the rat was transferred back to the operating table.
2. Using scissors, the thoracic and abdominal cavities were opened.
3. The ribs were cracked, to allow opening of the rib cage to access the heart.
4. The heart was removed by quickly cutting the aorta and superior and inferior vena cava. It was placed on an autoclaved and labelled foil, was weighed and stored on ice until the completion of the experiment.
5. The liver was removed by cutting its attachments; the hepatic vein, mesenchyme, etc. It was placed in a labelled centrifuge tube, was weighed and stored on ice until the completion of the experiment.
6. All samples were placed -80°C storage.

HPLC quantification of DOX, DOXOL and DNR

- Methods were pre-established in the MacLean Lab and were modified from an article by Alvarez-Cedron et al. (1999).
- Components were separated through HPLC with the Waters Alliance e2695 Separations Module system with a Waters 2475 Multi λ Fluorescence detector, with detection at 480 nm excitation and 560 nm emission. Analysis column used was an ACE-CN column (Canadian Life Science) with a particle size of 5µM and dimensions of 4.6mm by 250mm.
- Reservoir A: 100% HPLC grade Acetonitrile
- Reservoir B: 10mM sodium phosphate monobasic pH 4.0 (mobile phase)
- Reservoir C: MilliQ® H_2O
- Reservoir D: 100% Methanol
- Seal and Needle Wash: 10% HPLC grade Acetonitrile, 90% MilliQ® H_2O
- All solutions run through the system were vacuum filtered/degassed.
- When the system was idle, 20% Reservoir A and 80% Reservoir B was run through the column at a rate of 0.2 mL/min.
- If there were durations of extended idle (more than 3 weeks), 40% Reservoir C and 60% Reservoir D was run through the column at a rate of 0.2 mL/min.
- Purge inject and condition column functions were performed prior to each run and preceded injections of standards with known concentrations. Each sample run was 20 min. at a flow rate of 1.0 mL/min with the following gradient:

Table 6. HPLC gradients

Time (min.)	Flow (mL/min)	%A	%B	%C	%D	Curve
0.0	1.0	20.0	80.0	0	0	0
10.0	1.0	50.0	50.0	0	0	6
11.0	1.0	20.0	80.0	0	0	6
24.0	1.0	20.0	80.0	0	0	6

- Under this method, retention times were approximately:

DOXOL	6.650
DOX	7.950
DNR	9.350

- Processing: Integration was done manually and concentrations were determined using a calibration curve created for each run, based on the standards included in that run.

HPLC eluent and standard preparation

Mobile phase preparation

1. 1.19 g of sodium phosphate (NaH_2PO_4) monobasic (Fisher Chemical) was weighed and added to 1.00 L of MilliQ® H_2O (TOC~5 ppb).
2. The pH was adjusted to 4.0 by adding O-phosphoric acid 85% drop-wise.

Seal and needle wash preparation

1. 100 mL of 100% HPLC grade Acetonitrile was combined with 900 mL of MilliQ® H_2O.

Standard preparation

Standards were prepared to contain varying concentrations of both components of interest (DOX and DOXOL) and equal concentrations (0.625 µM) of the internal standard (DNR). The DOX (North-Eastern Ontario Cancer Centre) stock was at a concentration of 2.0 mg/mL or 3.47 mM. Both the DOXOL (Toronto Research Cheminal) and DNR (Sigma-Aldrich) stocks were at concentrations of 5.0 mM.

1. 10.0 µL of DOXOL and 14.1 µL of DOX stocks were added to 10 mL of MilliQ® H_2O. This mixture created a 5.0 µM solution of DOX and DOXOL.
2. The solution was vortexed thoroughly.
3. 0.75 mL of 5.0 µM DOX DOXOL was added to 0.75 mL of MilliQ® H_2O to obtain 1.5 mL of a 2.5 µM DOX DOXOL solution.
4. This solution was then serial diluted in the same manner until the concentration of the final standard was 0.0196 µM.
5. To include the DNR in each standard, the stock DNR had to first be diluted to 6.25 µM.
6. For the standards having a final volume of 0.75 mL, 75 µL of diluted DNR was added.
7. For the standards having a final volume of 1.5 mL, 150 µL of diluted DNR was added.

Extraction solutions preparation for HPLC analysis

Primary tissue extraction solution

0.625 µM daunorubicin in 0.067 M potassium phosphate

1. 1.167 g K_2HPO_4 was added to 100 mL MilliQ® H_2O.
2. 12.5 µL of 5.0 mM stock DNR was added.

Secondary tissue and primary plasma extraction solution

50/50 40% zinc/100% methanol

1. 40 g $ZnSO_4$ was added to 100 mL MilliQ® H_2O.
2. To this, 100 mL of 100% methanol was added.

Histological procedures

Specimen preservation

1. 0.5 mL micro-centrifuge vials were clearly labelled with the rat name and the tissue.
2. Approximately 0.3 mL of TissueTek® O.C.T Compound (Sakura Finetek USA) was added to the vials.
3. A section of right ventricle and a section of anterior lobe were removed from the partially frozen tissues, and embedded in their appropriate vials.
4. To optimize preservation, samples were first placed at -30°C, and allowed to freeze.
5. Samples were then transferred to -80°C for storage.

Slide preparation

1. The Leica® CM3050 S cryostat system was turned on, the blade and glass were inserted appropriately, and the chamber was allowed to cool to the optimal freezing temperature (for heart: -23°C to -24°C, for liver: -26°C to -27°C)
2. Chucks were prepared by placing a round dab of O.C.T. Compound in their centre and allowing it to freeze in the cryostat chamber.
3. The embedded sample was then removed from the vial, placed onto the prepared chuck using O.C.T. Compound and allowed to freeze.

4. The chuck was then placed into the object holder, which was manually advanced until it met the blade and a section could be sliced.
5. The settings were then adjusted to cut 30 µm sections, and sections were sliced and observed for consistent appearance (no splitting or wrinkling).
6. Good sections were melted onto appropriately labelled VWR® Superfrost® Plus Micro Slides (Figure 2.1, Chapter II).
7. Once the slide was full, 10-12 µL of Vectashield® Fluorescence Mounting Medium with DAPI (Vector Laboratories Inc.) was added to the slide with a pipette.
8. VWR® Cover slips were then placed on top and excess Vectashield® was removed with an absorbent wipe.
9. The edges were then sealed with clear nail polish.
10. All slides were stored in opaque slide cases at -4°C.

Slide observation

Histological slides were observed using a Nikon Eclipse 90i Fluorescence Microscope with QImaging Retiga EXi camera and iControl© and Simply PCI 6 ©1995-2005 software. Two different fluorescence filters were used; DAPI (440 nm, 40 nm bandwidth) and TRITC (590 nm, 34 nm bandwidth).

General procedure

1. The lamp was ignited.
2. The computer was turned on.
3. The microscope was turned on.
4. The camera was turned on.
5. iControl© was used to manually bring the slide into focus under the DAPI filter.

6. SimplePCI 6© was then used to focus the slide on the computer screen.
7. Without any further adjustment, one image was captured under the DAPI filter and another under the TRITC filter. They were therefore the same image, under two different fluorescence filters.
8. This was repeated for at least two sections of each tissue, including control tissue.
9. The contrast settings were adjusted in SimplePCI 6© for each image.
10. All heart images were set to DAPI Low: 1, High: 255 and TRITC Low: 0, High: 30
11. All liver images were set to DAPI Low: 1, High: 255 and TRITC Low: 0, High: 70.

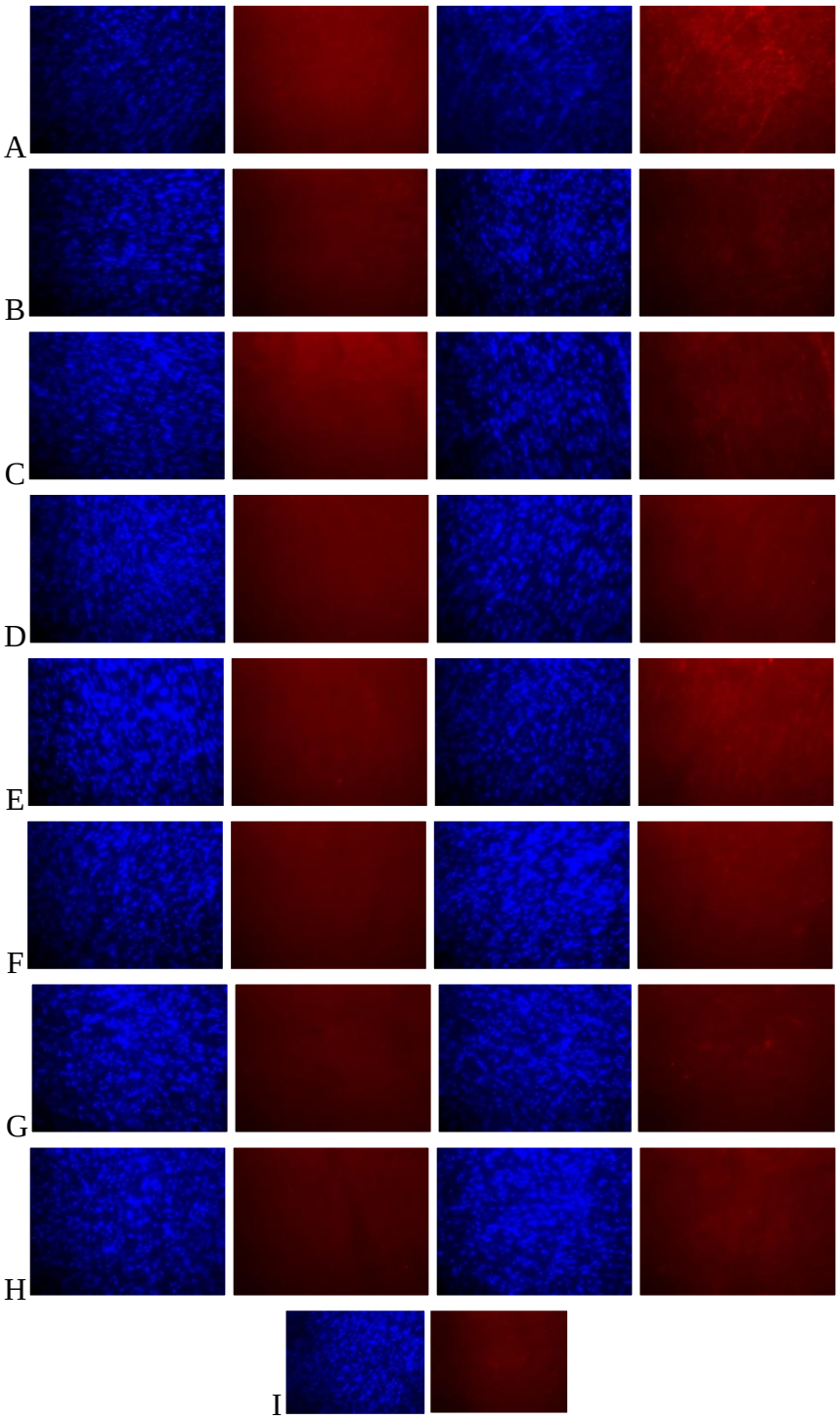

Figure 34: Histological images of heart tissue. In each panel from left to right; DAPI image for 1.5 mg/kg dose, TRITC image for 1.5 mg/kg dose, DAPI image for 4.5 mg/kg dose and TRITC image for 4.5 mg/kg dose. A) 24 hours post-injection. B) 48 hours post-injection. C) 72 hours post-injection. D) 96 hours post-injection. E) 120 hours post-injection. F) 144 hours post-injection. G) 168 hours post-injection. H) 192 hours post-injection. I) Control.

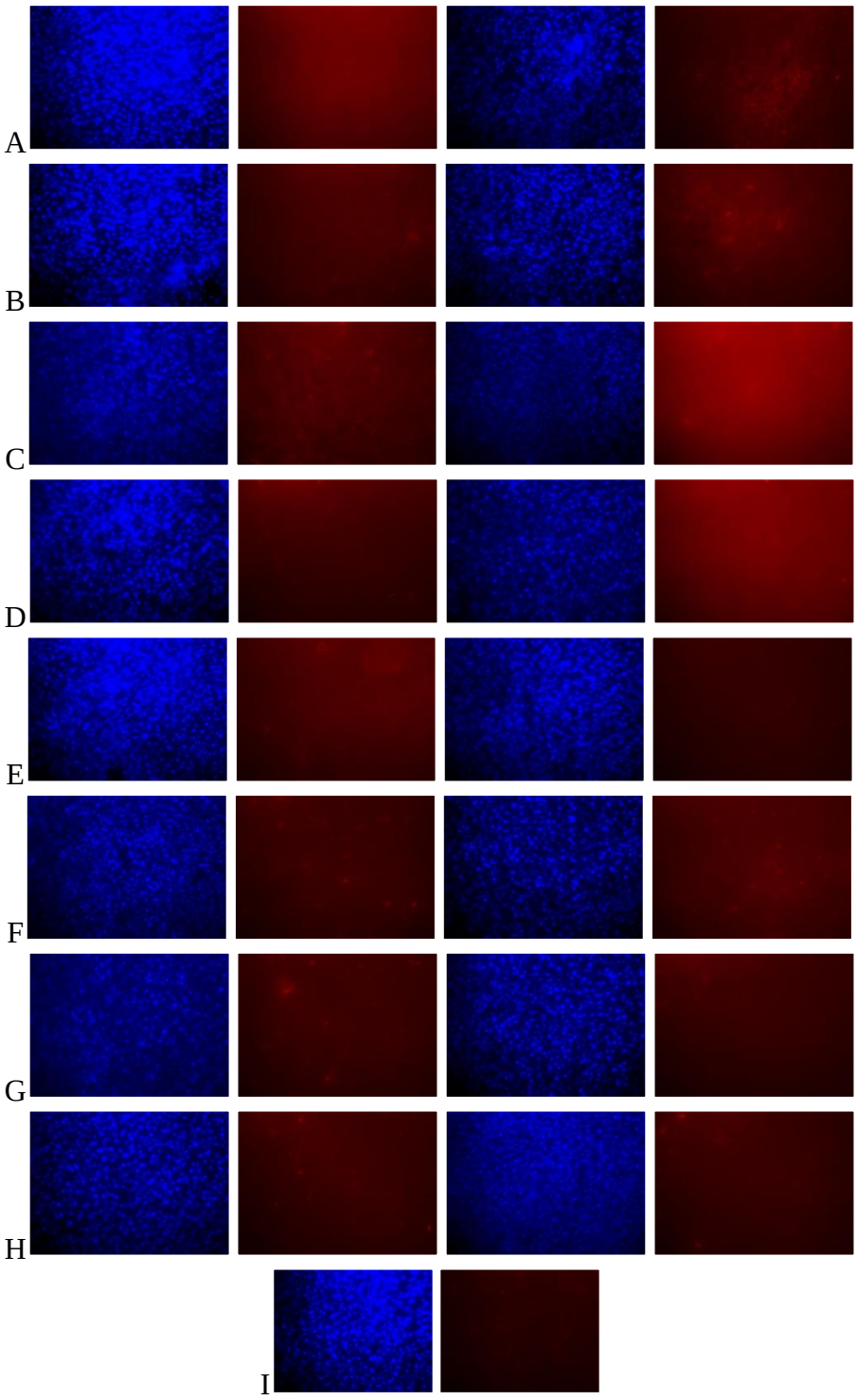

Figure 35: Histological images of liver tissue. In each panel from left to right; DAPI image for 1.5 mg/kg dose, TRITC image for 1.5 mg/kg dose, DAPI image for 4.5 mg/kg dose and TRITC image for 4.5 mg/kg dose. A) 24 hours post-injection. B) 48 hours post-injection. C) 72 hours post-injection. D) 96 hours post-injection. E) 120 hours post-injection. F) 144 hours post-injection. G) 168 hours post-injection. H) 192 hours post-injection. I) Control.